Tectonics of the Eastern Desert of Egypt: Key to Understanding the Neoproterozoic Evolution of the Arabian–Nubian Shield (East African Orogen)

Z. Hamimi, M. A. Abd El-Wahed, H. A. Gahlan and S. Z. Kamh

Abstract The tectonic evolution of the Arabian–Nubian Shield (ANS), the northern continuation of the East African Orogen (EAO), is enigmatic and a matter of controversy. The EAO is observed as a N–S trending major suture zone separating East and West Gondwanaland. It documents a prolonged tectonic history bracketed by the fragmentation of Rodinia Supercontinent and the amalgamation of Gondwana. The ANS is dominated by Neoproterozoic juvenile continental crust (i.e., crust formed directly from the mantle), formed by magmatic arc accretion and subsequent post-tectonic magmatism, and includes a mosaic of tectonic terranes juxtaposed along ophiolite-decorated megashears (suture zones). Among them is the Eastern Desert terrane (namely, Aswan or Gerf terrane in some literatures) which is regarded as the western extension of Midyan terrane in Western Arabian and shows most of the polydeformed history of the ANS. This chapter is devoted to discuss the Neoproterozoic crustal evolution of the Pan-African belt of the Eastern Desert terrane in an attempt to understand the tectonic setting of the ANS. Main points to be discussed in this chapter are: (1) infracrustal–supracrustal rocks, (2) thrusting, shearing, and folding relations; (3) gneiss domes versus metamorphic core complexes; (4) the conjugate pairs of Najd-related shears; (5) role of Najd Fault System in tectonic evolution of gneiss domes; (6) rates and transport directions of metaultramafic nappes; (7) the voluminous intrusives in northern Eastern

Z. Hamimi (✉)
Department of Geology, Faulty of Science, Benha University, Benha 13518, Egypt
e-mail: yahiahamimi@gmail.com

M. A. Abd El-Wahed · S. Z. Kamh
Geology Department, Faculty of Science, Tanta University, Tanta 31527, Egypt

H. A. Gahlan
Geology and Geophysics Department, College of Sciences, King Saud University, Riyadh 11451, Saudi Arabia

H. A. Gahlan
Department of Geology, Faculty of Science, Assiut University, Assiut 71516, Egypt

A. Bendaoud et al. (eds.), *The Geology of the Arab World—An Overview*,
Springer Geology, https://doi.org/10.1007/978-3-319-96794-3_1

Desert; (8) the post-amalgamation Hammamat sediments and their relation to Dokhan Volcanics; and (9) the northward decrease in intensity of deformation in the entire Eastern Desert.

1 Introduction

A general agreement is established that rifting of the Red Sea since the Oligocene and younger times led to uplifting and exhumation of the Neoproterozoic Arabian–Nubian Shield (ANS) (Hamimi et al. 2015b). The Egyptian Eastern Desert occupies the northwestern part of the ANS and is dominated by crystalline basement complex considered by many workers as the mirror image of the Neoproterozoic belt exposed at Western Arabia (Arabian Shield).

This chapter addresses the tectonic setting of the Egyptian Eastern Desert as a key to deciphering the Neoproterozoic tectonic evolution of the ANS and consequently the entire East African Orogen (EAO). Depending upon outstanding differences in exposed lithologies and remarkable contrast in physiographic features, Abdel Khalek (1979), Stern and Hedge (1985) and El-Gaby et al. (1988) subdivided the Egyptian Eastern Desert into three main provinces; Northern Eastern Desert (NED), Central Eastern Desert (CED) and Southern Eastern Desert (SED). Such threefold division has been one of the few broadly accepted concepts in the tectonic analysis of the Egyptian Neoproterozoic basement (Fowler and Osman 2009). The provinces juxtapose along two major structural elements; Qena-Safaga Shear Zone separates NED from CED, and Idfu-Mersa Alam Shear Zone splits CED from SED (Fig. 3). Fowler and Osman (2009) considered the northerly dipping Sha'it–Nugrus shear zone as the boundary separating the CED from the SED. The NED is dominated by voluminous granitoids, together with slightly deformed–unmetamorphosed Dokhan Volcanics and post-amalgamation Hammamat volcano-sedimentary sequence. The CED encompasses gneisses–migmatites-sheared granitoids and remobilized equivalents outcropping as elliptical domal-like structures, in addition to volcano-sedimentary succession (mainly volcanogenic metagraywackes and metamudstones) and ophiolitic metaultramafics. Lithologic units encountered in the SED resemble those of the CED with the exception of high percentage of gneisses and migmatitic gneisses, as well as the ophilitic metaultramafics that form conspicuous tectonically transported nappes. Gneissic and migmatitic rocks of the SED occupy much larger, more complexly shaped areas associated with batholiths of foliated granodiorite (Fowler and Osman 2009). Moreover, the typical greenschist facies of volcanogenic metagraywackes and metamudstones of the CED are also comparable to the high-grade schistose-metasediments of the SED (El-Gaby et al. 1988; Hermina et al. 1989; Hassan and Hashad 1990). Besides the lithologic differences, the previously mentioned provinces of the Egyptian Eastern Desert display remarkable differences in structural architecture (Hamimi et al. 2015b). The NED is dominated by fault/joint systems and marked by younger granitoid intrusions. Fold-related faults are dominant in the CED and are commonly

associated with pull-apart basins linked to Najd Fault System. In the SED, fold-thrust belts prevail and thrusts are first-order kinematics that are later over-printed by map-scale transpression.

2 Proposed Models for the Arabian–Nubian Shield, East African Orogen

According to the concept of supercontinental cycle, continental blocks and cratons converge into single supercontinent, split and disperse into numerous continents, then amalgamate once again. This scenario, which is estimated to be 300–500 Ma long, occurred more than once throughout earth's history giving Pangaea and preceding supercontinents such as Rodinia and Colombia (Hoffman 1999). Several lines of evidence indicated that rifting and fragmentation of Rodinian Supercontinents lasted over 300 Ma and reassembly of the old continental blocks resulted in the formation of Gondwana supercontinent. Gondwana comprises two continental blocks juxtapose along a 3000 km stretched EAO (Stern 1994). The EAO extends in a N- to NNW-direction from Sinai Peninsula to Mozambique. The East African Orogen has long been considered the best exposed bowels of former mountain building that there are results of continent–continent collision and the bulldozing together of many oceanic arcs and remnants of oceanic lithosphere that once separated the cratons (Drury 2013). It consists of several Neoproterozoic juvenile island arc terranes accreted on the westward Saharan Metacraton (Fig. 1), during a long orogenic cycle started with the breakup of Rodinia (Li et al. 2004) and continued to the final amalgamation of Gondwana (Pisarevsky et al. 2003; Collins and Pisarevsky 2005).

Several models have been proposed to discuss the tectonic evolution of the ANS which represents the northern extension of the EAO and upper crustal equivalent of the Mozambique belt (Hamimi et al. 2013a, b).

(1) Infracrustal orogenic model, whereby ophiolites and island arc volcanics and volcaniclastics were thrusted over an old craton consisting of high-grade gneisses, migmatites, and remobilized equivalents during Neoproterozoic time (e.g., Akaad and Noweir 1980; El-Gaby et al. 1988; Abdel Khalek et al. 1992; Khudeir and Asran 1992).
(2) Turkic-type orogenic model, whereby much of the ANS formed in broad fore-arc complexes (Şengor and Natal'in 1996).
(3) Hot-spot model, whereby much of the ANS is due to accretion of oceanic plateau formed by upwelling mantle plumes (Stein and Goldstein 1996).
(4) Arc assembly (arc accretion) model, whereby EAO juvenile crust was generated around and within a Pacific-sized ocean (Mozambique Ocean). This model was proposed first by Vail (1985) and Stoeser and Camp (1985), and modified by Stern (1994).

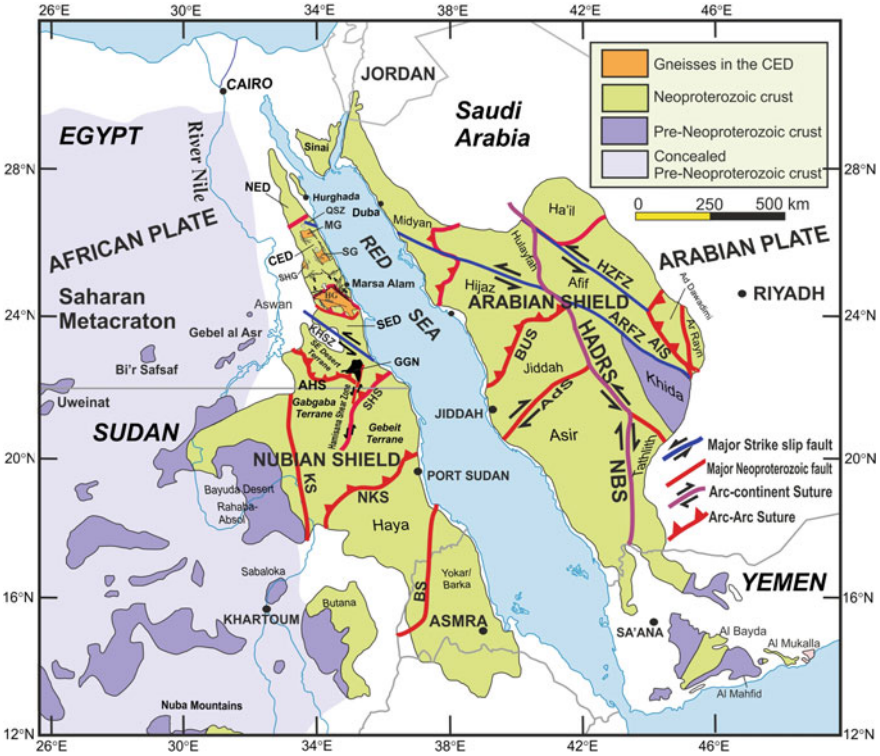

Fig. 1 Relationship between the Arabian–Nubian Shield (ANS) to the adjacent older continental crust. The border with the Saharan Metacraton, on the west, is the effective contact between ANS and West Gondwana: a border, on the east, with putative East Gondwanan crust, is not certain. NED = North Eastern Desert; CED = Central Eastern Desert; SED = South Eastern Desert; QSZ = Queih Shear Zone; MG = Meatiq Gneisses; SG = Sibai Gneisses; MG = Hafafit Gneisses; SHG = Shalul Gneisses; KHSZ = Kharit-Hodein shear zone: SHS = Sol Hamed Suture; AHS = Allaqi–Heiani Suture; GGN = Gabal Gerf Nappe; NKS = Nakasib Suture; KS = Keraf Suture; BS = Baraka Suture; AIS = Al Amar Suture; ADS = Ad Damm Suture; BUS = Bir Umq Suture; YS = Yanbu Suture; HADRS = Hulayfah-Ad Dafinah-Ruwah; NBS = Nabatih Suture; HZFZ = Halaban-Zarghat Fault Zone; ARFZ = Al Rika Fault Zone (compiled from Johnson et al. 2011; Abdeen and Abdelghaffar 2011; Fritz et al. 2013; Abd El-Wahed et al. 2016)

3 Rock Succession in the Egyptian Nubian Shield

The Precambrian igneous–metamorphic complex (basement) of Egypt, covers ~100,000 km^2, crops out along the Red Sea hills in the Eastern (Arabian) Desert and southern Sinai Peninsula as well as limited areas in the south Western (Libyan) Desert (Oweinat area) (Fig. 2) (El- Gaby et al. 1990; Hassan and Hashad 1990). The basement complex of Egypt is part of the Arabian–Nubian Shield (ANS). The ANS is the largest tract of juvenile continental crust of Neoproterozoic age on Earth (Patchett and Chase 2002). It forms the suture between East and West

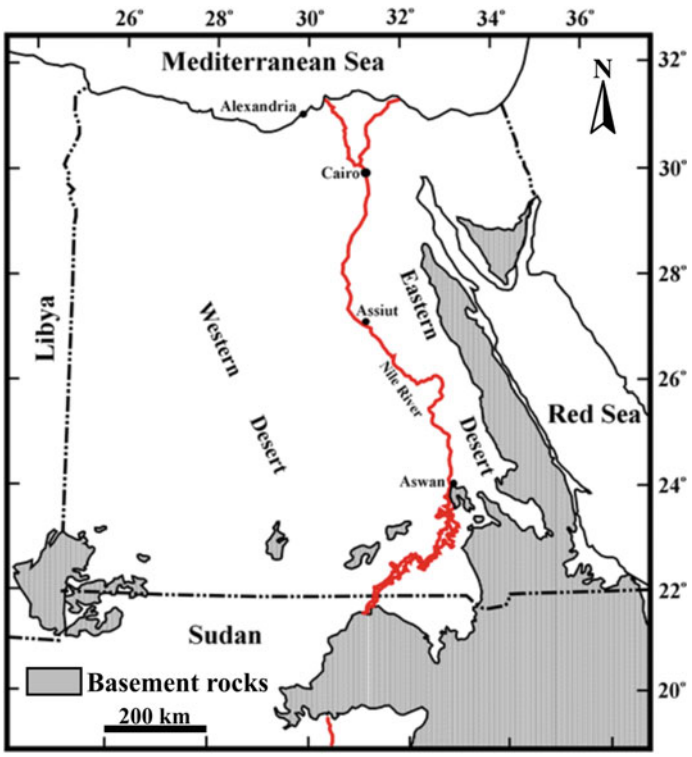

Fig. 2 Distribution of the Precambrian basement rocks in Egypt (El-Gaby et al. 1990). Rocks of Archean age are confirmed in the Western/Libyan Desert only

Gondwana at the northern end of the East African Orogen. The ANS has a complex history including a record of the breakup of Rodinia at circa 900–800 Ma, and the evolution of numerous arc systems, oceanic plateaux, oceanic crust, and sedimentary basins (Stern 1994; Stein and Goldstein 1996; Johnson 1998; Kusky et al. 2003; Kusky 2004). The ANS can be represented by a complex amalgam of arc, ophiolite and micro-continental terranes that had been resulted from the Neoproterozoic closure of the Mozambique Ocean (e.g., Kusky et al. 2003). The shield was subsequently over buried by the Phanerozoic sediments. In the Oligocene and younger times, the shield had been exposed by uplift and erosion on the Red Sea flanks (Stern et al. 2004). Accordingly, the basement complex is well exposed along the Eastern Desert of Egypt and western Arabia.

Generally, the ANS/basement of Egypt comprises three main tectonostratigraphic units (e.g., Ali et al. 2012) from bottom upward as follows: (1) high-grade gneisses and migmatites, (2) arc-type volcanic/volcano-sedimentary units, along with dismembered ophiolites, and (3) the Ediacaran Hammamat and Dokhan supracrustal sequences. And granitoids intrude all the three units.

3.1 Gneisses and Migmatites

Gneisses and migmatites constitute the infrastructural rocks of the Egyptian basement complex, as well as the ANS. They comprise 7% of the surface outcrops of the Egyptian basement. Pohl (1979) inferred that gneiss domes represent the northern continuation of the Mozambique belt. They show tectonic windows or continental basement being exposed in the uplifted regions of the Pan-African belt (e.g., El-Gaby et al. 1984). Among the most famous gneiss domes of the Egyptian Eastern Desert: Meatiq, Um Had, Sibai, El Shalul, Hafafite, Migif, Beitan, and Fiqo from the North- to South Eastern Desert (Fig. 3) (e.g., El-Gaby et al. 1984; Hamimi et al. 1994; Hamimi 1996; Gahlan 2006; Fowler et al. 2007; Abd El-Wahed 2007, 2008; Andersen et al. 2009, 2010; Ali et al. 2010, 2012; Lundmark et al. 2012, among others). They are structurally below arc and ophiolite rocks.

Briefly, the infrastructural rocks comprise schists, gneisses, and migmatites constituting the so-called *Tier-I* (e.g., Bennet and Mosely 1987; Greiling et al. 1994). They were derived from an ancient sedimentary succession accumulated along a passive continental margin, being affected by low-*P* and high-*T* regional metamorphism up to the upper amphibolite facies. The sedimentary sequence was also intercalated by basic igneous sills (ortho-amphibolites) as well as marls (para-amphibolites) and quartzite layers. The metamorphic grade and grain size change gradually by moving toward the core of the antiform, from common metamorphites (i.e., schists) to partially migmatized metatexites before reaching the high-grade weakly foliated homogenized mesocratic to leucocratic diatexites which occupy the core of the antiform. The homogenized diatexites comprise tonalite to granodiorite gneisses. The gneiss domes are commonly surrounded folded thrust belt of low-grade supracrustal rock assemblage, namely, island arc metavolcanic and metavolcano-sedimentary sequences, and ophiolites.

A variety of ages have been proposed for the Egyptian Eastern Desert gneisses; pre-Neoproterozoic/pre-Pan-African (e.g., El-Ramly and Akaad 1960; El-Ramly 1972; El-Gaby et al. 1984, 1990; Hamimi et al. 1994; Khudeir et al. 2008) or juvenile/Pan-African (El-Ramly et al. 1984; Greiling et al. 1984, 1988; Kröner et al. 1994; Andresen et al. 2009, 2010; Ali et al. 2010, 2012; Augland et al. 2012; Lundmark et al. 2012). The isotopic dating of gneiss domes at Meatiq (631 ± 2 Ma, Andersen et al. 2009), El Shalul (631 ± 6 Ma, Ali et al. 2012), Hafafit (659 ± 5, Lundmark et al. 2012) and Beitan (~725 ± 9 Ma, Ali et al. 2015) has denied the pre-Neoproterozoic age for those gneisses. Although the pre-Neoproterozoic zircons are recognized in the juvenile Eastern Desert basement rocks (Ali et al. 2015, and references therein), which indicate a contribution from an older crustal component to the Eastern Desert juvenile rocks. Isotopic data (U–Pb zircon and Sm–Nd whole rock) further indicate that most of the Eastern Desert curst was derived from a depleted mantle source (e.g., Moghazi et al. 1998; Moussa et al. 2008; Andresen et al. 2009; Ali et al. 2009, 2010, 2012; Liégeois and Stern 2010; Augland et al. 2012; Lundmark et al. 2012).

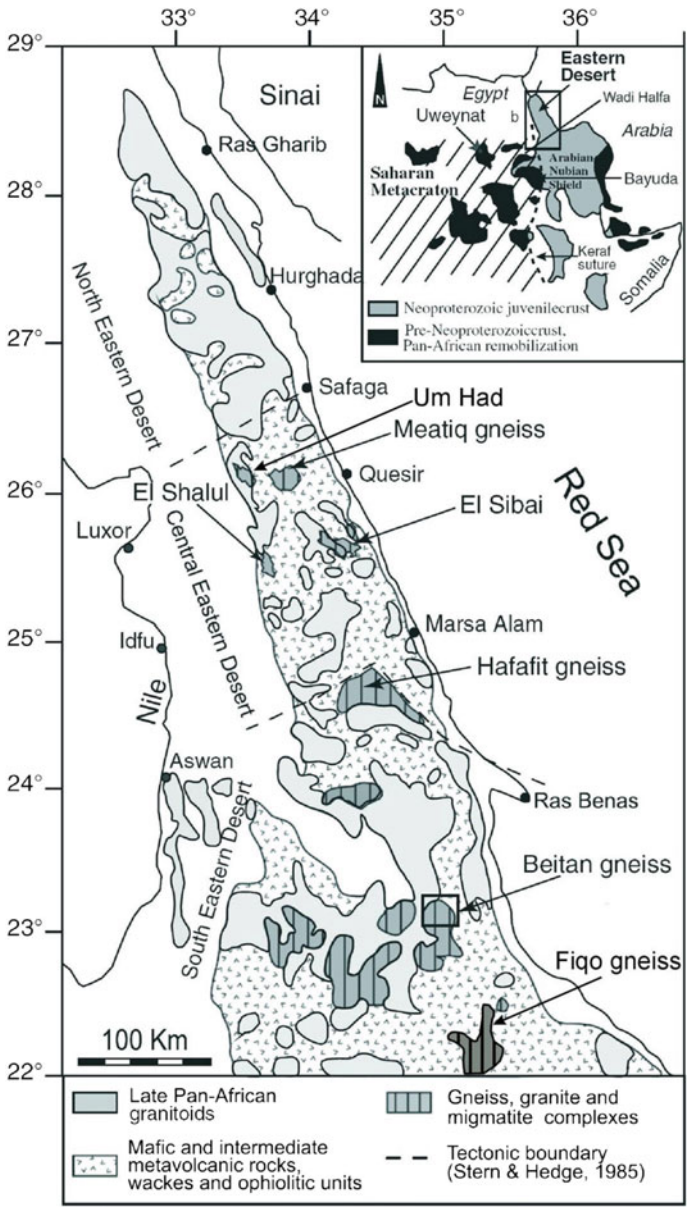

Fig. 3 Distribution of the most famous gneiss domes in the Central and South Eastern Desert of Egypt, modified after Ali et al. (2015) and locality of the Fiqo gneisses is after Gahaln (2006). The inset is a general geological map of the Arabian–Nubian Shield, Saharan Metacraton, and Archean and Paleoproterozoic crust that were remobilized during the Neoproterozoic era

3.2 *Relict Oceanic Lithosphere*

It is widely accepted that the ANS ophiolites represent remnants of Neoproterozoic oceanic lithosphere (~870–690 Ma) obducted along destructive plate boundaries during the Pan-African orogeny (~750–650 Ma) (Stern 1994; Ali et al. 2010). A variety of tectonomagmatic scenarios have been proposed for the Egyptian ophiolites, including: (i) back-arc basins (e.g., Ahmed et al. 2001; Farahat et al. 2004b; Abd El-Rahman et al. 2009a); (ii) mid-ocean ridges (MOR) (e.g., Zimmer et al. 1995; Khalil 2007); and/or (iii) forearcs (e.g., Stern et al. 2004; Gahlan 2006; Azer and Stern 2007; Abd El-Rahman et al. 2009b; Ahmed 2013; Gahlan et al. 2015).

The Egyptian ophiolites seem to be formed at ~730–750 Ma (e.g., Allaqi ~730 Ma, Ali et al. 2010; Fawakhir 736.5 ± 1.5 Ma, Andersen et al. 2009; Gerf ~750 Ma, Zimmer et al. 1995; Ghadir 746 ± 19 Ma, Kröner et al. 1992; Gerf 741 ± 21 Ma; Kröner et al. 1992) (Fig. 4).

According to the Penrose Conference ophiolite model (Anonymous 1972), the Egyptian ophiolites are variably dismembered due to tectonic disruption. A pseudo-lithostratigraphic column for the Egyptian ophiolites can display a sequence from mantle section, upward through mafic crust to the overlying mafic volcanic rocks (Fig. 5) (Gahlan 2006).

The mantle section is represented by sheet-like bodies of serpentinized ultramafics dominated by harzburgite and dunite. Chromitite pods are commonly small-scale and observed in the shallowest parts of the mantle section. The uppermost part of mantle

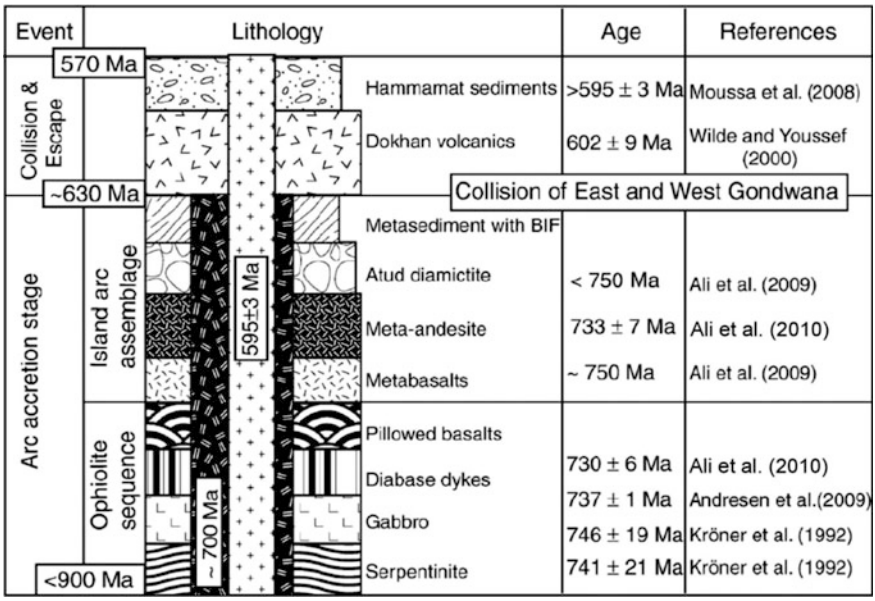

Fig. 4 An evolutionary diagram shows major tectonic events of the Neoproterozoic basement complex of Egypt (Ali et al. 2010, and references therein)

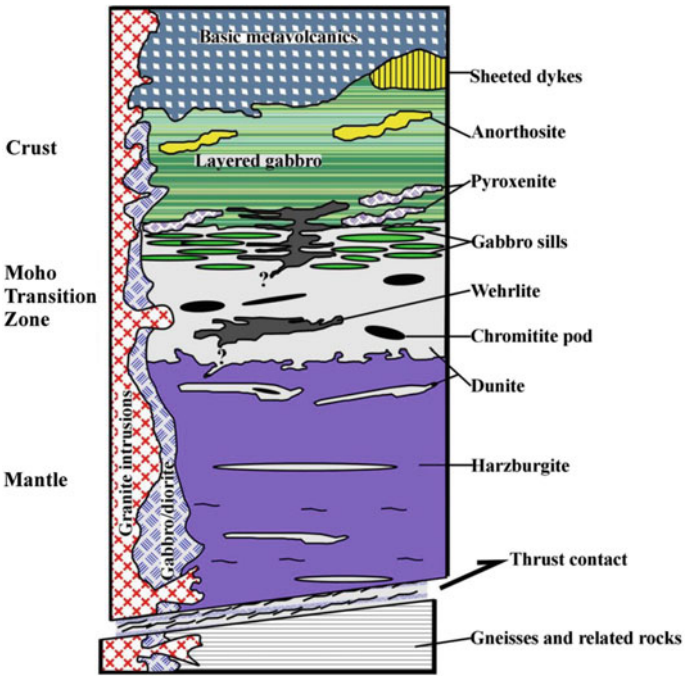

Fig. 5 A general pseudo-lithostratigraphic column of the Egyptian ophiolites, an example from the Abu Dahr ophiolite (Gahlan et al. 2015)

sometimes contains large masses of serpentinized dunite containing concordant gabbro sills or layers of serpentinized ultramafic cumulates, representing the so-called Moho Transition Zone (MTZ) (Fig. 5). The ultramafic cumulates are represented by wehrlites and pyroxenites, being restricted to the Moho transition zone and the lower crustal sequence (e.g., Ras Salatit ophiolite, Gahlan et al. 2012) (Fig. 5). Toward the sole thrust and along shear zones, the serpentinized ultramafics are transformed into schistose serpentinites and talc-carbonates.

The crustal section is represented by metagabbro and metavolcanic rocks. The metagabbros range from medium-grained to appinitic pyroxene metagabbro, Hb-metagabbro, and meta-anorthosite. Isomodal-type igneous layering and foliation are observed. The sheeted dykes were locally observed in the best cases as massive 100% dykes with chilled margins discriminate the contacts between them (e.g., Gerf ophiolite, Gahlan 2006; Sol Hamed ophiolite, Gahlan et al. submitted). The metavolcanics are represented by basalts and basaltic andesites. They are locally pillowed and associated with ophiolitic metasedimentary rocks. They stratigraphically and structurally overlie the metagabbros. Locally, near and along thrust contacts, the metavolcanic rocks are transformed into chlorite and actinolite schists.

3.3 Island Arc Assemblage

The island arc rock assemblage of the Egyptian basement includes (1) an intrusive gabbro–diorite–tonalite suit, and (2) calc-alkaline volcanic and volcano-sedimentary rocks, with rare sedimentary iron formation and carbonates (e.g., El-Gaby et al. 1984; Mohamed and Hassanen 1996; Abu El-Ela 1997; Kharbish 2010; Azer et al. 2016, and references therein). The island arc rocks are commonly regionally deformed, sheared, and metamorphosed up to the lower amphibolite facies. They show a calc-alkaline nature; namely, LILE enrichment, negative Nb and P_2O_5 anomalies, and jagged primitive mantle-normalized trace-element pattern compared to the smooth MORB pattern.

According to Be'eri-Shlevin et al. (2009b, 2011), the calc-alkaline magmatism in the ANS can be divided into two stages; the first stage (625–650 Ma) includes deformed syn- to late-orogenic island arc intrusive and the associated extrusive rocks, and the second stage (590–625 Ma) includes less deformed post-collision calc-alkaline magmatic rocks.

3.4 Dokhan Volcanics

The Dokhan volcanics are K-rich calc-alkaline volcanic rocks that characterize the stage after cratonization of the shield in the Neoproterozoic ($\sim$590–610 Ma) (Fig. 4). They record the second major volcanic episode in the Neoproterozoic crust of the ANS (e.g., Abdel Wahed et al. 2012). The Dokhan volcanics are largely restricted to southern Sinai, North, and Central Eastern Desert of Egypt, in decreasing order of abundance (Fig. 5). Additionally, Gahlan (2003) recorded the Dokhan volcanics in the southernmost Eastern Desert, along the Egyptian–Sudanese boarder, at Wadi Soaorib.

They form a thick sequence of variegated stratified andesitic to rhyolitic lava flows and their pyroclastics as well as ignimbritic rhyolites of Ediacaran age (615 $\pm$ 4 Ma, Breitkreuz et al. 2010; Basta et al. 1980). The Dokhan volcanics are characterized by K-rich nature, great abundance of acidic volcanics, common presence of ignimbrites and welded tuffs, LILE enrichment relative to HFSE, low-pressure fractionation, low Nb and Ta, depletion of Sr and Ti, and high total REEs with LREE enriched over HREE (e.g., El-Gaby et al. 1991; Abdel Wahed et al. 2012). Moreover, these volcanics provide evidences of fractional crystallization and crustal contamination magma processes.

A variety of origins have been proposed for the Dokhan volcanic: (1) compressional tectonomagmatic regime/active continental margin (e.g., Basta et al. 1980; El-Gaby et al. 1989; Abdel Rahman 1996); (2) extensional tectonomagmatic regime/rift system (e.g., Stern et al. 1984); (3) and/or transitional tectonomagmatic regime between extensional and compressional (e.g., Mohamed et al. 2000; Eliwa et al. 2006).

3.5 *Hammamat Molasse Sediments*

The Hammamat sediments are late-orogenic molasse-type fluvial sediments deposited in foreland, strike-slip, intermontane basins (e.g., El-Gaby et al. 1984; Fritz and Messner 1999; Abd El-Wahed 2010). They commonly crop out in N–S extent along the North- and Central Eastern Desert of Egypt (e.g., Hassan and Hashad 1990). They mark a significant change in the Pan-African tectonics, the end of compressional and the onset of extensional regime (Stern and Hedge 1985).

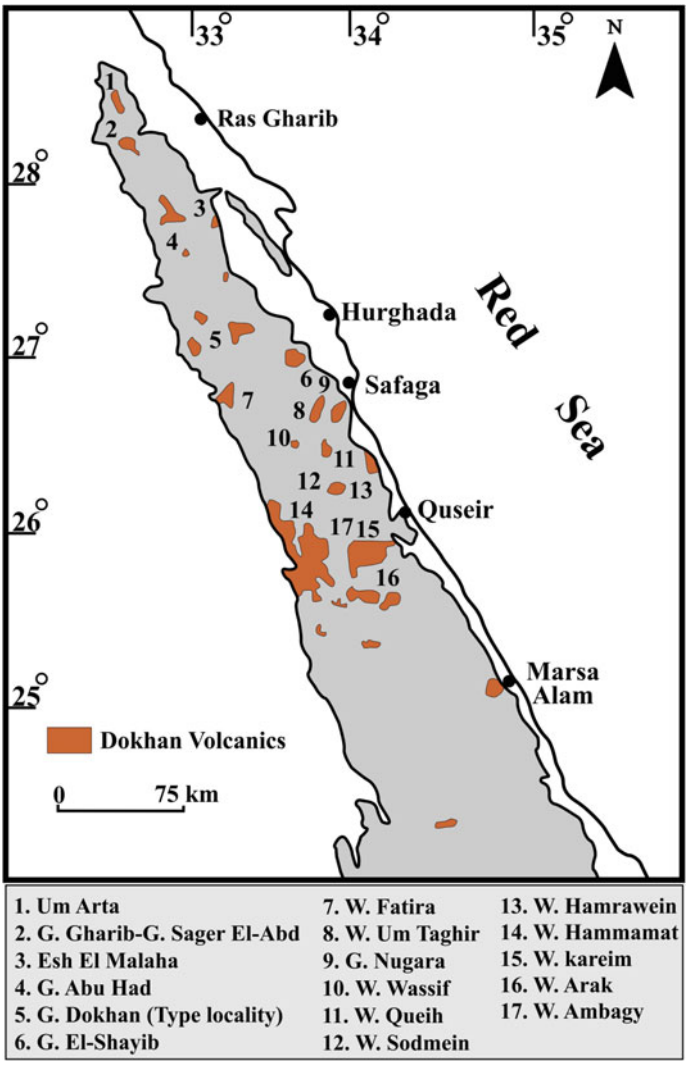

Fig. 6 Distribution of the most famous Dokhan volcanic outcrops in the Eastern Desert of Egypt (El Ramly 1972; Hashad 1980)

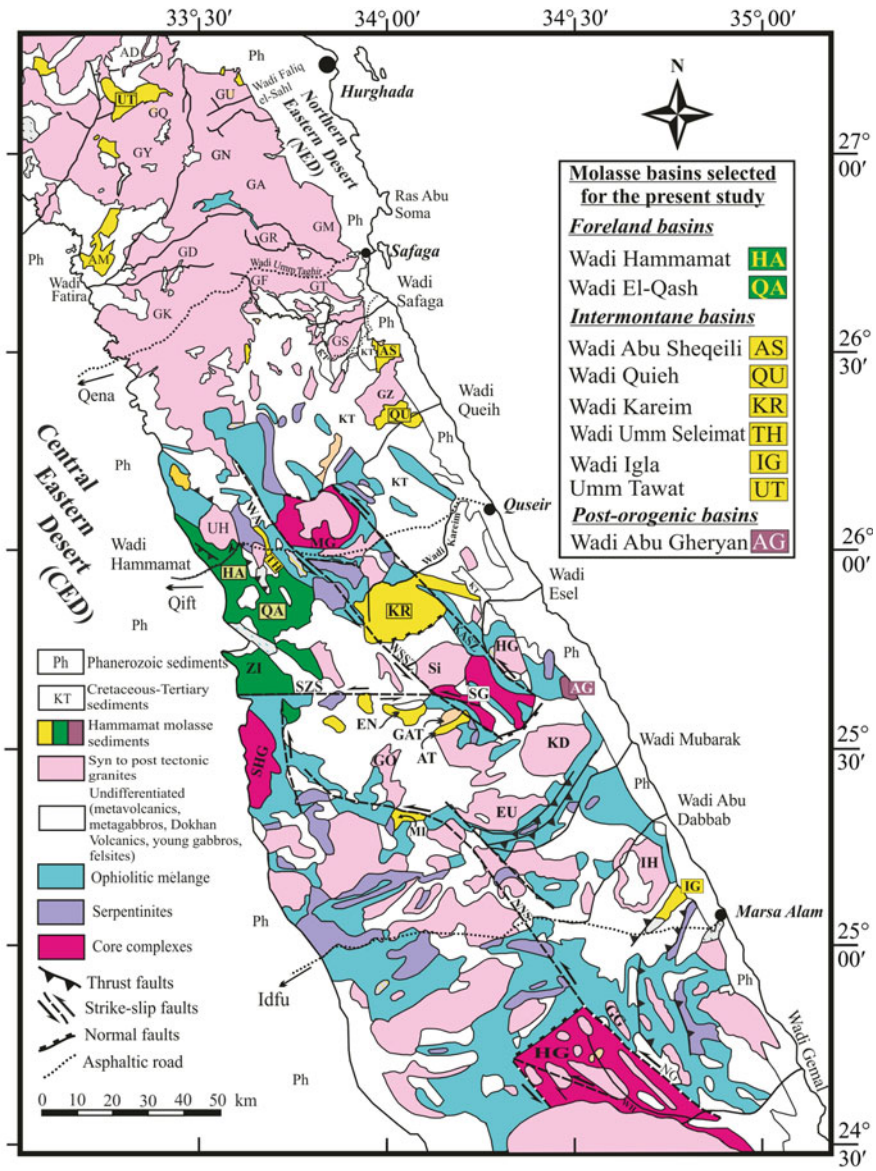

The lower part of the Hammamat sequence comprises red-colored clastics (Igla formation), which passes upward into greenish gray subgraywackes, volcanic arenites, and conglomerate banks representing fanglomerates (El-Gaby et al. 1984). According to Willis et al. (1988), the lower part of the Hammamat sequence comprises polymictic breccia and the upper part comprises sandstone and shale.

◄**Fig. 7** Simplified geological map of the Central and part of the Northern Eastern Desert of Egypt showing distribution of Hammamat molasse basins (after Abd El-Wahed 2010; Compiled from the Geological Map of Egypt (El-Ramly 1972) and the geological map of Quseir (Klitzch et al. 1987). Major structures are after Fritz et al. (1996), Bregar et al. (2002), Shalaby et al. (2005) and Abd El-Wahed 2008). HG, Hafafit Gneiss; WH, Wadi Hafafit; NG, Wadi Nugrus; GG, Gebel (G.) Nugrus; IG, Wadi Igla molasse basin; IH, Igl Al-Ahmar monzogranite, GX, G. Umm Nagat; NNS, Um Nar-Nugrus shear zone; EU, Gebel El-Umra older granite; MI, El-Miyah molasse basin; KD, Kadabora monzogranite pluton; SHG, El Shalul gneisses; AT, Atawi molasse basin; GAT; Gebel Atawi Alkali feldspar granite; EN, Andiya molasse basin; AG, Abu Gheryan molasse basin; Si, Gebel Sibai alkali feldspar granite; SG, Sibai gneisses; WSSZ, Wadi Sitra shear zone; KASZ, Kab Ahmed Shear zone, HG; Homrat Ghaunam alkali feldspar granite; ZI, Wadi Zeidun molasse basin; SZS, Wadi Zeidoun-Wadi El-Shush strike-slip fault; QA, Wadi El-Qash molasse basin; KR, Kareim molasse basin; TH, Um Esh-Um Seleimat molasse basin; HA, Hammamat molasse basin; UH, Um Had granite pluton; WA, Wadi Atalla; MG, Meatiq gneisses; QU, Wadi Quieh molasse basin; AS, Abu Sheqeili molasse basin; GZ, G. Umm Zarabit; GK, G. Kafari; GS, G. Gasus; GD, G. el-Dob; GF, G. Abu Furad; GT, G. Umm Taghir; GR, G. Ras Barud; GM, G. el-Magal; GA, G. Umm Anab; GY, G. Samyuk; GN, G. Shayib el Banat; GQ, G. Qattar; GU, G. Umm Araka; UT, Umm Tawat molasse basin and AD, Gebel Dokhan

They are typically well bedded and commonly overlie the Dokhan volcanics. The Hammamat sequence is largely derived from the erosion of the Dokhan volcanics (El-Gaby et al. 1984). And the sequence in turn is intruded by the syn- to late-orogenic granitoids (younger granites). Alteration is manifested by hematitization, epidotization, and kaolinitization.

Most of the Eastern Desert molasse basins were evolved between 650 and 580 Ma (Fig. 6) in individual basins with different individual tectonic settings (e.g., Shalaby et al. 2006; Abd El-Wahed 2010). Geochemistry revealed that the Hammamat molasse sedimentary rocks were originated from felsic to intermediate igneous sources formed in a continental arc setting.

Abd El-Wahed (2010) concluded that the deformational history of the molasse basins includes two main thrusting events overprinted by an event of sinistral shearing along the Najd Fault System (NFS). The NNW-directed thrusts and the NE-, ENE-, and WSW-trending folds are the structures related to NNW–SSE shortening (650–640 Ma). The SW- and NE-directed thrusts are due to ENE–ESE constriction during oblique convergence and arc accretion around 640–620 Ma. Fritz and Messner (1999) and Abd El-Wahed (2010) classified the Hammamat molasse basins in the Central and part of the Northern Eastern Desert (Fig. 7) into: (i) The foreland basins (e.g., Wadi Hammamat basin, Wadi El-Qash basin); (ii) Intermontane basins (e.g., Wadi Queih basin, Wadi Abu Sheqeili basin, Wadi Kareim basin, Wadi Igla basin, Wadi Um Seleimat basin, Gebel Umm Tawat basin); and (iii) Post-orogenic basins (e.g., Wadi Abu Gheryan basin). The basins which are characterized by prevalence of thrust-related structures include foreland basins (Wadi Hammamat, Wadi El-Qash) and two of the intermontane basins (Wadi Umm Tawat, Wadi Abu Sheqeili basins) (Abd El-Wahed 2010). The other intermontane basins are markedly pull-apart basins characterized by structures related to thrusting overprinted by strike-slip faulting (e.g., Wadi Queih, Wadi Igla, Wadi Um Seleimat). Some basins

exhibit structures developed by the sinistral shearing only (e.g., Wadi Kareim, Wadi Atawi, and Wadi El-Miyah basins) (Abd El-Wahed 2010).

3.6 Granites

The Egyptian granites can exclusively be divided into three major groups: (1) older gray granites and (2) younger pink granites, which include (3) A-type (alkaline/peralkaline) granites; all possibly constitute one granite series from less to more evolved (e.g., El-Ramly and Akaad 1960; El-Gaby 1975; Hussein et al. 1982; Farahat et al. 2004a, 2007; Ali et al. 2013).

(1) The older gray granites (615–820 Ma, Stern and Hedge 1985) comprise ~27% of the cropping out Egyptian basement (Stern 1979). They show a composition ranges from qz-diorite to granodiorite. They are syn- to late-orogenic, subduction-related, and calc-alkalic I-type granitoids (e.g., Rise et al. 1983; Hassan and Hashad 1990; Kroner et al. 1994; Moghazi 2002; El Mahallawi and Ahmed 2012). Hussein et al. (1982) identified these granites as G_1 granites. Most of the older gray granites are pre-collision of arc assemblages (650–580 Ma, Stern 1994) and variably deformed.
(2) The younger pink granites (590–610 Ma, Moussa et al. 2008; Ali et al 2012, and reference therein) comprise ~16% of the cropping out Egyptian basement (Stern 1979). They show a composition ranges from alkali feldspar granite to normal granite (e.g., Ali et al. 2012; El-Bialy and Omar 2015, and references therein). They are late-orogenic, suture related, and highly fractionated calc-alkalic I-type granitoids (e.g., El-Bialy and Omar 2015, and references therein). Hussein et al. (1982) identified these granites as G_2 granites.
(3) The A-type granites (~590–610 Ma, Be'eri-Shlevin et al. 2009a) are recorded in Sinai, North Eastern Desert, and South Eastern Desert, in decreasing order of abundance (e.g., Stern 1979). They show a composition ranges from alkali feldspar granite to syenite (e.g., Gahlan et al. 2016, and references therein). They are alkaline/peralkaline, anorogenic, and within-plate granitoids (e.g., Abdel Rahman and El-Kibbi 2001). Hussein et al. (1982) discriminated these granites as G_3 granites.

A variety of origins have been proposed for the aforementioned granite groups; (a) partial melting of the crust (e.g., Moghazi et al. 2001; Farahat et al. 2011; El Mahallawi and Ahmed 2012) or (b) fractionation of a mantle derived magma (e.g., Finger et al. 2008; Moussa et al. 2008; Ali et al. 2012).

4 Landsat- and ASTER-Based Mapping of the Egyptian Nubian Shield

The Egyptian Arabian–Nubian Shield consists of extensive outcrops of metamorphosed gneissic domes, ophiolitic-related assemblages, island arc metavolcanics, and their volcaniclastic associations together with clastic Molasse-type sediments,

which they intruded by suites of mafic, syn-late to post-tectonic volcanics and granitoids. Remotely sensed processed data including Enhanced Landsat Thematic Mapper (ETM+) and Advanced Spaceborne Thermal Emission Reflection Radiometer (ASTER) have been used by many workers in lithological discrimination and mineral exploration in the Egyptian Nubian Shield (e.g., Kusky and Ramadan 2002; Sadek 2004, 2005; Gad and Kusky 2006; Amer et al. 2010; Sadek and Hassan 2012; Gabr et al. 2015; Abou El-Magd et al. 2013; Asran et al. 2013; Hassan and Ramadan 2014; Hassan et al. 2015; Sadek et al. 2015), where these data were utilized in the geological mapping at various scales and have shown a great success (Qiu et al. 2006; Gaber et al. 2010; Zoheir and Emam 2014 and Kumar et al. 2015). From the lunch of spaceborne multispectral sensors, particularly Landsat (TM and ETM+) in 1982 and 1999 with five and eight spectral channels, respectively, they have been well employed for geological applications (Gad and Kusky 2006). Moreover, the launch of ASTER in December 1999 with three spectral bands in the Visible/near Infrared (VNIR) region, six spectral bands in the Shortwave Infrared (SWIR) region and five spectral bands in the Thermal Infrared (TIR) region with 15, 30 and 90 m spatial resolution has provided a new prospective of investigating the geological materials (Rowan and Mars 2003; Gad and Kusky 2007; Gaber et al. 2010).

Khan et al. (2007) pointed out that the remote sensing data has been used increasingly during the last two decades for mapping, structural analysis, and mineral exploration. There is a wide acceptance that these data conveys useful information for mapping different rock types and their alteration products (Torres-Vera and Prol-Ledesma 2003; Ramadan and Kontny 2004). The recent developments in sensor technology have enabled remote sensing to become an increasingly important tool for mapping lithologies, structures, and ore deposits, particularly for remote areas with little or no access, or areas that lack detailed topographic or geologic base maps (Qaoud 2014). Numerous and success trials for mapping different areas of the Egyptian Nubian shield using Landsat (ETM+) and ASTER were performed by many scientists, especially after the free availability of the Landsat images through the Global Land Cover Facility (GLCF) (www.landcover.org) which authorized by the National Aeronautics and Space Administration (NASA). These studies produced new geologic maps as well as improved pervious geologic maps for these areas, where the resulted maps were verified by the fieldwork, geochemical and pertographical studies.

4.1 Remote Sensing Techniques and Lithological Discrimination

To carry out lithologic mapping and to identify mineral deposits in arid and semi-arid environments, remote sensing data have been analyzed using several digital image processing techniques such as image enhancement, fusion, band

rationing, and principal component transformation (e.g., Sultan et al. 1986; Kusky and Ramadan 2002; Gad and Kusky 2007; Youssef et al. 2009; Madani and Emam 2011; Ali-Bik et al. 2012 and Zoheir and Emam 2012). Thus, the development of the specific remote sensing methods and data is considered as a critical part of geological mapping over the last years. Many scientists have statistically selected

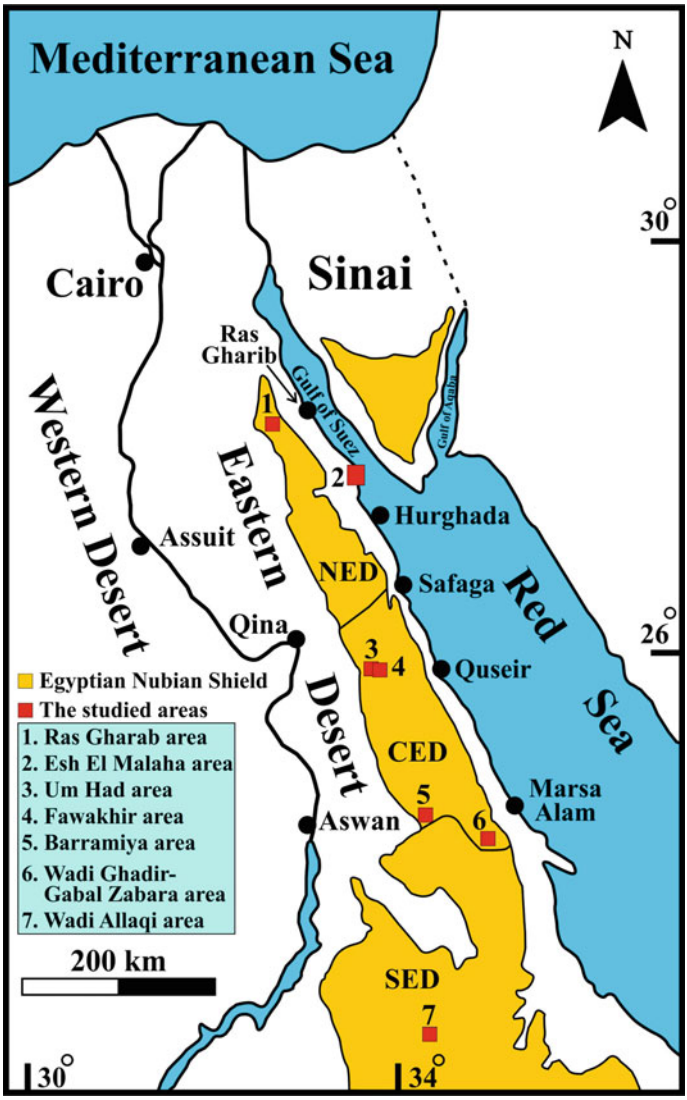

Fig. 8 Location map for seven areas in the Egyptian Nubian shield had been subjected to Landsat and ASTER geological mapping. NED = Northern Eastern Desert, CED = Central Eastern Desert, and SED = Southern Eastern Desert

Landsat TM enhanced false-color composite to map geological terranes with high degree of confidence (Souza Filho and Drury 1997).

Remote sensing techniques usually offer a medium for a successful discrimination and mapping of exposed rocks and associated weathering products (Yenne et al. 2015), providing information that is relevant to maps of bedrock geology (Rowan et al. 2005 and David and Wooil 2012). The reflectance characteristics of individual lithological classes (i.e., rock or soil types) are mainly used as a function of the presence of minerals to be utilized (Yenne et al. 2015). It is essential to note that Landsat bands 4, 5, and 7 are most successfully used to discriminate between major rock types (Rothery 1987) which achieved through several processes.

The enhanced resolutions, high Signal-to-Noise Ratio (SNR), the effective spectral coverage and global data availability makes ASTER more suitable particularly for operational geological applications (Kumar et al. 2015). The three subsystems of ASTER sensor, i.e., VNIR, SWIR, and TIR, has different roles to play in spectroscopy for geological applications such as the VNIR region provides spectral features of transition metals such as iron, SWIR region is very effective for analyzing spectral characteristics of carbonate, hydrate, and hydroxide minerals, and TIR region is effective for characterization of silicates (Clark 1999; Gad and Kusky 2007). The ASTER sensor acquires earth's surface imagery in the VNIR, SWIR, and TIR wavelength regions and has offered a great opportunity of using these data sets for mapping of various lithological units (Aboelkheir et al. 2010; Tangestani et al. 2011), minerals (Salem et al. 2014; Salem and Soliman 2015).

Various image enhancement techniques such as Principle Component Analysis (PCA), Minimum Noise Fraction (MNF), Band Ratios (BRs), Band Combinations (BCs) and Spectral Indices (SIs) as well as image classifications can be used (Gad and Kusky 2006, 2007). The present study offers some of these remote sensing techniques to discriminate the various lithological units in selected areas in the Egyptian Nubian Shield (Fig. 8). Actually, aforementioned image processing techniques will be applied after the needed preprocessing techniques (e.g., geometric, atmospheric, and radiometric corrections) performed to the Landsat and ASTER images.

4.2 False-Color Composites (FCC)

Color composite is an image produced by displaying multiple spectral bands as colors different from the spectral range in which they were taken. This method is commonly used for displaying multiband (multichannel) imagery (Kalelioğlu et al. 2009). This is usually achieved by assigning three of the image bands to the fundamental colors red (R), green (G) and blue (B), the combination of which results in a RGB (false) color composite image. The selected band combination should be the most informative one and has the highest sum of standard deviation and lowest correlation among band pairs. Seleim and Hammed (2016) selected the False-Color Composite (FCC) of RGB 742 of Landsat 8 as the best one to

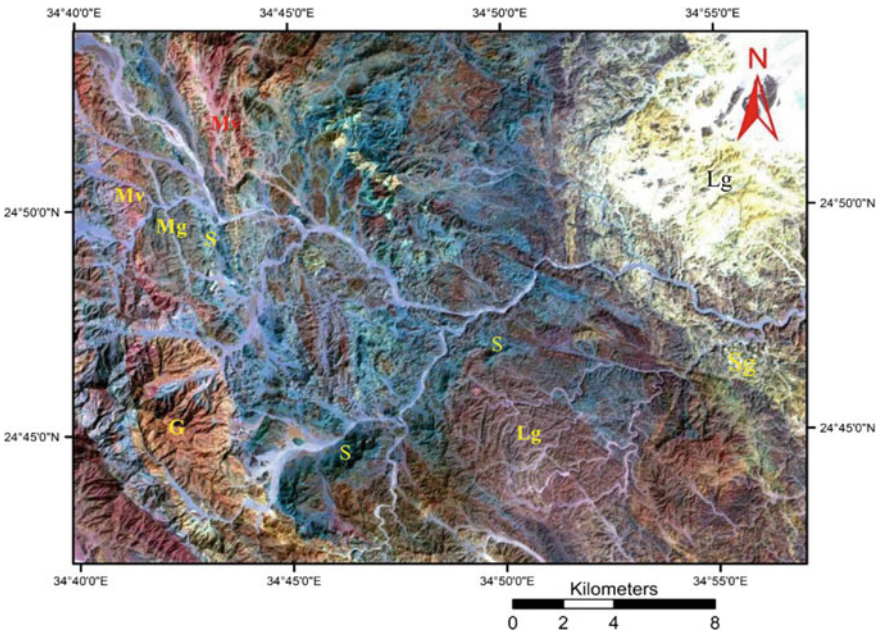

Fig. 9 False-color composite of Landsat 7 (ETM+) image RGB 742 of Wadi Ghadir-Gabal Zabara area at the central Eastern Desert of Egypt (after Kamel et al. 2016). Gneiss (Gn), serpentinites (Sp), metagabbroic (Mgb), metavolcanics (Mv), syn-tectonic granite (Sgr), late-tectonic gabbro (Lgb), and late-tectonic granite (Lgr)

discriminate the rock units in Esh El Malaha area at the North Eastern Desert of Egypt. Where the FCC of RGB 742 of Landsat 7 success to separate the rock types in Wadi Ghadir-Gabal Zabara area and Wadi Allaqi area at the central and southern Eastern Desert of Egypt, respectively (Salem and Soliman 2015; Kamel et al. 2016). Kamel et al. (op. cit) pointed out that the RGB 742 band combination success to discriminate the serpentinites, metavolcanics, metagabbros, and syn- and late-tectonic granites rocks in Wadi Ghadir-Gabal Zabara area obviously (Fig. 9). The FCC RGB 731 of ASTER has the ability to differentiate between granitic rocks and serpentinites at Fawakhir area (Abou El-Maged et al. 2015; Fig. 10) and to discriminate the different rock types in the Barramiya district (Salem et al. 2014) at the central Eastern Desert of Egypt.

4.3 Principal Component Analysis (PCA)

The principal component analysis (PCA) is the image processing technique commonly used for analysis of correlated multidimensional data. It is multivariate statistical method used to compress multispectral data sets by calculating a new

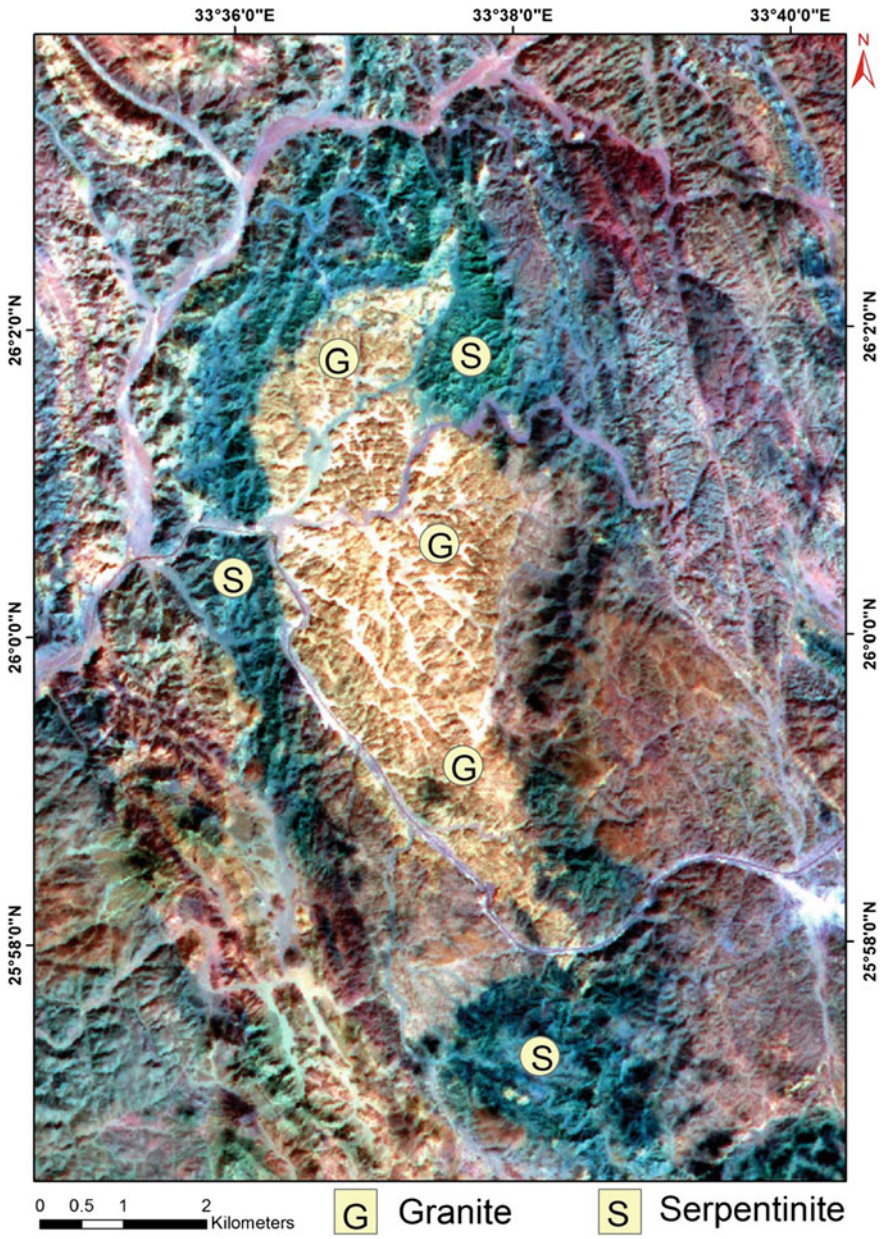

Fig. 10 False-color composite of ASTER image RGB 731 of Fawakhir area at the central Eastern Desert of Egypt (after Abou El-Maged et al. 2015)

coordinate system and redistribute data onto a new set of axes in multidimensional space (Drury 1987; Gupta 1991). This technique has several advantages, where most of the variance in a multispectral data set is compressed into one or two PC images. Moreover, noise may be relegated to the less correlated PC images and the spectral differences between materials may be more apparent in PC images than in individual bands (Sabins 1997). Seleim and Hammed (2016) adopted three PCA RGB combinations of PC2, PC1, PC3; PC5, PC3, PC2 and PC4, PC5, PC2 of Landsat 8 to discriminate the lithologic units in Esh El Malaha area at the North Eastern Desert of Egypt. They success to separate the metavolcanics, Dokhan volcanics, and granitoid rocks as well as sedimentary cover using the fore mentioned PCs images. Where the PCA RGB combination of PC2, PC1, PC4 of Landsat 7 is the good one to differentiate between the different rocks assemblage of Wadi Ghadir-Gabal Zabara area at the central Eastern Desert of Egypt (Kamel et al. 2016). Moreover, Qaoud (2014) recognized the gneisses, serpentinites, Hammamat sediments, and granitoids in Um Had area at the central Eastern Desert of Egypt using PCA RGB combination of PC4, PC2, PC3 of Landsat 7 (Fig. 11). In addition, different PCs combinations of ASTER images played a role to differentiate between

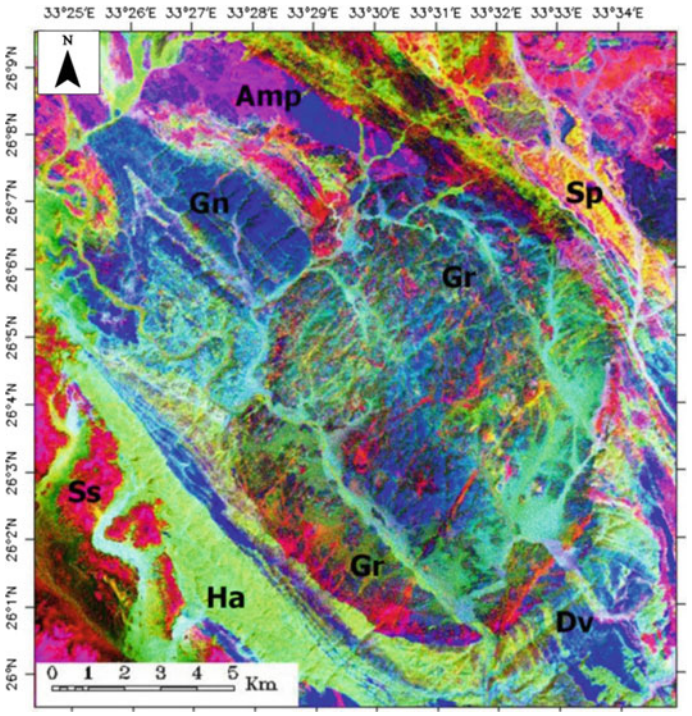

Fig. 11 Landsat (ETM+) PCA RGB combination of PC4, PC2, PC3 of Um Had area at the central Eastern Desert of Egypt (after Qaoud 2014). Hammamat sediments (Ha), Amphibolites (Amp), Gneisses (Gn), and Serpentinites (Sp)

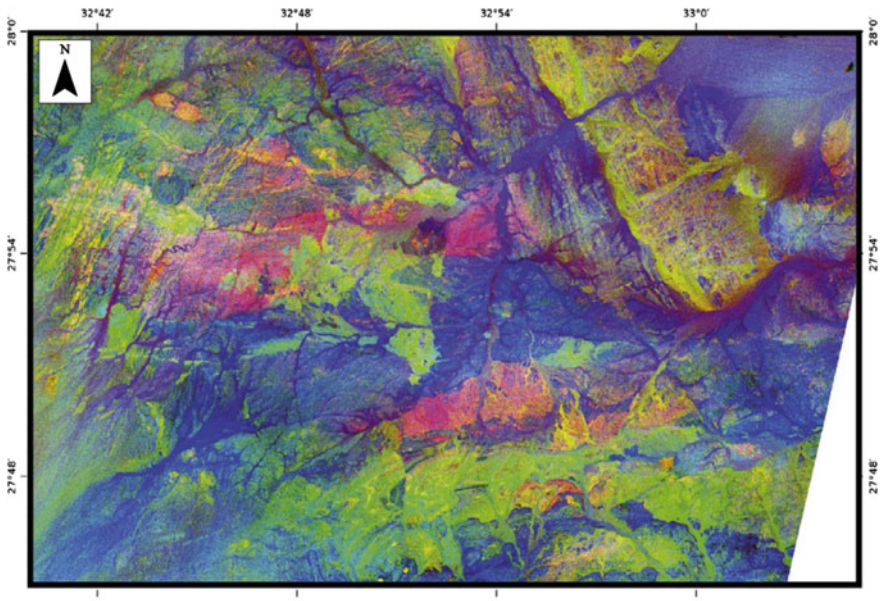

Fig. 12 ASTER PCA RGB combination of PC5, PC7, PC6 of Ras Gharib area at the North Eastern Desert of Egypt (after Jakob et al. 2015)

rock types in different areas of the Eastern Desert of Egypt. Jakob et al. (2015) used PCA RGB combination of PC5, PC7, PC6 to recognize the rock types in Ras Gharib area (Fig. 12) but Salem et al. (2014) adopted PC3, PC4, PC2 PCA RGB combination to differentiate between rock units in the Barramiya district.

4.4 Band Ratioing

The ratio images were prepared simply by dividing the Digital Number (DN) values of each pixel in one band by the DN values of another band (Drury 1993). Band ratio technique enhances the objects based on the differences in reflectivity between the numerator and denominator spectral bands. There are some effective factors controlling the lithological mapping using remote sensing techniques including the increased concentration of minerals relative to the background in the locality and the mineral assemblage characteristics (Frei and Jutz 1990). The main advantage of band ratio images is that they used to reduce the variable effects of illumination condition, thus suppressing of the expression of topography (Crane 1971). Band ratios have been used successfully in lithological mappings for the Arabian–Nubian shield and for other areas worldwide (Gad and Kusky 2006), where the band selection for the different ratio images used is based on the spectral signature of these rocks.

The band ratio transformation of Landsat ETM+ and ASTER data is useful for qualitative detection of hydrothermal alteration minerals (Di Tommaso and Rubinstein 2007), and also has wide acceptance in geological mapping in the Eastern Desert of Egypt (e.g., Qiu et al. 2006; Amer et al. 2010; Aboelkhair et al. 2010; Madani and Emam 2011). For example, Landsat ETM+ band ratios (5/7, 5/1, 5/4 * 3/4) in RGB coloring mode have been used for mapping serpentinites in the Egyptian Nubian Shield (Sultan et al. 1986). They concluded that these band ratios can be used to distinguish serpentinites from the surrounding mafic rocks with high amounts of magnetite and hydroxyl-bearing minerals in arid regions. Gad and Kusky (2006) used the false-color combinations of ETM+ band ratios (5/3, 5/1, 7/5) and (7/5, 5/4, 3/1) for mapping serpentinites in Barramiya area in the central Eastern Desert of Egypt (Fig. 13). They suggested that these band ratios can be used as well as the Sultan et al. (1986) band ratios for mapping serpentinites in the Eastern Desert of Egypt. Kamel et al. (2016) adopted Landsat ETM+ band ratios

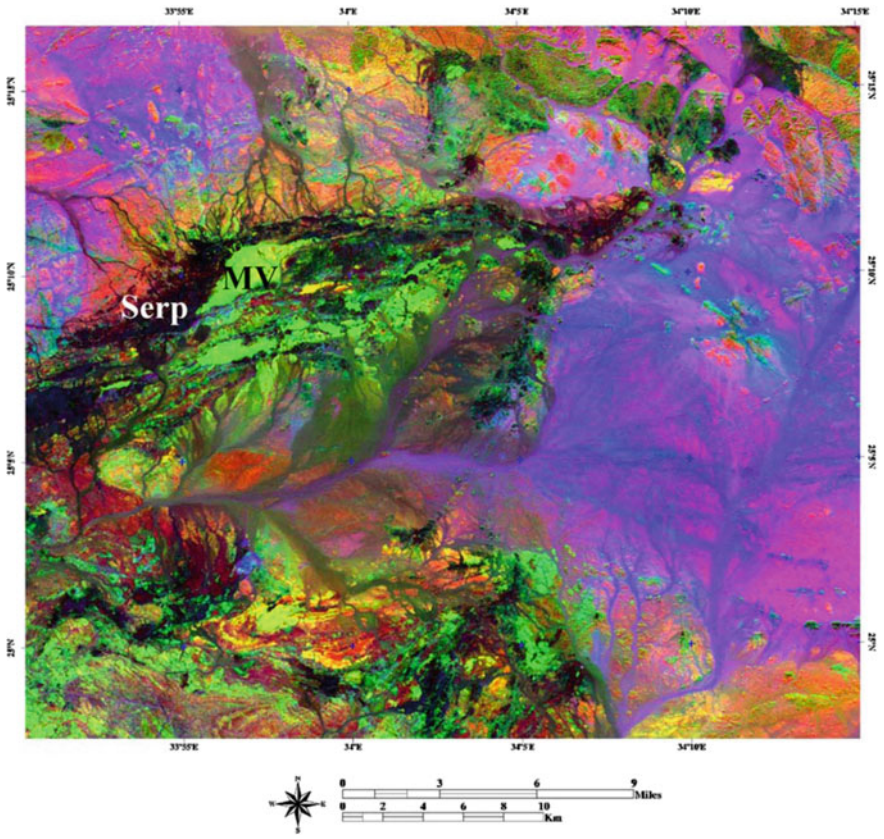

Fig. 13 Landsat TM RGB band ratio image (7/5, 5/4, 3/1) for the Barramiya area at the central Eastern Desert of Egypt (after Gad and Kusky 2006). Serpentinites (Serp) and Metavolcanics (Mv)

(5/1, 3/2, 7/2) and (3/1, 4/2, 5/7) to differentiate serpentinites and granites from their surrounding rocks, respectively. Moreover, Youssef et al. (2009) used the false-color combination of Landsat ETM+ band ratios (5/3, 5/1, 7/5) to discriminate between different granitic phases of the Kadabora granitic intrusion in the central Eastern Desert of Egypt.

Abdeen et al. (2001) used band ratios (4/7, 3/4, 2/1) of ASTER image, which are equivalent to (5/7, 4/5, 3/1) Landsat TM image, also named as Abram's combination, for mapping units of the Neoproterozoic Allaqi Suture of southeast Egypt, mainly serpentinites, marble, and granite. Amer et al. (2010) used ASTER band ratios ((2 + 4)/3, (5 + 7)/6, (7 + 9)/8) to distinguish between ophiolites and granites and for general lithological mapping of arid areas. Zoheir and Emam (2012) found that the band ratio (4/7, 2/4, 6/8) of ASTER images, the most efficient in differentiating all lithologic units and hydrothermally altered zones around Gabal Egat within the Wadi Allaqi region at the southern Eastern Desert (Fig. 14). Moreover, Jakob et al. (2015) considered the band ratios of (7/6, 2/1, 4/6) and (8/6, 2/1, 4/8) of ASTER images produced images of high contrast and good discrimination between different lithological units of Ras Gharib area in the north of the Eastern Desert of Egypt.

4.5 Image Classification Techniques

Classification is the process by which pixels having similar spectral characteristics are consequently assumed to belong to the same class that can be identified and assigned a unique color. The base of image classification is in comparing it to predefined class, which requires definition of the classes and methods for comparison. Definition of the predefined classes is an interactive process and is carried out during the training process or collecting the spectral signature. After the training sample sets have been defined, classification of the image can be carried out by applying a classification algorithm. The choice of a particular algorithm depends on the purpose of the classification, the characteristics of the image and training data. There are two types of image classification can be identified unsupervised and supervised. Where the first one needs a prior knowledge about the study area, but the second one needs to build training areas from the fieldwork or old geologic maps of the study area to use them as a base to classification.

Several workers were produced geological maps for a selected areas at the Egyptian Nubian Shield based on the supervised classification of Landsat (ETM+) and ASTER images with satisfied accuracies. Jakob et al. (2015) differentiated between the rock units in Ras Gharib area using the Support Vector Machine (SVM) algorithm to Landsat and ASTER images and produced a geologic map with overall accuracy 99.81% (Figs. 12 and 15). They prepared geological map shows clear improvements and variations to the earlier version of Breitkreuz et al. (2010) by set up new borders between lithologic units and adding three new rock types to the pervious map. Kamel et al. (2016) performed the maximum likelihood

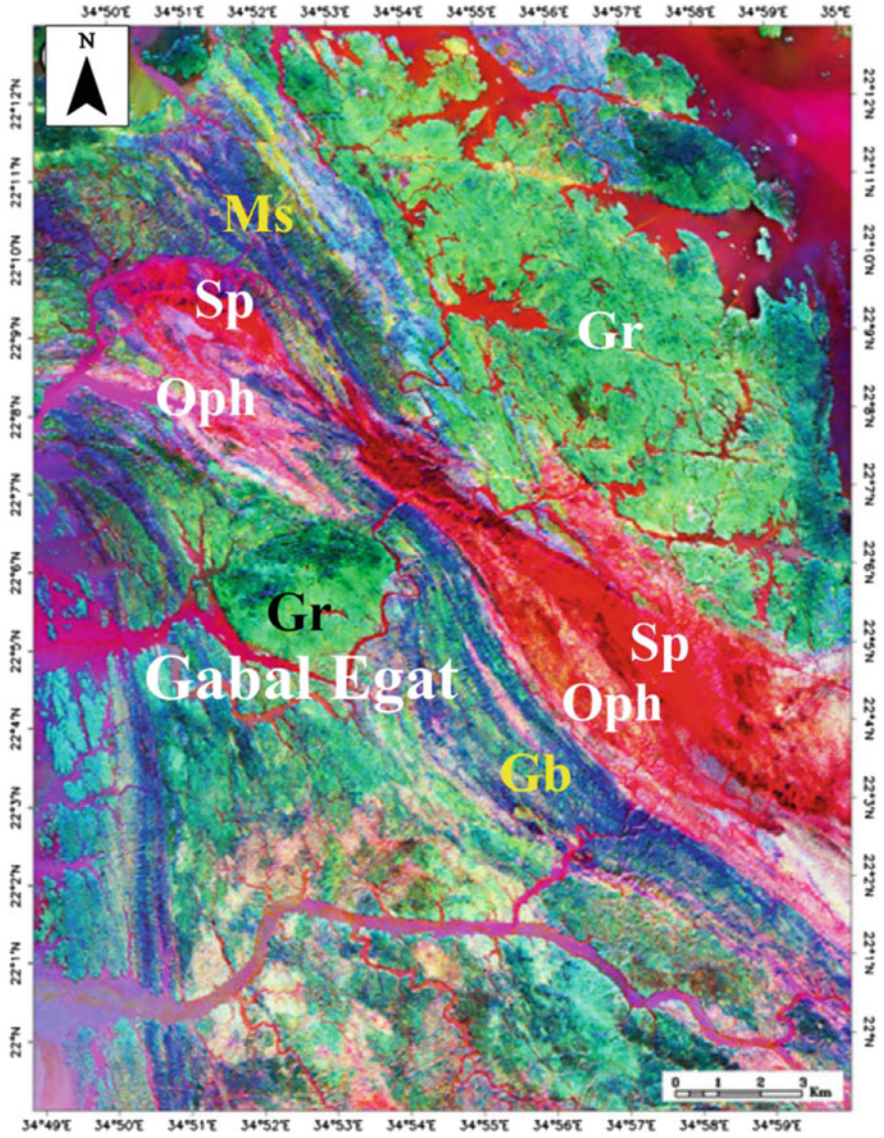

Fig. 14 ASTER RGB band ratio image (4/7, 2/4, 6/8) for Wadi Allaqi region at the South Eastern Desert of Egypt (after Zoheir and Emam 2012). Serpentinites (Sp), Ophiolites (Oph), MetaGabggros (Gb), Metasediments (Ms), and Granites (Gr)

algorithm to Landsat 7 image to discriminate between the different rocks in Wadi Ghadir-Gabal Zabara area at the central Eastern Desert of Egypt. They displayed the defined rock units of granite gneiss, serpentinites, metagabbros, metavolcanics, Melange, and late-tectonic gabbro syn- and late-tectonic granites in a thematic map

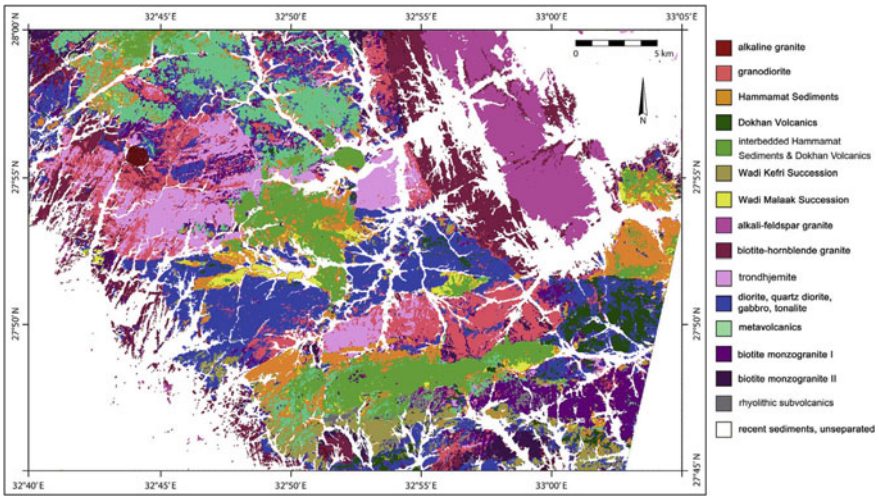

Fig. 15 The classified geologic map of Ras Gharib area, North Eastern Desert, Egypt (after Jakob et al. 2015)

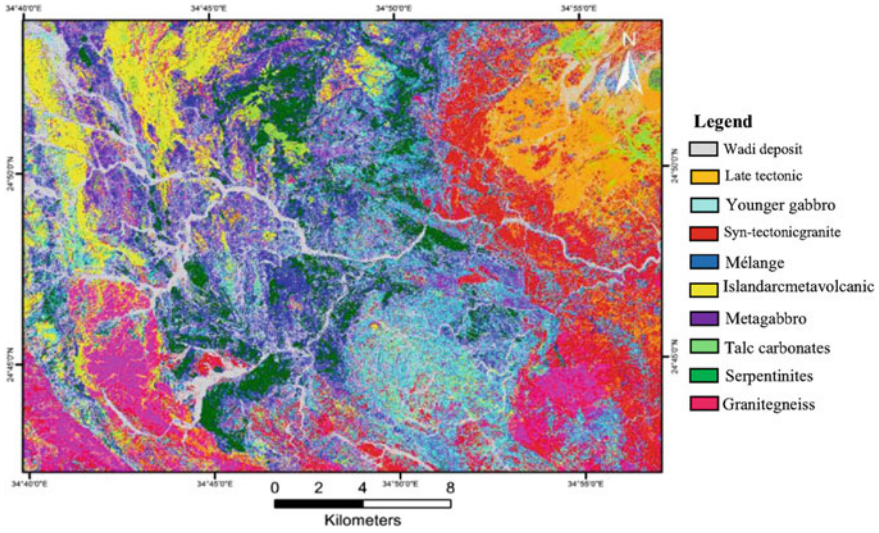

Fig. 16 The classified geologic map of Wadi Ghadir-Gabal Zabara area at the central Eastern Desert of Egypt (after Kamel et al. 2016)

(Fig. 16). Moreover, Seleim and Hammed (2016) produced a new geologic map of Esh El Malaha area at the north of the Eastern Desert of Egypt, with 13 classes using Mahalanobis distance algorithm to Landsat 8 image (Fig. 17). They added that the new lithologic map produced from the remote sensing data shows more

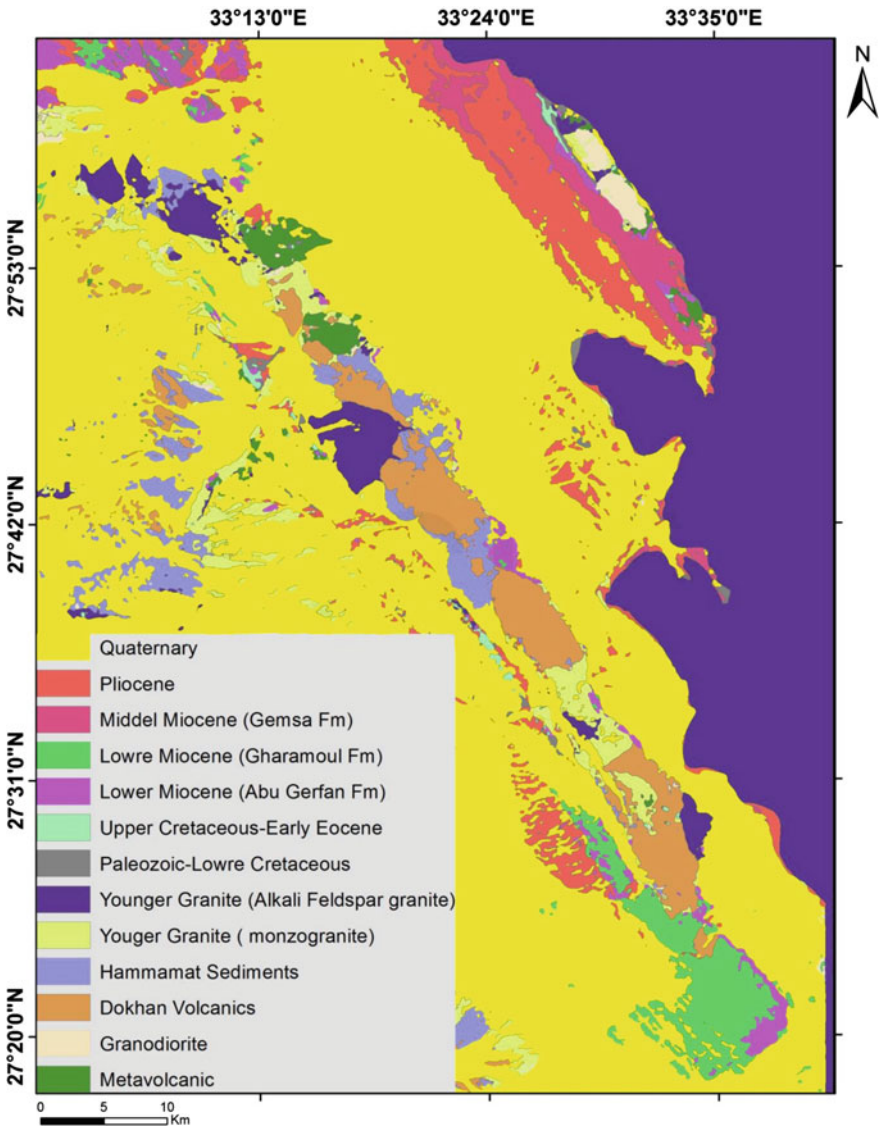

Fig. 17 The classified geologic map of Esh El Malaha area at the North Eastern Desert of Egypt (after Seleim and Hammed 2016)

clear improvement and variations than the previously published maps and can discriminate easily between the granitic rock phases at the north of Gabal El Zeit.

Finally, Landsat and ASTER multispectral remote sensing imagery provides a potentially useful data source that can be used for discriminate between the geological units in the Egyptian Nubian Shield. The processing techniques for these

data enable the rapid and inexpensive mapping of surface geological and mineralogical features, especially in arid regions. Several enhancements of Landsat and ASTER images such as band ratios, false-color composites, and principal component analysis as well as image classification are used and evaluated to obtain new geologic maps or improve the previous geologic ones. Where many studies stated that the maps derived from remote sensing data agree well with the field derived maps and show details unobtainable from conventional ground-based mapping.

5 Structural Succession and Sequence of Tectonic Events

Detailed field investigations of structural fabrics encountered in the Neoproterozoic crystalline basement outcropping in the Egyptian Eastern Desert, along with their overprinting relations, allow us to establish a plausible structural succession comprising three successive deformations ($D_1 \rightarrow D_3$). The D_1 deformation, termed here as Syn-accretion phase, resulted in the formation of syn-accretionary structures and embraces two progressive stages; D_1a and D_1b. Both stages took place at greenschist facies condition as indicated by minerals forming slip lineations and slickenlines. The D_1a was a shortening stage, concurrent with the E–W assembly of Gondwanalands, led to the formation of W- and WSW-propagated thrusts such as those encountered in Wadi Beitan, Allaqi–Heiani Belt (Abdeen and Abdelghaffar 2011), and Wadi Ghadir in the SED (Greiling et al. 1994). W- and WSW-propagation of D_1a-thrusting was responsible for the formation of obvious thrust-related folds, as in Wadi Beitan and Um Shilman areas. The D_1b was a progressive stage, concomitant with the N-directed escape of the entire ANS, and resulted in the formation of N- (to NNW-) propagated thrusts and thrust-propagation folds which are best typified in Wadi El Mayet, Wadi Mubarak, and Wadi El-Umra in the CED (Shalaby et al. 2005; Abd El-Wahed and Kamh 2010). The D_2 deformation, termed here as post-accretion phase, was also a shortening phase, played a noteworthy role in the structural shaping of the basement complex of the Egyptian Eastern Desert. A wide variety of post-accretionary transpressive structures affiliated to this phase, including the sinistral transcurrent shearing along the NNW-directed Najd Shear Corridor (e.g., Nugrus and Atalla Shear Zones), the dextral transcurrent shearing along the NE-directed megashears (e.g., Idfu-Mersa Alam and Qena-Safaga Shear Zones), and the post-accretionary shear zone-related gneiss domes (e.g., Meatiq, Sibai, Shalul, and Hafafit gneiss domes) (Fritz et al. 1996, 2002, 2013; Loizenbauer et al. 2001; Abd El-Wahed 2008, 2014; Abdeen et al. 2014; Abd El-Wahed et al. 2016; Stern 2017). Deposition of the Hammamat Volcano-sedimentary Sequence in fault-controlled down sags and pull aparts occurred during also during the D_2 deformation. The D_3 deformation, was an extensional long-lasting phase, associated the crustal relaxation followed the Gondwana assembly and the subsequent Red Sea rifting since the Oligocene and younger times. Rejuvenation of the preexisting Neoproterozoic fractures and shear zones, as well as rift-related structures are related to this

deformation phase. Also, the ring complexes of the Eastern Desert of Egypt are connected to this phase. These complexes represent the northward continuation of the East African chain of ring complexes, range in age from Cambrian (554 Ma) to Late Cretaceous (89 Ma), and include a wide variety of rock types, ranging from basic to acidic and from undersaturated to quartz-bearing (El-Ramly and Hussein 1983). However, the previously mentioned structures will be dealt with in a way or another in the following sessions.

6 Thrusting and Thrust Duplex System

The Eastern Desert of Egypt, the northwestern part of the Arabian–Nubian Shield, has experienced a polyphase deformation history involving many successive events. The oldest deformation event (D_1) in the Eastern Desert is recorded in its southern part, where fold-thrust belts prevail and thrusts are the first-order kinematic later overprinted by map-scale transpression. The Southern Eastern Desert in general seems to generally represent a deeper level of exposure than the Central Eastern Desert and is less affected by Najd shearing. The major structures in the south are manifested by accretion-induced sutures developed at ca. 750–720 Ma. $D_{1a,\ b}$ is represented by NNW or SSW direction of thrust transport in the Allaqi–Heiani shear zone (Abdeen and Abdelghaffar 2011). The Allaqi–Heiani Shear Zone (Figs. 18 and 19) involves an early N–S shortening followed by a late E–W shortening. The N–S shortening is associated with accretion and obduction of the South Eastern Desert island arc rocks over the Gabgaba island arc rocks to its south (Abdeen and Abdelghaffar 2011). The late E–W shortening is associated with a post-accretion phase probably related to the latest stage of the Pan-African orogen or to the Najd orogen (Abdeen and Abdelghaffar 2011).

The tectonic evolution of the Allaqi–Heiani shear zone is characterized by a polyphase deformation history involving, at least, two phases of deformation (Abdeen and Abdelghaffar 2011). D_1 phase involves N–S to NNE–SSW shortening due to collision between the South Eastern Desert (Aswan) terrane and the Gabgaba terrane (Figs. 18 and 19) between ca. 800 and 700 Ma (Kröner et al. 1992). D_1 structures include WNW–ESE trending imbricate thrust sheets dipping gently toward the NNE indicating a nappe transport toward SW, megascopic, and mesoscopic folds verging to SSW, shear foliations along thrust planes, and SSW plunging stretching lineation. The ENE–WSW collision led to the formation of D_2 structures including NNW–SSE-oriented folds and reactivation of older thrust faults as D_2 transpressional shear zones.

Fold-related faults are dominant in the Central Eastern Desert and are commonly associated with pull-apart basins linked to Najd System (Hamimi et al. 2015b). The most recent subdivision of deformation events in the Central Eastern Desert (Makroum 2001; Fritz et al. 1996, 2002; Loizenbauer et al. 2001; Shalaby et al. 2005; Abd El-Wahed 2008, 2014; Abd El-Wahed and Kamh 2010; Abdeen et al. 2014; Hamimi et al. 2015b; Abd El-Wahed et al. 2016) arranged as follows: (1) D_1

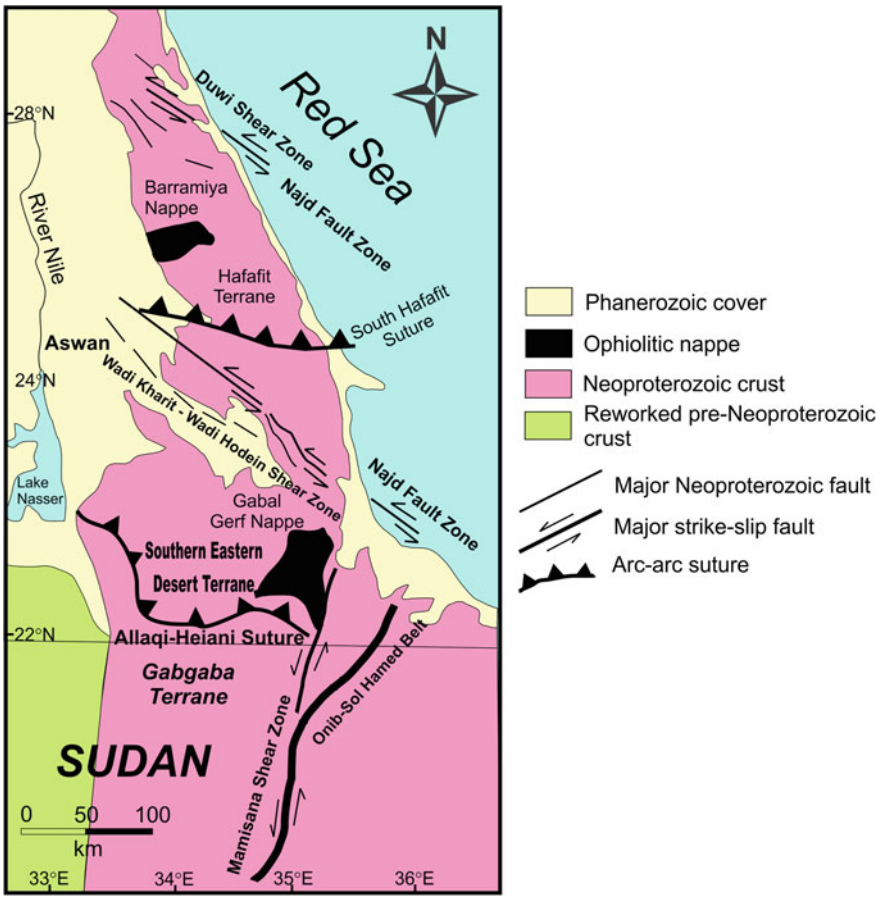

Fig. 18 Simplified tectonic sketch map showing location of the Allaqi–Heiani and the South Hafafit sutures (after Greiling et al. 1994; Abdeen and Abdelghaffar 2011)

linked to NNW- and WSW-propagated thrusts. D_1 deformation took place at greenschist facies conditions (Neumayr et al. 1998) and related to the Pan-African deformation associated with oblique convergence of the arc and back-arc assemblage onto the Nile craton around 620–640 Ma (Fritz et al. 1996) (3) D_{2a} attributed to sinistral movement along the NW-trending shear zones of the Najd Fault System (Fig. 19). (4) D_{2b} associated with dextral movement along NE-trending shear zones. D_2 is linked to the formation of crustal-scale northwest–southeast sinistral shear zones of the Najd Fault System (Stern 1985) followed by exhumation of core complexes within orogen-parallel extension around 620–580 Ma. D_3 deformation occurred much later and may be related to brittle deformation associated with the Red Sea rifting.

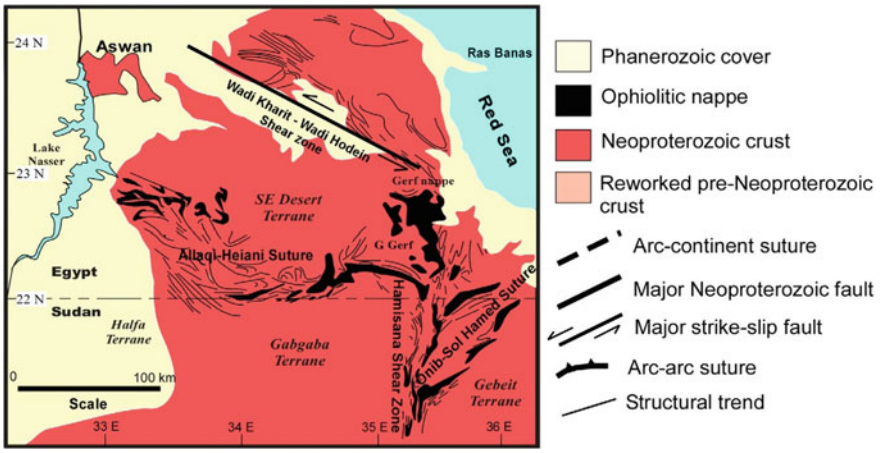

Fig. 19 Simplified tectonic sketch map showing the location of the Allaqi–Heiani–Gerf–Onib–Sol Hamed suture and the Hamisana Shear Zone (after Abdeen and Abdelghaffar 2011)

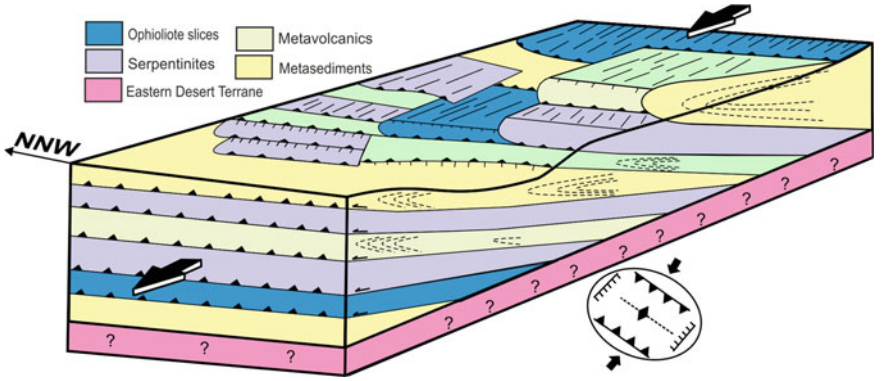

Fig. 20 Early NNW–SSE shortening associated with accretion of relict island arcs and thrusting of ophiolites over old continent (680–660 Ma)

The early NNW–SSE shortening event (D_1) is related to oblique island arc accretion (740–680 Ma) and characterized by stacking and imbrications of Pan-African nappe from SSW to NNW (Fig. 20). NNW–SSE shortening is documented by top-to-NNW large-scale thrusting and folding, distributed over the Eastern Desert of Egypt (Greiling et al. 1994; Abd El-Wahed 2014; Abdeen et al. 2014). A regional nappe transport toward the NW is documented in the Central Eastern Desert from Meatiq, Sibai, Hafafit core complexes (Greiling 1997; Fritz et al. 1996; Loizenbauer et al. 2001; Abd El-Wahed 2008) and from Wadi Mubarak belt (Shalaby et al. 2005; Abd El-Wahed and Kamh 2010). The structure associated with these events includes imbricated shear zones (Fig. 21) forming thrust duplex

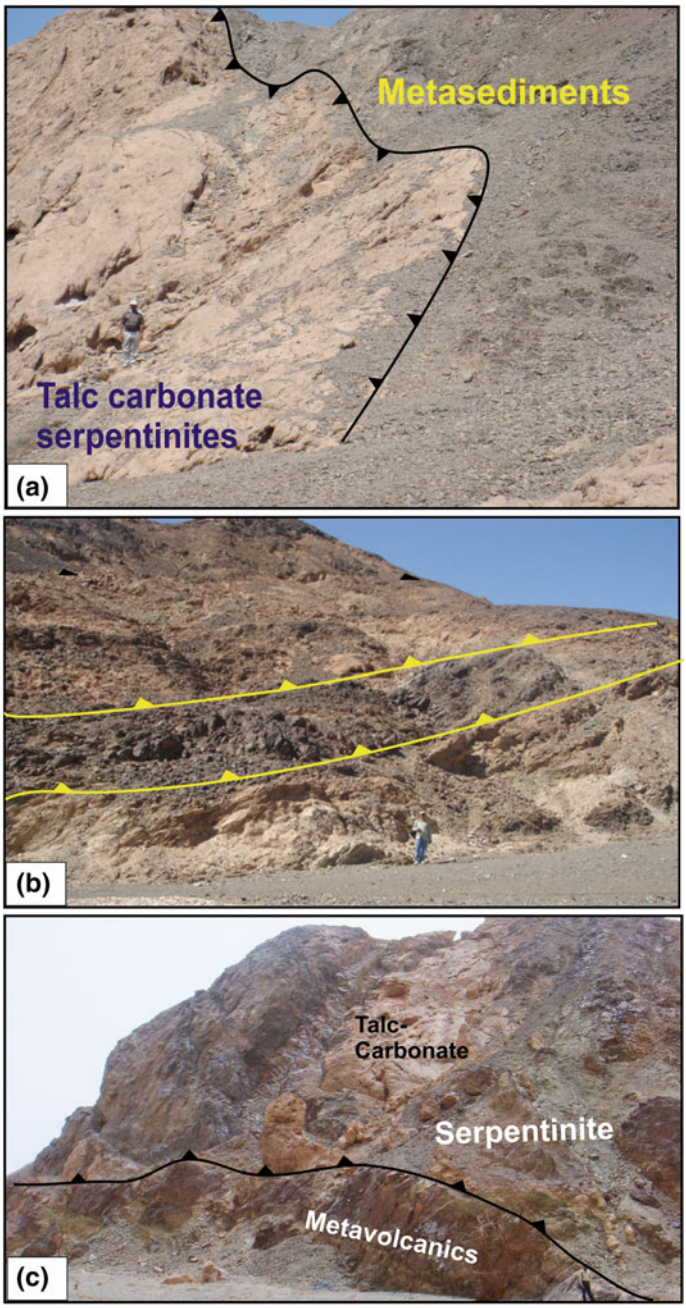

Fig. 21 Example of imbricate thrusts from the Central Eastern Desert of Egypt **a** imbricate thrusts between talc-carbonate serpentinites and volcaniclastic metasediments, looking WSW (After Abd El-Wahed and Kamh 2010); **b** imbricate thrusts between serpentinites and talc–carbonate pods, Wadi Barramiya, looking NW; and **c** EW-oriented imbricate thrusts along Wadi Dungash

structures (e.g., thrust duplexes and the ramp which formed the summit of Gabel El Mayet, Shalaby et al. 2005), E- and NE-trending bedding and fracture cleavage, NE- and ENE-trending map-scale, and mesoscopic folds.

The Northern Eastern Desert is very different than either the Central the Southern Eastern Deserts. Gneisses, ophiolites, and Najd deformation are absent. Faults and joint systems are dominant, and thrusts where observed are attenuated as most of the sector is masked by younger granitoid intrusions. Brittle deformation in the northern sector is evidently late. The nature and overprinting relationships between the pervasive structures at all scales in the Northern Eastern Desert point toward structural younging toward the north (Stern 2017).

7 Suture Zones

7.1 Allaqi–Heiani Suture

Allaqi–Heiani zone represents the most obvious structural feature in the extreme SED of Egypt (Figs. 1, 18, 19 and 22). This zone was described for the first time by Taylor et al. (1993) and has been mentioned in numerous studies later on (e.g., Greiling et al. 1994; EGSMA 1996; El-Kazzaz and Hamimi 1999; Hamimi and El-Kazzaz 2000). It extends over 200 km (average width ≈ 3 km) from Gabal Um Shilman and probably to Nasser Lake in the west to the NNE-trending Hamisana Shear Zone in the east. It could be traced easily on the satellite imagery and aerial photomosaics (scale 1:50.000) covering Gabgaba-Elba Topographic Sheets (scale 1:250.000). The strike of this zone is remarkably variable from E–W, NW–SE and N–S. Such strike variation makes it to be perpendicular to the main Wadi Allaqi to the west and align the southern flank of the same wadi to the east, where it is apparently cut by the NE-oriented Hamisana Shear Zone (Greiling et al. 1994). Kusky and Ramadan (2002) carried out integrated remote sensing and field work to distinguish exposed lithologic units, and to investigate overprinting relations between geologic structures along Allaqi–Heiani zone in the vicinity of Gabal Um Shilman. They considered the zone as an arc/arc collision suture zone (750–720 Ma) formed when the Gerf terrane (Eastern Desert or Aswan terrane) in the north overrode the Gabgaba terrane in the south, prior to the closure of the Mozambique Ocean (830–720 Ma). In this context, Abdelsalam and Stern (1996) proposed four Neoproterozoic deformations ($D_1 \rightarrow D_4$) for the development of the Allaqi–Heiani suture zone. D_1 and D_2 are associated with early collisional stages between the Gerf terrane in the north and Haya and Gabgaba terranes in the south, whereas D_3 and D_4 are associated with later stages of collision. Abdelsalam et al. (2003) believed that the Neoproterozic Allaqi–Heiani suture is the western extension of the Allaqi–Heiani–Onib–Sol Hamed–Yanbu suture (Fig. 22) that represents one of arc–arc sutures in the Arabian–Nubian Shield. From the authors opinion, this suture is worthy to understand Neoproterozoic evolution of the Arabian–Nubian Shield because: (1) It is the northernmost linear ophiolitic belt that defines an

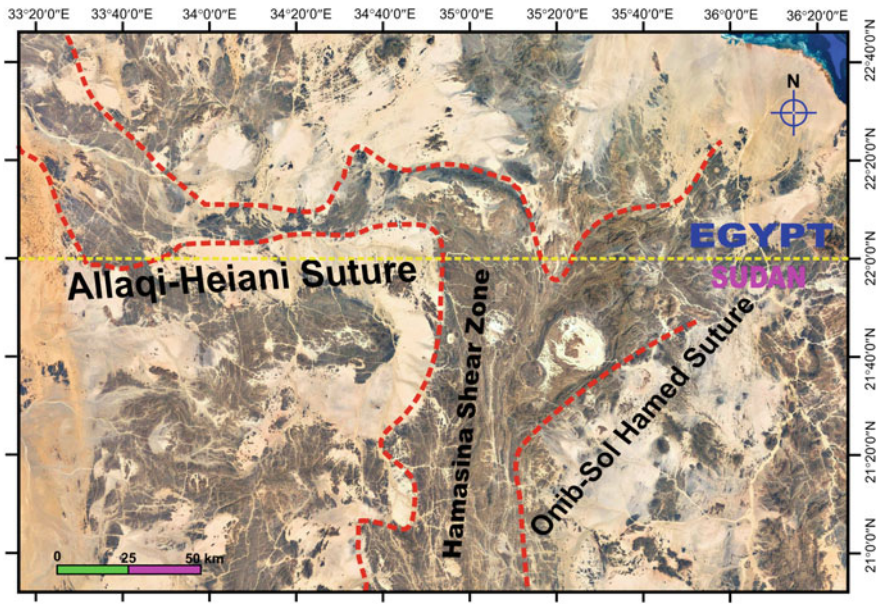

Fig. 22 ETM+ false-color image combination of bands 7, 4, 2 in (RGB) showing the Allaqi–Heiani and Onib–Sol Hamed suture zones

arc–arc suture in the Arabian–Nubian Shield (Kröner et al. 1987a; Stern 1994; Abdelsalam and Stern 1996); (2) It is the only suture in the ANS where a complete ophiolite is preserved at Gabal Gerf (Zimmer et al. 1995); (3) The suture extends in a general east-west direction and its western end is at a high angle to the proposed N-trending, western margin of the ANS; and (4) Recent tectonic models have resulted in conflicting views about the continuity of the Allaqi–Heiani suture, its structural style, and the overall tectonic transport direction involved. The authors concluded that the Allaqi–Heiani Suture is an E–W to NW–SE trending fold/thrust belt forming three allochthons and one autochthonous block. Such conclusion is inconsistent with that given by El-Kazzaz and Taylor (2000) who used facing direction and folded thrust patterns to demonstrate north-verging and top-to-north transport direction. The Allaqi–Heiani suture zone shows sinistral sense of shear indicated by shear band mylonitic foliation, mineral and mica fish, and S-C fabrics. Progressive shearing produced a complex history of folding with development of planar and nonplanar refolded sheath folds.

Abdeen and Abdelghaffar (2011) subdivided the Allaqi–Heiani belt into three structural domains. The western domain (I) is characterized by NNE dipping thrusts and SSW-vergent folds. The central domain (II) includes upright tight to isoclinal NNW–SSE-oriented folds and transpressional faults. The eastern domain (III) shows NNW–SSE-oriented open folds. Structural analysis indicates that the area has a polyphase deformation history involving at least two events. Event D_1 was an N–S to NNE–SSW regional shortening generating the SSW-verging folds

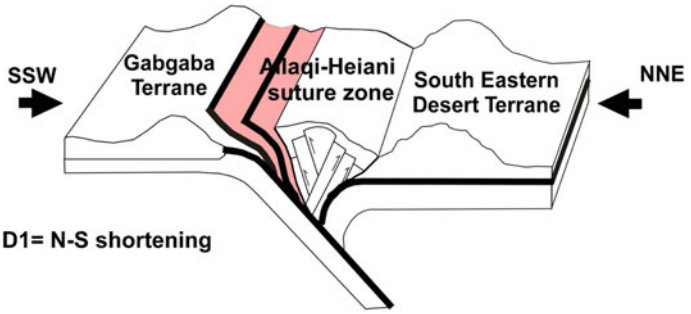

Fig. 23 Schematic sketch showing the tectonic evolution of the central Allaqi–Heiani suture zone during the Neoproterozoic East African Orogen. D1 phase showing the results of the N–S compression between the South Eastern Desert terrane and the Gabgaba terrane (after Abdeen and Abdelghaffar 2011)

and the NNE dipping thrusts (Fig. 23). Event D_2 was an ENE–WSW shortening producing NNW–SSE-oriented folds in the central and eastern parts of the study area and reactivating older thrusts with oblique-slip reverse fault movement.

7.2 South Hafafit Suture (?)

Suture is simply an ophiolite-decorated shear zone defining closure of ocean or back-arc basin. In orogenic belts, indications for suturing are multiple but the most significant at all is the distribution of ophiolitic serpentinites in a linear pattern. In the Eastern Desert of Egypt, the complete ophiolite sequence was described for the first time by El-Sharkawi and El-Bayoumi (1979) in Wadi Ghadir area. Since that time, the ophiolitic affinity of the Egyptian serpentinites has been the subject matter of detailed discussion. Some workers (e.g., Akaad 1997; Akaad and Abu El Ela 2002) raised doubt about the ophiolitic nature and tend to consider these suites as intruded magams. However, a number of criteria demonstrate the tectonic obduction of the Egyptian serpentinites in convergent zone. Enigmatic point, from our opinions, do all serpentinites suites could be considered as suture zone? Greiling et al. (1994) introduced the term South Hafafit Suture to the south of the Wadi Hafafit island arc terrane (Fig. 18), which juxtaposes Hafafit terrane to the north and Aswan terrane to the south. They believed that such suture restores for a lateral transport distance of at least 300 km to the SE to form the eastward continuation of the previously mentioned Allaqi–Heiani suture zone. The Aswan terrane is considered to be the equivalent and westward continuation of the Hafafit terrane, and the terrane to the south of the South Hafafit suture, is regarded to extend as far south as the Onib–Sol Hamed Belt, is an equivalent of the Gabgaba terrane. Nevertheless, such restoration needs to be confirmed elsewhere in the CED and SED of Egypt.

8 Major Shear Zones in the Egyptian Eastern Desert

Shear zones (high-strain zones) are known to form important mechanical weaknesses that affect the rheology of the continental lithosphere and its kinematic response of deformation (Bulter et al. 1995). They are the deep counterpart or extension of faults, where both are strain localization structures, both involve displacement parallel to the walls, and both tend to grow in width and length during displacement accumulation (Fossen 2010). These zones play the noteworthy roles as deformation-buffer zones in the upper and lower crust of continents and island arcs, accommodating the crustal thinning (extension) and thickening (shortening) (Coward 1990). The accommodation patterns of crustal thinning and thickening depend on the preexisting anisotropy (geometry of preexisting fracture zones), spatial variation in temperature and spatial distribution of the various rock materials with various mechanical properties, and stress state and its variation in time and space (Sakakibara 1995). Based on ductility, shear zones are subdivided into brittle, brittle–ductile (semi-brittle), ductile–brittle and ductile shear zones, and based on deformation mechanism they are discriminated into brittle/frictional or plastic shear zones. In brittle shear zones, the deformation is localized in a narrow fracture surface separating the wall rocks, whereas in ductile shear zones the deformation is spread out through a wider zone, the deformation state varying continuously from wall to wall (Ramsay and Huber 1987). In the last decades, a large number of studies have been focused on kinematic analysis of shear zones, such as the sense of shear (e.g., Hanmer and Passchier 1991; Hippertt 1993; Greiling et al. 1994; Doblas et al. 1997; Greiling 1997; Hamimi 1999; de Wall et al. 2001; Abdelsalam et al. 2003; Hamimi et al. 2012a, b), non-coaxiality or kinematic vorticity number (e.g., Ratchbacher et al. 1991; Ishii 1992; Hamimi et al. 2015a), finite strain value and its direction (e.g., Hudleston 1983; Treagus 1983), three dimensional shape and finite strain (*k*-value) (e.g., Gapais et al. 1987) and its strain path (e.g., Lacassin and Van Den Driesshce 1983; El-Kazzaz and Taylor 2000).

In the Eastern Desert of Egypt, the shear zones are the most prominent tectonic features that playing a major role in the structural shaping of the Neoproterozoic Pan-African belt. They have given much more attention since the work of El-Gaby (1983) who considered Qena-Safaga Zone as a conspicuous right-lateral shear zone juxtaposes remobilized older continental crust and infolded, locally metamorphosed, Dokhan Volcanics and molasses Hammamat Sediments to the north, and ophiolites, island arc metavolcanics, and metavolcaniclastics to the south. Further studies investigated and referred to megashear zones in Eastern Desert include: Dixon et al. (1987), El-Gaby et al. (1988), Sultan et al. (1988), Greiling et al. (1994), Abdelsalam and Stern (1996), El-Kalioubi and Osman (1996), Fritz et al. (1996), Abdel Khalek et al. (1999), Hamimi and El-Kazzaz (2000), Wallbrecher et al. (1999), El-Kazzaz and Taylor (2000), Fowler and El-Kalioubi (2002), Shalaby et al. (2005), Fowler and Osman (2009), Abd El-Wahed (2008, 2014) Abd El-Wahed and Kamh (2010), Abdeen et al. (2014), Hamimi et al. (2015b), Abd El-Wahed et al. (2016) and Stern (2017). However, the eye-catching shear trend in

the Eastern Desert is the NW- (to NNW-) trend. This trend is typified by Wadi Kharit–Wadi Hodein, Nugrus, and Atallah Shear Zones. Other obvious shear zones are NE-, ENE-, N- to NNE-oriented, such as Qena-Safaga, Idfu-Mersa Alam, and Hamisana Shear Zones. The N- to NNE-oriented shear trend is less pronounced compared to the other trends.

8.1 Wadi Kharit–Wadi Hodein Shear Zone

Wadi Kharit–Wadi Hodein Shear Zone (≈186 km long) is a distinctive high angle NW-oriented transcurrent shear zone (Figs. 1 and 18) in the SED of Egypt exhibiting sinistral sense of shear confirmed by various kinematic indicators such as veins, deflected markers, S-C structures, microscale foliations, porphyroclasts, mica fish and mineral fish. Opinions differ about the tectonic affinity of this shear zone, where some workers (e.g., El-Gaby et al. 1988; Stern et al. 1990) proved that it is a Najd-related shear system (analog of the 655–540 Ma, Najd Fault System in the Egyptian Eastern Desert), others (e.g., Fritz et al. 1996; Fowler and El Kalioubi 2004) considered it as a youngest major structural element in the Egyptian Eastern Desert, or even a transpressional corridor (Greiling et al. 1994; Nano et al. 2002). Ramadan and Kontny (2004) reported gold mineralization in listvenite-type wall-rock alteration at Gabal El-Anbat in the vicinity of this shear zone. Greiling et al. (1994) supposed that the Wadi Kharit–Wadi Hodein Shear Zone has connected the —perhaps once continuous—previously mentioned Allaqi and South Hafafit sutures (before being overprinted by the Hamisana Shear). Hamimi et al. (2016) reported a dextral sense of shear along the main Wadi Kharit overprinting the main sinistral shearing, which may demonstrate switching in tectonic regime from sinistral to dextral along the Najd Shear Corridor in the Egyptian Eastern Desert.

8.2 Nugrus Shear Zone

Nugrus Shear Zone (Fig. 24) is a NW-oriented high-strain zone reaching up to 750 m in maximum width, and constitutes the boundary between Wadi Ghadir area (East) and Hafafit Core Complex (West). It is steeply dipping toward the NE direction and separates hanging wall low-grade ophiolitic metaultramafic nappes and volcanogenic metasediments from Migif-Hafafit high-grade gneisses in its footwall.

Geochronologically, the data suggests that the emplacement of low-grade nappes above gneisses occurred at around 680 Ma. The timing of the Nugrus Shear Zone shearing is a distinctly younger shearing event at around 600 Ma (Fowler and Osman 2009). This corroborates the conclusion by (Greiling et al. 1994) that extensional collapse in the region began at about 600 Ma, and accelerated during the period 595–575 Ma. Greiling (1985) stated that Nugrus Shear Zone age is

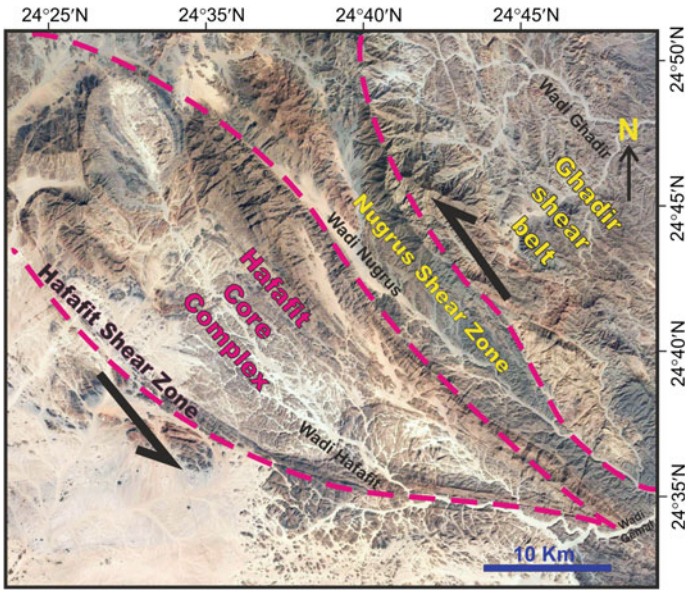

Fig. 24 ETM+ false-color image showing Hafafit Core Complex and Nugrus shear zone

bracketed between 680 Ma (the age of sheared trondhjemite) to 595 Ma (age of post-tectonic granite). Relatively, Mohamed (1993) mentioned the activity time on the Nugrus shear zone was bracketed between the intrusion of the older granitoids and the younger granitoids. Rb/Sr whole rock ages of 610 ± 20 Ma and 594 ± 12 Ma for leucogranites intruded into the schists bordering the Sha'it-Nugrus Shear Zone was given by (Moghazi et al. 2004).

A wide variety of structures are recorded along strike of the shear zone including mylonitic foliation, shear bands, S-C foliations and deformed objects with monoclinic symmetry (Fig. 24). These structures reflect the sinistral sense of shearing which is also confirmed under the microscope by sigmoidal structure and mineral fish. These structures overprint arc collision-related nappe structures (≈680 Ma) and are therefore post-arc collision (Fowler and Osman 2009). The structural architecture of Wadi Nugrus was and still is a matter of debate. It was interpreted in terms of (a) thrust duplexes (Greiling et al. 1988; El-Ramly et al. 1993), (b) Najd-related Shear Zone with sinistral sense of shear (Fritz et al. 1996; Makroum 2003; Abd El-Wahed et al. 2016), and (c) as part of a northerly dipping Sha'it–Nugrus shear zone which is a post-arc collision low-angle normal ductile shear zone separating CED from SED (Fowler and Osman 2009). The steep NE dip of shear-related schistosity and low-pitching slip lineations along Wadi Nugrus are due to NW–SE folding of the Sha'it–Nugrus shear zone, and do not indicate a sinistral strike-slip shear zone (Fowler and Osman 2009).

The footwall of NSZ is Migif-Hafafit gneisses deemed to be of high-temperature–low-pressure amphibolite facies (El-Ramly et al. 1984, 1993).

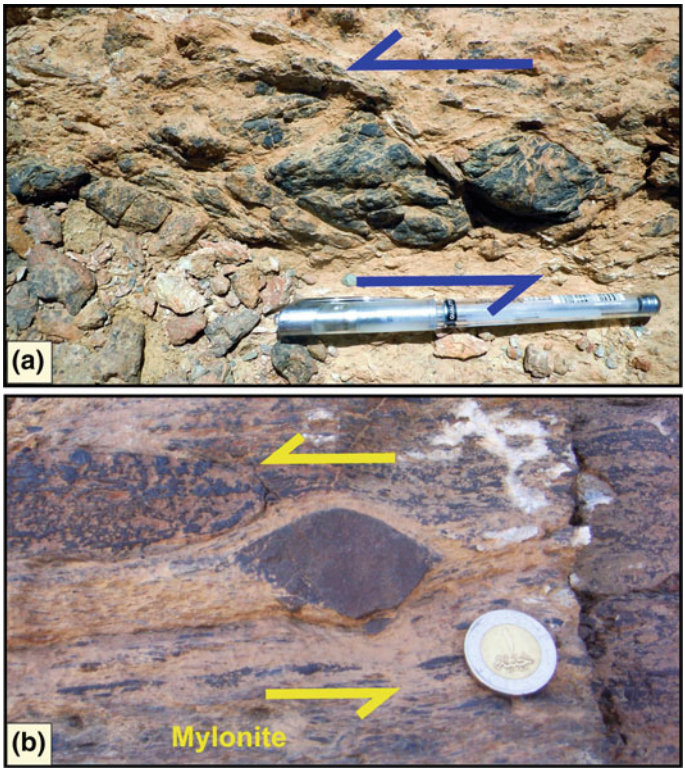

Fig. 25 σ-type serpentinite porphyroclasts indicating sinistral sense of shear, northern part of Nugrus shear zone

Numerically, the metamorphic conditions were estimated by (Asran and Kabesh 2003) as 720–740 °C for Migif-Hafafit amphibolites and 800–820 °C for associated migmatites, both under pressures of 6–7 kbars. The pressure conditions were confirmed as 6–8 kbars by (Abd El-Naby and Frisch 2006) (Fig. 25).

8.3 Atalla Shear Zone

Atalla Shear Zone is a NW-oriented steeply dipping zone showing sinistral transcurrent regime (Figs. 26 and 27). It is marked by the Atalla felsite mass (28.4 km long by 7.2 maximum width) (Akaad and Noweir 1977; Akaad 1996). The Atalla felsite was considered by many workers as pertaining to the "post-Hammamat felsites" (e.g., Noweir 1968). Conversely, Essawy and Abu Zeid (1972) considered the Atalla felsite and the associated siliceous metatuffs and acidic flows as rocks belonging to ummetamorphosed old volcanics of the Dokhan type. Akaad and

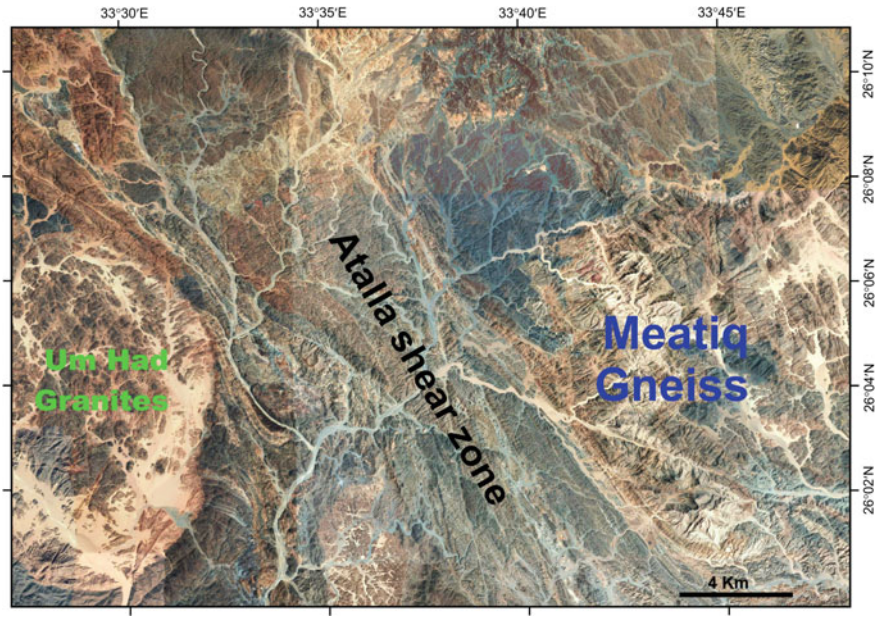

Fig. 26 ETM+ false-color image showing Atalla shear zone

Noweir (1977) and Akaad et al. (1979) considered the Atalla felsite as older than Um Had granite pluton, and this is proved in the field where the felsite extruded the mélange rocks (serpentinites, metasediments metavolcanics, and acidic tuffs) and both of them are intruded by Um Had granite. Because of the effect of Atalla Shear Zone, the huge felsite mass and the mélange rocks are strongly sheared and cataclased, exhibiting stretching lineations and slickenlines particularly at their margins. Kinematic indicators with monoclinic symmetry that encountered at outcrop scale reflect sinistral sense of shearing.

Akawy (2003, 2007) concluded that the structural pattern of the Atalla Shear Zone consists of thrust faults dipping toward the NE with a transport direction toward the SW. Folds developed upon the thrusting represent the second generation of structures. The fold axes trend in a NW–SE direction. The folds occur on centimeter-to-kilometer scales. The thrust faults and folds were cut by four sets of faults, which trend NW–SE, E–W, N–S and NE–SW. The oldest faults are mainly compressive (strike-slip faults) which were superseded by extensional (normal faults).

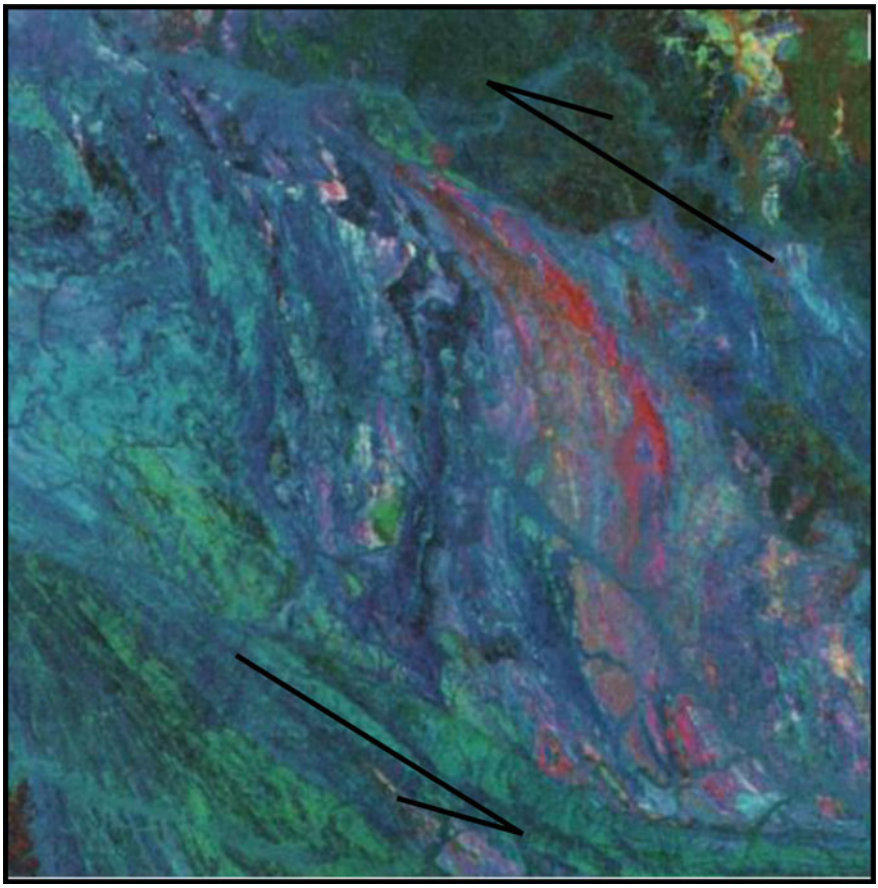

Fig. 27 Landsat image showing kinematic indicator with monoclinic symmetry reflecting sinistral shearing along Atalla Shear Zone (after Sultan et al. 1988)

8.4 Qena-Safaga Shear Zone

Qena-Safaga Shear Zone (Fig. 28) is a semi-ductile–semi-brittle subvertical shear zone (5 km average width), running along Qena-Safaga line in a NE–SW direction, at nearly right angle to the Red Sea. It passes through two lithologically different domains; Pan-African basement complex in the east and Phanerozoic sediments in the west. In the basement domain, the shear zone juxtaposes Dokhan Volcanics and post-amalgamation Hammamat volcano-sedimentary sequence to the north from ophiolites, arc metavolcanics, and metavolcaniclastics to the south. Qena-Safaga Shear Zone has a long-lasting tectonic history since the Precambrian time and shows dextral sense of movement proved by the remarkable displacement of the basement rocks, particularly near 22 km from Safaga Coastal City. Dextral shear

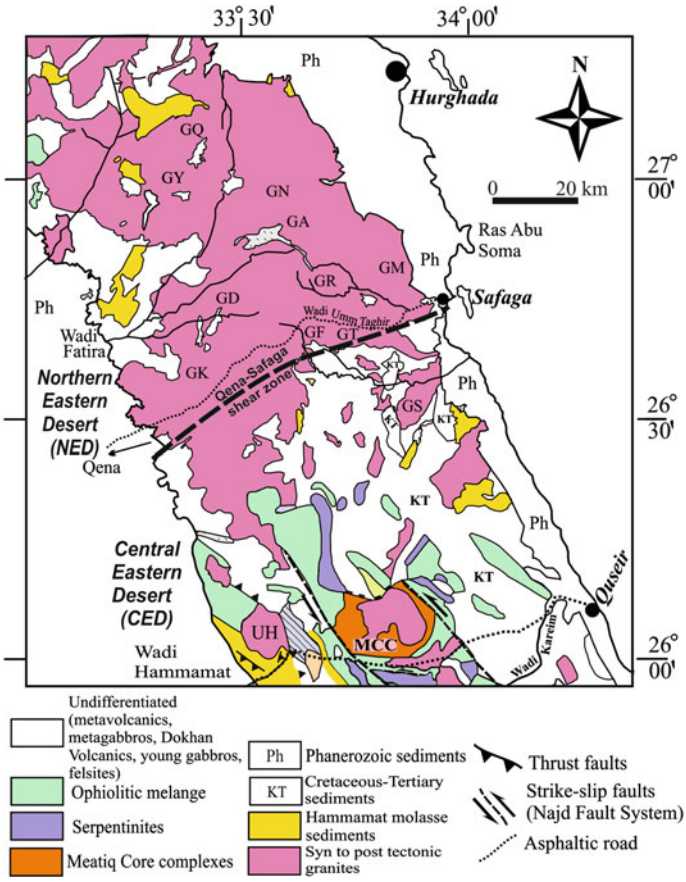

Fig. 28 Simplified geological map of northern part of the Central Eastern Desert and the southern part of the Northern Eastern Desert of Egypt (After Abd El-Wahed and Abu Anbar 2009). Compiled from the Geological Map of Egypt (El-Ramly 1972) and the geological map of Quseir (Klitzch et al. 1987). Major structures are after Fritz et al. (1996). UH, Um Had granite pluton; MCC, Meatiq core complex; GK, G. Kafari; GS, G. Gasus; GD, G. El-Dob; GF, G. Abu Furad; GT, G. Umm Taghir; GR, G. Ras Barud; GM, G. El-Magal; GA, G. Umm Inab; GY, G. Samyuk; GN, G. Shayib El Banat; GQ, G. Qattar. The thick gray line is the Qena-Safaga line of El-Gaby et al. (1994) and represents the approximate boundary between CND and NED

criteria are also recorded some 2 km to the south of the Qena-Safaga asphaltic road. In places, sinistral sense of movement is detected, reflecting reactivation along the shear zone. El-Gaby et al. (1988) suggested that the pronounced reactivation which was during the Tertiary had been responsible for the creation of Qena Bend in the course of the River Nile. In this context, some authors (e.g., El Kazzaz 1999) believed that Qena-Safaga Shear Zone is an active tectonic zone till the present time. The presence of tensile and en echelon opening fractures within the recent

sediments, especially between 20 and 30 km to the east of Qena City, together with high magnitude seismicity (up to 3.9) are rather evidence conforming this opinion.

8.5 *Mubarak–Barramiya Shear Belt*

The Mubarak–Barramiya shear belt is a huge NE-trending shear belt (about 90 km in length and 40 km in width) occupies the area between Wadi Mubarak and Wadi Ghadir on the Red Sea coast and extends through the whole width of the Eastern Desert to include the area between Wadi Barramiya and Wadi Sha'it to the west (Fig. 29). Hassaan and El-Sawy (2009) considered Barramiya, Atud–Sukari; Um Khariga-Wadi Abu Dabbab as sutures and/or shear zones. Greiling et al. (1994) considered E–W trending Idfu-Mersa shear zone originated as extension collapse during a post-collision event. However, Salloum et al. (1989) considered Idfu-Mersa Alam Shear Zone as a major E–W deep seated fault, overprinted by several thrusts and strike-slip faults having N–S, NE–SW and NW–SE directions

The Mubarak–Barramiya Shear Belt runs NE–SW to ENE–WSW in the CED (Figs. 29 and 30) and deforms supracrustal successions and structures associated with the NW-trending shear fabric. It constitutes well-defined ophiolite-decorated linear belt where serpentinites represent the most characteristic lithological unit. The geology of The Mubarak–Barramiya shear belt is commonly described in terms of three major lithotectonic units, namely, (i) ophiolite slices and ophiolitic mélange, (ii) island arc metavolcanic and metasedimentary successions, and (iii) syn- to post-orogenic gabbroic to granitic intrusions. The ophiolites display imbricate thrust sheets and slices of dismembered ophiolite suites distributed along several localities within the Mubarak–Barramiya shear belt (Shalaby et al. 2005; Abd El-Wahed and Kamh 2010; Abd El-Wahed 2014; Abd El-Wahed et al. 2016).

The Mubarak–Barramiya shear belt is post-accretionary deformational belts in the Arabian–Nubian Shield and characterize by the following evolutionary sequence (Abd El-Wahed 2014): (1) Early NW–SE shortening (D_1) associated with accretion of island arcs and obduction of ophiolites over old continent. D_1 produced NNW-directed thrusts and ENE–WSW-oriented folds in the CED. (2) an E–W-directed shortening deformation was superimposed due to oblique collision between the Arabian–Nubian Shield and the Nile Craton (D_2) this produced NW-trending upright folds, NE-dipping and SW-dipping thrusts, and discreet NW–SE tending shear zones in the CED. NNW-directed thrusts belonging to D_1 were folded around NNW–SSE trending fold axes. Continuing E–W shortening rotated the folded thrust to steeply dipping orientations and initiation of major NW-trending sinistral shear zones and culminated in the initiation of major dextral strike–slip shear zones (D_3) as conjugate sets with the NW-trending sinistral shear zones at c. 640–540 Ma ago. The structures associated with the NW-sinistral shear zones are strongly superimposed by the NE-trending transpressional deformation of the Mubarak–Barramiya Shear Belt.

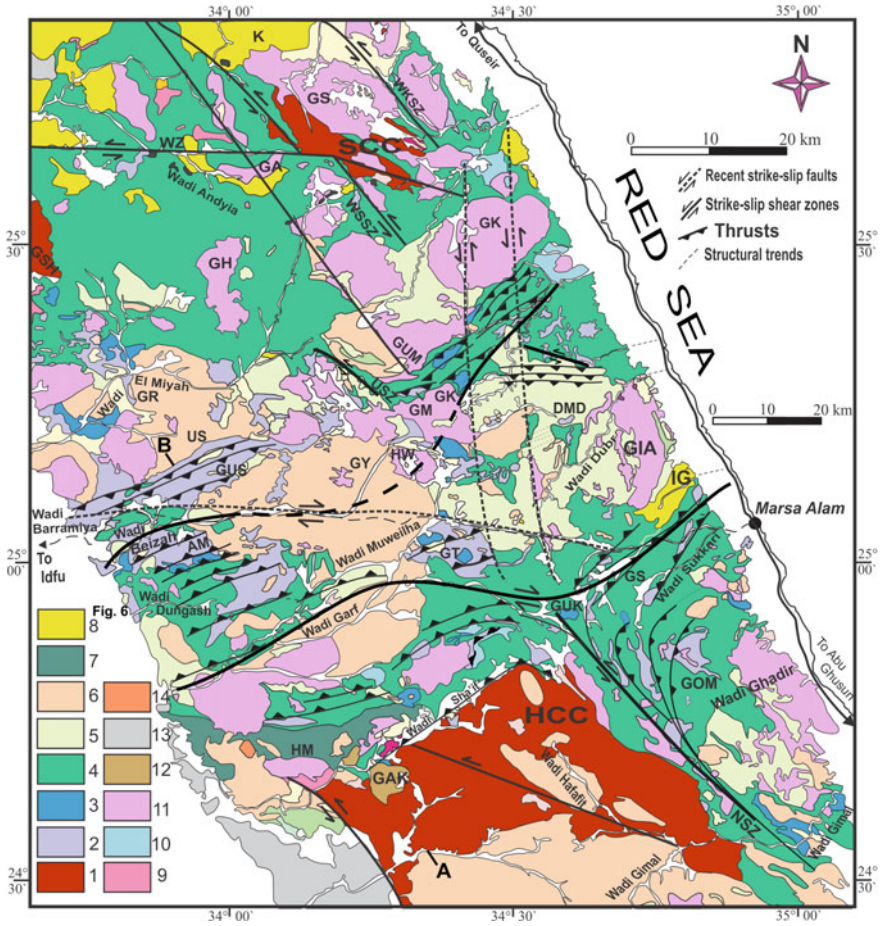

Fig. 29 Geological map of the southern part of the Central Eastern Desert of Egypt (modified after Klitzsch et al. 1987). 1; core complexes 2; serpentinites, 3; ophiolitic metagabbros, 4; metavolcanics and metasediments, 5; syn-tetonic intrusive metagabbros, 6; syn-tectonic granite, 7; Dokhan volcanics, 8; molasse sediments, 9; felsites, 10; gabbros, 11; post- to late-tectonic granites; 12; ring complex, 13; Natash volcanics, and 14; trachyte plugs. GAK; Gebel Abu Khruq, HG; Hafafit gniess, GOM; Wadi Ghadir ophiolitic mèlange, HM; Hamash gold mine, NSZ; Wadi Nugrus shear zone, GS; Gebel Sukkari and Sukkari gold mine, GUK; Gebel Um Khariga, IG; Igla molasse basin, DMD; Dubr metagabbro–diorite complex, GIA; Gebel Igl Al-Ahmar, HW, Gebel Homrat Waggad, GY, Gebel El-Yatima, GUS; Gebel Umm Salim, US, Gebel Umm Saltit, GK; Gebel Abu Karanish, GM, Gebel Al Miyyat, USZ; Um Nar shear zone, GUM; Gebel El-Umra, GK; Gebel Kadabora, GA; GH; Gebel El-Hidilawi, GU; Gebel Umm Atawi, SHG; El Shalul gneiss, GR; Gebel El Rukham; SG; Sibai gneiss, GS; Gebel Sibai, WZ; Wadi Zeidon, WSSZ; Wadi Sitra shear zone, WKSZ; Wadi Kab Ahmed shear zone, and K; Kareim molasse basin. The major structures are after Akaad et al. (1993), Fritz et al. (1996), Helmy et al. (2004), Shalaby et al. (2005), Abd El-Wahed (2008) and Abd El-Wahed and Kamh (2010)

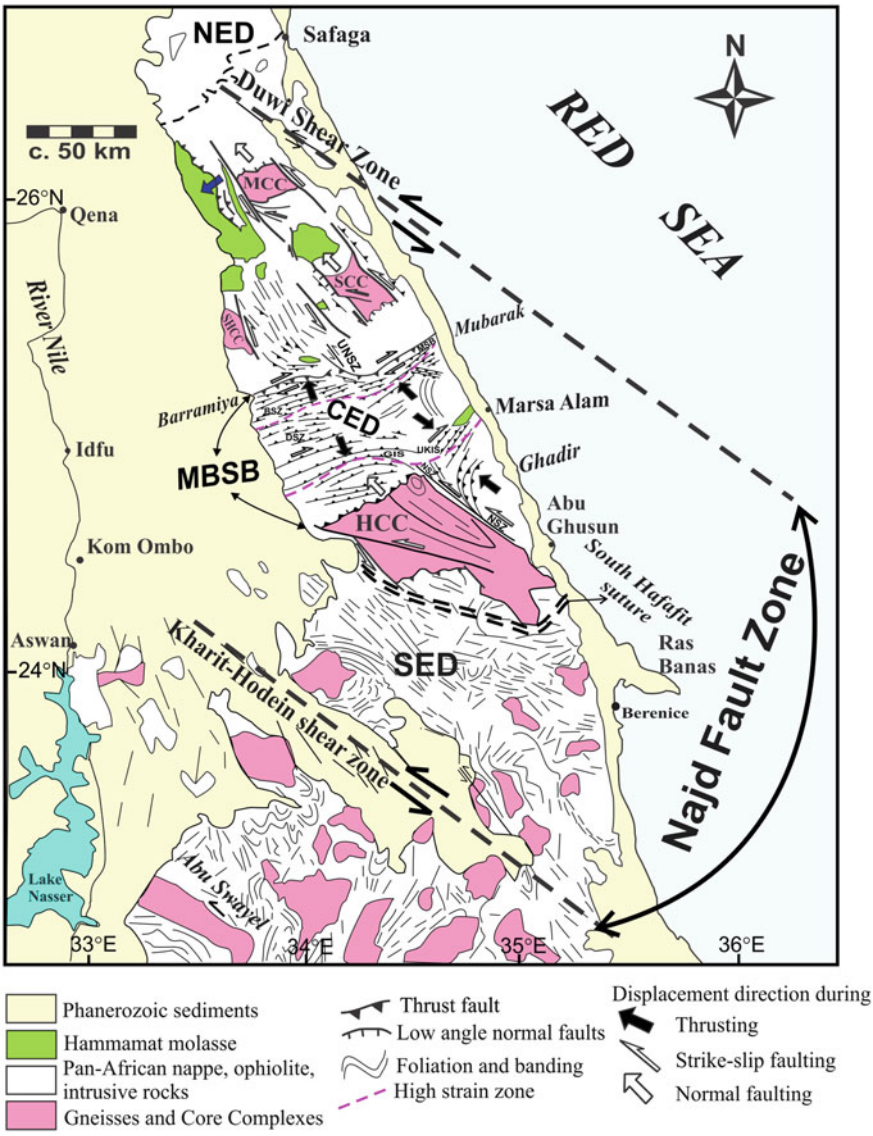

Fig. 30 Major structures in the Central Eastern Desert (CED). The Najd Fault Zone in the Eastern Desert is enclosed between Kharit-Hodein shear zone in the south and Duwi Shear Zone to the north. SED; South Eastern Desert, CED; Central Eastern Desert, NED; Northern Eastern Desert, NSZ, Nugrus shear zone, UNSZ, Um Nar shear zone, HCC; Hafafit Core Complex, SCC; Sibai Core Complex; MCC; Meatiq Core Complex; and MBSB, Mubarak–Baramiya shear belt. This map is compiled from Greiling et al. (1994), Fritz et al. (1996), de Wall et al. (2001) and (Abd El-Wahed 2014)

8.6 Hamisana Shear Zone

Hamisana Shear Zone (660–610 Ma) belongs to the post-accretionary structures (Fig. 22) that formed in the ANS post-dating arc–arc collision and distinct from the assembly between the ANS and Gondwana fragments (Abdelsalam and Stern 1996). It extends in N- to NNE–direction from northern Sudan and because of its sinistral sense of shear causes remarkable dragging of the Allaqi–Heiani Suture Zone and goes further north bounding the Gerf metaultramafic nappe from the east, then continues to meet the Red Sea Coast. Abdelsalam and Stern (1996) proposed dextral sense of shear along the Hamisana Shear Zone based on the deteral off-setting of the Yoshgah Suture (Stern et al. 1989, 1990). The geometric aspect and kinematic history of the Hamisana Shear Zone have been the subject matter of controversy where it is interpreted in terms of a major high-strain zone, a suture zone, and a large-scale transpressional transcurrent zone. Miller and Dixon (1992) argued that transpression in itself is polyphase and this is consistent with the geometric relationship between the eastern extension of the Allaqi Suture Zone and the Hamisana Shear Zone. de Wall et al. (2001) carried out integrated field and AMS studies, and demonstrated that deformation in the Hamisana Shear Zone is dominated by pure shear under upper greenschist/amphibolite grade metamorphic conditions, producing E–W shortening, but with a strong N–S-extensional component. The authors demonstrated that deformation was responsible for folding of regional-scale thrusts (including the base of Gerf and Onib ophiolitic nappes) and indicate that high-strain deformation is younger than ophiolite emplacement and suturing of arc–arc terranes. The obtained data led these authors to conclude that the Hamisana Shear Zone is dominated by late-orogenic compressional deformation and cannot be related to either large-scale transpressional orogeny or major escape tectonics.

Hamisana Shear Zone (Fig. 22) is cut by NW-striking faults and shear zones related to the Najd Fault System, although the amount of displacement and extent of deformation associated with the Najd system is controversial (e.g., Sultan et al. 1988; Smith et al. 1999; Kusky and Ramadan 2002). Four deformational phases have been identified (Stern et al. 1990). The oldest (D_1) records emplacement of the ophiolitic rocks. This produced a complex imbrication of ophiolitic and metavolcanic sequences. D_2 folding around north-trending axes produced a regional cleavage (S_2), subhorizontal intersection lineation (L_2), and tight, upright to inclined fold (F_2). D_3 is coaxial with D_2 and refolds S_2, locally producing pencil structures and crenulations in the western Hamisana. The resultant pervasive northsouth fabric is truncated by narrow, north-northeast-trending D_3 dextral shear zones. These become more dominant in the extreme south as the Hamisana shear zone turns southwest. Later kinks (D_4) and brittle faults have variable movement sense and account for limited regional strain. Thus, the principal ductile deformation in the Hamisana is characterized by nearly coaxial folding about a northsouth axis, indicating shortening normal to the zone.

9 Najd Shear Corridor

The first requirement for comprehensive understanding of the Eastern Desert regional tectonic setting is the entire fathoming of the Najd Fault System (NFS) and its complex arrays of secondary structures. The NFS has a great importance due to its great size, role in the exhumation of metamorphic core complexes and prominence in Gondwana cratonization. Moore (1979) described this system as a major transcurrent (strike-slip) fault system, of Proterozoic age in the Arabian Shield (Fig. 1). He suggested a similarity of NFS to many of the world's major transcurrent fault systems, including the San Andreas (USA) and Alpine (New Zealand) faults in terms of its length (possible length of more than 2000 km), and added the system is a braided complex of parallel and curved en echelon faults. For the NFS and especially close to the terminations of some major faults a complex association of secondary structures including strike-slip, oblique-slip, thrusts, and normal faults, in addition to folds and dike swarms are usually present forming an intricate array. Therefore, we should keep in our mind that the importance and complexity of NFS is augmented by this array of secondary structures that give an allusion to synchronous compressional and extensional conditions in various parts of the fault zones.

The NFS was identified originally as a huge late Proterozoic and early Phanerozoic NW-trending brittle–ductile shear zone with 300 km width and length over 1100 km extending across the northern part of the ANS (Brown and Jackson 1960; Stern 1985; Johnson et al. 2011). The displacement along the strike of the NFS was reported by (Brown 1972) as 240 km cumulative displacement but field displacements can be demonstrated as only tens of kilometers for faults (Johnson et al. 2011). The NFS and other NW-trending strike-slip faults in the ANS are regarded also as post-accretionary structures and were interpreted to be the result of the squeezing of the Arabian–Nubian Shield between East and West Gondwana (Berhe 1990; Stern 1994; Abdelsalam 1994; Abdelsalam and Stern 1996; Abdelsalam et al. 2003). The formation of NFS is a result of simple shear that allowed the Nubian and southern Arabian shield to move several hundred kilometers sinistrally with respect to northern Arabia (Moore 1979).

From the Arabian Shield, the northwestern extensions are probably in the Eastern Desert of Egypt and to the southeast, the line of faulting coincides with structures in the south Yemen coast and in the bed of the Arabian Sea (Brown 1972). In southern Jordan rocks, the shear zone is inferred to be present and disrupted by much younger Cenozoic slip on the Dead Sea Transform (El-Rabaa et al. 2001). In the Mozambique Belt in Kenya and Madagascar, Similar NW-trending shear zones were identified (Raharimahefa and Kusky 2010). The influence of the NFS also continued to southeast into parts of India and the Lut block of Iran as was reported by (Al-Husseini 2000) from Magnetic and gravity data. Thus, the NFS attains more than 2000 km (Moore 1979) total possible length making this system one of the greatest shear systems known on Earth.

Geochronologically, the absolute radiometric ages obtained from small intrusions denoted that the faults were active from late Proterozoic into early Phanerozoic times, 580–530 Ma ago (Fleck et al. 1979). The late stages (630–535 Ma) of the Pan-African

event witnessed the NFS development in the form of huge shear zone system striking NW–SE (Stern 1985; Johnson et al. 2011).

Geophysically, subsurface aeromagnetic maps interpretation denoted a continuity of the NFS beneath the surface faults arrays concluding that this system is broader at depth than the outcropping fault complex (Moore 1979). At depth and under amphibolite facies prevailing conditions, an early shear ductile activity of the NFS is prevailing which is turned into brittle shearing at the shallower levels (Johnson et al. 2011; Fritz et al. 2013). Hydrothermal activity, in turn was pervasive indicating abnormally high heat transfer in the time of faulting. The hydrothermal alteration is probably also a reflection of the mechanical importance of fluid pressure in the mechanism of faulting at this structural level (Phillips 1972).

Deformation was followed by brittle failure during the main faulting episodes. The currently exposed structural level in the Southern Najd was that of ductile to semi-brittle deformation (Moore 1979). In addition to strike-slip movement, minor thrusting, oblique-slip faulting, and normal faulting have occurred in some areas. Thrust faults and folds adjacent to terrane containing normal faults can be seen. These unusual assemblages of minor structures define local areas of anomalous compression or dilation within the fault belt. The compressional regimes, in which thrusting and folding accompany second-order wrench faulting, occur on the northeast side of the northwest terminations and on the southwest side of southeast terminations and in the "overlap" between en echelon major faults. The compressional regimes are complemented by "dilation" on the opposite side of the master fault, marked by normal faulting and extension fissure formation. The dilational areas offer the most mechanically favorable loci for dike intrusion during the faulting events (syn-tectonically) and, subsequently, for hydrothermal vein emplacement.

Strictly speaking, the NFS is dominated by NW-trending shears, and best typified in the Egyptian Eastern Desert by the previously mentioned Kharit-Hodein, Nugrus, and Atalla Shear Zones (Fig. 30). On the other hand, the theoretical complements (major NE-trending dextral faults) to the main system are rare (Moore 1979). The NE- (to ENE-) trending dextral shears are regarded as the conjugate pairs of the NW trend and are represented in the Eastern Desert by Qena-Safaga and Mubarak–Baramiya shear belt (Fig. 30). It is worth mentioning to denote that the NFS is a coherent structure that can be explained by a single regional event (Moore 1979). The sinistral strike–slip shearing along the NW-oriented Najd-related Shear Zones was accompanied by transpressional and transtensional tectonic regimes (Fritz et al. 1996; Abd El-Wahed 2014; Abd El-Wahed et al. 2016; Stern 2017).

10 Shear Zone-Related Gneiss Domes

As mentioned before, the Eastern Desert of Egypt is characterized mainly by the prevalence of a NW-trending tectonic fabric marking the NW–SE sinistral shear zone (Fig. 30) of the NFS (Abd El-Wahed and Kamh 2010). Another important structural feature in the Eastern Desert is presence of a series of gneiss domes

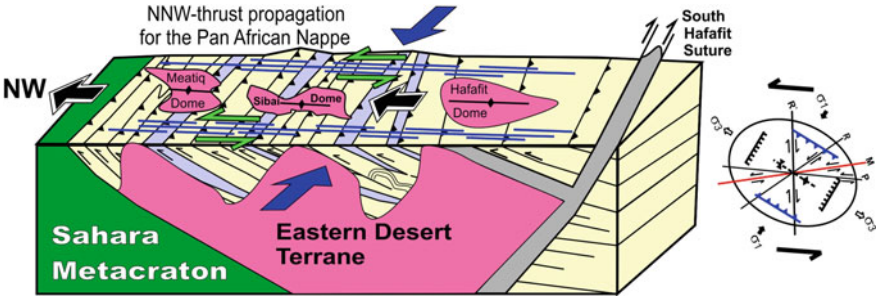

Fig. 31 E–W shortening associated with a post-accretion phase produced sinistral shearing along NW–SE shear zones (660–560 Ma)

(Figs. 30 and 31) or core complexes (e.g., Meatiq, Sibai, El- Shalul, and Hafafit) (Hamimi et al. 1994; Hamimi 1996, Fritz et al. 1996, 2002, 2013; Loizenbauer et al. 2001; Abd El-Wahed 2008; Abdeen et al. 2014). These domes are bounded in the northeast and southwest by NW-trending sinistral strike–slip shear zones related to the NFS such as Nugrus Shear Zone to the east of Hafafit Culmination (Fig. 24). Gneiss domes have either been interpreted as (1) antiformal stacks formed during thrusting (e.g., Greiling et al. 1994), (2) core complexes formed during orogen-parallel crustal extension (e.g., Fritz et al. 1996; Bregar et al. 2002; Abd El-Wahed 2008), and (3) interference patterns of sheath folds (Fowler and El Kalioubi 2002). Geochronology suggests that extension and exhumation of gneiss domes commenced around 620–606 Ma (Fritz et al. 2002; Andresen et al. 2009). The gneiss domes in the Eastern Desert (e.g., Meatiq, Sibai, Shalul, and Hafafit) are distributed along a NW-trending major zone that extends for more than 400 km between Wadi Hodien in the south to Wadi Quieh in the north (Figs. 30 and 32).

Fig. 32 Field photographs showing the southern part of El Shalul Dome, looking E (after Hamimi et al. 1994)

11 Transpressional Regime in the Egyptian Eastern Desert

Transpressional deformation has played an important role in the late Neoproterozoic evolution of the Eastern Desert of Egypt and the ANS as a whole. Transpression is strike-slip deformation that deviate from simple shear because of a component of, respectively, shortening or extension orthogonal to the deformation zone (Harland 1971; Tikoff and Greene 1997; Dewey et al. 1998). It is a combination of a strike-slip component and a shortening component orthogonal to the deformation zone and includes a deformation developed between two undeformed blocks resulting from both simple and pure shear (Sanderson and Marchini 1984; Fossen et al. 1994; Fossen and Tikoff 1998; Jones et al. 2004).

Transpressional shear zones are characterized by an association of structures that suggest zone-normal shortening and zone-parallel shearing. In wrench-dominated transpression, stretching lineations are either horizontal (low strain) or vertical (high strain), whereas they are always vertical in a pure shear dominated transpression. Vertical stretching lineations within a vertically oriented shear zone, perpendicular to the simple shear component of deformation and the direction of tectonic movement, were first interpreted to be the result of transpressional deformation by Hudleston et al. (1988). Theoretical models of heterogeneous transpression (Jiang and Williams 1998) interpret these lineations as can range from horizontal to vertical continuously, depending upon the value of finite strain.

Transpression occurs in a wide variety of tectonic settings and scales during deformation of the earth's lithosphere such as the Archean North Caribou greenstone belt (Gagnon et al. 2016), the Pan-African Kaoko belt in Namibia (Goscombe and Gray 2008; Knopásek et al. 2005), Southern Uplands of SE Scotland (Tavarnelli et al. 2004), Kushtagi schist belt, India (Matin 2006), Sanandaj–Sirjan metamorphic belt, Zagros mountains, Iran (Sarkarinejad and Azizi 2008; Shafiei Bafti and Mohajjel 2015), Al Jabal Al Akhdar, Libya (Abd El-Wahed and Kamh 2013), Central Asian Orogenic Belt (Li et al. 2016), Cauvery shear zone, southern Granulite Terrain, India (Chetty and Bhaskar Rao 2006), Dom Feliciano Belt, Uruguay (Oriolo et al. 2016) Salem–Attur shear zone, south India (Kumar and Prasannakumar 2009), Egyptian Eastern Desert (Fritz et al. 1996, 2002, 2013; Bregar et al. 2002; Shalaby et al. 2005; Abd El-Wahed 2008, 2010, 2014; Abd El-Wahed and Kamh 2010; Zoheir 2008, 2011; Zoheir and Weihed 2013; Abd El-Wahed et al. 2016), and Arabian Shield (Hamimi et al. 2013a, b, 2014).

In the Eastern Desert of Egypt, transpressional deformation is recognized as post-collisional structures (Greiling et al. 1994; Fritz et al. 1996; Abd El-Wahed and Kamh 2010; Abdeen and Abdelghaffar 2011) identified by localized transpressional strike-slip shear zones (Greiling et al. 1994; Fritz et al. 1996, 2013; Abd El-Wahed and Kamh 2010) deforming the early compressional structures. The best examples for transpressional strike-slip shear zones in the Eastern Desert of Egypt are the Allaqi–Heiani shear zone (Figs. 18, 19 and 22), the NW-oriented Wadi Kharit–Wadi Hodein (Figs. 18, 19 and 30), and the N-oriented Hamisana in

southern Eastern Desert (Greiling et al. 1994), and the Najd Fault Zones in the CED. The sinistral strike–slip shearing along the NFS was accompanied by transpressional and transtensional tectonic regimes (Fritz et al. 1996). Transpression resulted in formation of ESE- to ENE-shortening that produced NNW- to N-trending folds throughout the CED. These are superimposed on early NNW-directed thrusts and related structures (Makroum 2001; Shalaby et al. 2005; Abd El-Wahed and Kamh 2010; Abd El-Wahed 2014; Abdeen et al. 2014; Abd El-Wahed et al. 2016).

Early transpression in the Eastern Desert of Egypt produced the Allaqi Allaqi–Heiani shear belt and final transpression is documented in the Wadi Kharit–Wadi Hodein Zones (Greiling et al. 1994). Abdeen and Abdelghaffar (2011) described two major deformation events from Allaqi–Heiani Shear Belt; (i) D_1 was an N–S to NNE–SSW regional shortening generating the SSW-verging folds and the NNE dipping thrusts, and (ii) D_2 was an ENE–WSW shortening producing NNW–SSE-oriented folds and reactivating older thrusts with oblique-slip reverse fault movement. D_1 is related to the terrane accretion during the early Pan-African orogen and associated with collision between the Eastern Desert terrane and the Gabgaba terrane along the Allaqi–Heiani Shear Belt, whereas D_2 is related to Najd Orogen due to collision between East- and West-Gondwanalands at ca. 750–650 Ma associating the closure of the Mozambique Ocean. Collision between East- and West- Gondwanalands deformed the Allaqi–Heiani Shear Belt along N–S trending shortening zones and produced NW–SE and NE–SW-oriented sinistral and dextral transpressional faults, respectively (Abdeen and Abdelghaffar 2011).

Allaqi–Heiani shear belt is apparently linked by the high angle sinistral strike-slip Wadi Kharit–Wadi Hodein Shear Zone with a tectonic transport of about 300 km toward the W/NW. The Wadi Kharit–Wadi Hodein Shear Zone is characterized by compressional/transpressional deformation and interpreted as an equivalent of the NFS (Greiling et al. 1994; Zoheir 2011). The Hamisana Shear Zone is one of the largest transpressional shear zone in NE Africa, covers an area of about 15,000 km^2. It has been interpreted as a Precambrian suture, as a zone of strike-slip displacement, or as a zone of crustal shortening (e.g., Stern et al. 1989; Miller and Dixon 1992; de Wall et al. 2001; Sakran et al. 2001; Takla et al. 2002; Ali-Bik et al. 2014). The Hamisana Shear Zone represents a transpressional shearing event post-dating the terrane accretion (Smith et al. 1999). On the contrary, a post-accretion origin is postulated for the Hamisana Shear Zone by many workers (e.g., Stern et al. 1989, 1990; Miller and Dixon 1992; de Wall et al. 2001). Stern et al. (1989) bracketed the shearing event of the Hamisana Shear Zone between 660 and 510 Ma post-dating the terrane accretion. They related the Hamisana Shear Zone to the Najd Tectonic System.

The most important transpressional shear zones in the CED of Egypt are Nugrus Shear Zone, Mubarak–Baramiya shear belt and the major shear zones bounding the gneiss domes. Nugrus Shear Zone interpreted as thrust accommodating westward or SW-ward ophiolitic material transport over the continental margin (El-Gaby et al. 1990; El-Bayoumi and Greiling 1984; El-Ramly et al. 1984) or as roof thrust (Greiling et al. 1994 and Greiling 1997). Many workers considered Nugrus Shear

zone as a Najd-related transpressional strike-slip shear zone (e.g., Fritz et al. 1996; Shalaby et al. 2006; Abd El-Wahed et al. 2016).

Nugrus Shear Zone and Mubarak–Baramiya Shear Belt are dominated NW-sinistral and NE-dextral shear zone characterized by wrench-dominated transpressional structures such as oppositely dipping thrusts, subhorizontal lineation (Fig. 33a), pop-up structures, and flower-like cleavage (Figs. 33b and 34). The Mubarak–Baramiya Shear Belt is composed of a network of anastomosed shear

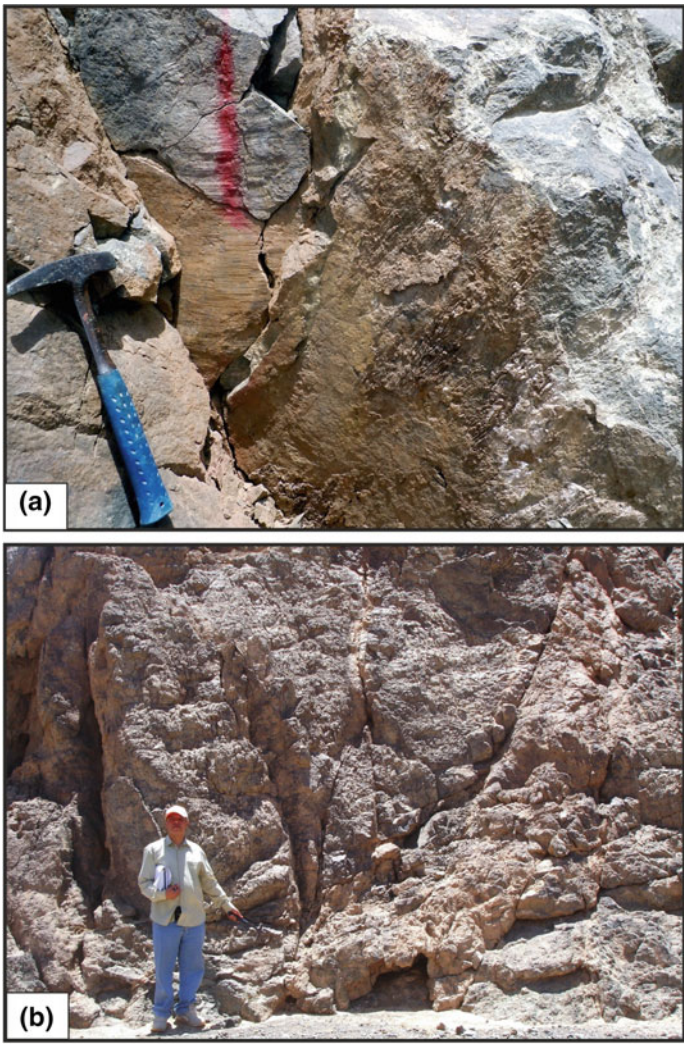

Fig. 33 **a** Subhorizontal slickensides overprinted by steeply dipping striae in sheared metavolcanics along Wadi Al Alam, Central Eastern Desert, looking NW; **b** flower-like cleavage in serpentinites, Wadi Barramiya, Central Eastern Desert, looking SW

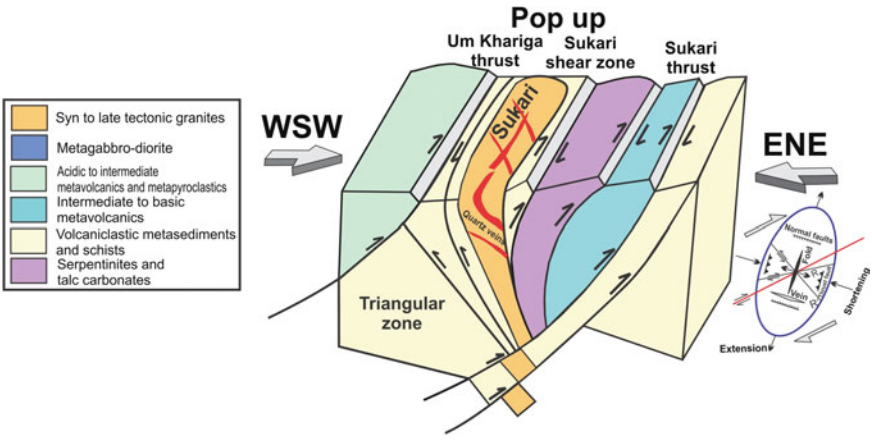

Fig. 34 A schematic block diagram showing the geometry and kinematics of pop-up structure along Sukari shear zone, northern Nugrus shear zone (after Abd El-Wahed et al. 2016)

zones arising from conjugate shears with a prevalent dextral sense (Abd El-Wahed and Kamh 2010). The transpression-related sinistral shear regime is superimposed by the dominant dextral transpression along NE–SW trending Wadi El-Umra Shear Zone. This dextral shearing is characterized by development of NNE- to NE-trending cleavage, strike-slip duplex, NNE- and NE-trending folds, and NNW-directed thrusts. These two events represent a single progressive phase associated with sinistral transpressional deformation, which is related to a younger E–W shortening event (Abd El-Wahed 2014). E–W-directed shortening is due to oblique convergence between East and West Gondwana along the Mozambique belt. Transpressional structures in the NE–SW trending Mubarak–Barramiya Shear Belt (Figs. 29 and 30) indicate highly oblique convergence leading to wrench-dominated dextral transpression and development of a major flower structure between Wadi Mubarak and Hafafit dome occupying the whole width of the CED (Abd El-Wahed 2014).

Transpression has also been used to explain the geometry and kinematics of gold-bearing quartz veins in the Eastern Desert of Egypt (Hassaan et al. 2009; Zoheir 2008, 2011; Zoheir and Lehmann 2011; Abd El-Wahed 2014). The syn-orogenic gold mineralization in the Eastern Desert relates to transpressional NW-sinistral (Fig. 34) and NE-dextral strike-slip shear zones related to the NFS and hosted by volcaniclastic metasediments and altered ophiolitic serpentinites (Abd El-Wahed et al. 2016). Structural analysis of the shear fabrics in Sukari gold mine area indicates that the geometry of the mineralized quartz veins and alteration patterns are controlled by the regional NNW- and NE-trending conjugate zones of transpression (Abd El-Wahed et al. 2016). Gold-bearing quartz veins are located within steeply dipping NW- and SE-dipping thrusts and NE- and NS-oriented

dextral and sinistral shear zones around Sukari mine area, and along E-dipping back thrusts and NW–SE and N-S fractures in Sukari granite (Abd El-Wahed et al. 2016).

The high grade of gold mineralization in Sukari is mainly controlled by SE-dipping back thrusts branched from the major NW-dipping Sukari Thrust. The gold mineralization in Sukari gold mine and neighboring areas in the Eastern Desert of Egypt is mainly controlled by the conjugate shear zones of the NFS. In the SED, many of the mineralized quartz veins and alteration patterns are controlled by the regional, NNW-trending zone of transpression, such as the Wadi Kharit–Wadi Hodein Shear Zone, which is related to the 655–540 Ma, Najd Shear Corridor (Zoheir 2011).

12 The Active Seismotectonic Zone in the Egyptian Eastern Desert

The abovementioned fractures and shear zones traversing the Eastern Desert of Egypt show no indications for reactivation at present time. The only known active seismotectonic zone in the entire Pan-African belt of the Eastern Desert is Abu Dabbab zone which represents one of five seismotectonic zones in Egypt (Hamimi and Hagag 2017). Abu Dabbab zone is an ENE-oriented narrow zone, lying some 30 km north of Marsa Alam City along the Red Sea Coast. This zone could easily be affiliated to the ENE Najd-related Shear Zones, such as Idfu-Mersa Alam Shear Zone, in terms of direction and sense of shear, but it differs where it shows daily recorded microearthquakes with local magnitudes (ML < 2.0). Besides, November 12, 1955 and July 2, 1984, two giant earthquakes were recorded with magnitudes 5.6 and 5.2, respectively (Fairhead and Girdler 1970; Badawy et al. 2008). The recorded seismic activity from Abu Dabbab region by the Egyptian National Seismic Network (ENSN) ranges from 10 to 15 events/day to more than 60 events/day, and sometimes attained 100 events/day during swarms (Badawy et al. 2008; Mohamed et al. 2013). Such enigmatic seismic record has attracted the attention of many workers (e.g., Fairhead and Girdler 1970; Daggett et al. 1986; Hassoup 1987; Kebeasy 1990; El-Hady 1993; Ibrahim and Yokoyama 1998; Badawy et al. 2008; Hosny et al. 2009, 2012; Azza et al. 2012; Mohamed et al. 2013) to decipher origin of the earthquakes. The magmatic origin of the seismicity and associated shallow and deep earthquakes is promoting most of the publications dealt with the tectonic setting and seismic activity of Abu Dabbab area. Sabet et al. (1976) suggested that the tectonic evolution of the area was associated with volcanic activity, whereas Daggett et al. (1986) attributed Abu Dabbab seismicity to the subsurface volcanic environment of a cooling pluton. Meanwhile, Hassoup (1987) interpreted this seismicity in the light of the subsurface structural heterogeneity. Hosny et al. (2009) proposed a structural model for the area based on seismic velocity tomography, and related the P and S-wave velocity anomaly to magmatic intrusion. Recently,

El Khrepy et al. (2015) reveal strong arguments for the tectonic origin of the seismicity of Abu Dabbab area in despite of the prevalent magmatic origin.

Hamimi and Hagag (2016) proposed a new tectonic model for Abu Dabbab seismogenic zone based on integrated field-structural investigations, and EMR/seismic data. The obtained results led the authors to indicate a present-day faulting activity in the area and to determine the depth of the brittle–ductile transition zone underlies the Abu Dabbab area. The transition zone is estimated to be existed at a relatively shallow depth (10–12 km) depending upon the following main criteria: (1) the absence of a large seismic main shock, (2) the periodically recorded swarm's hypocenters of focal depths not deeper than 16 km, (3) the high *Vp*/*Vs* ratio (from seismic tomography) until 12 km depth, (4) the occurring of tensile earthquakes of high compensated linear vector dipole (CLVD) ratios, and (5) the high heat flow rates (about 92 $mW/m^2 \pm 10$, which is more than twice the average value of Egyptian Eastern Desert; 47 mW/m^2). The authors came to the conclusion that there is a mechanical decoupling between the shallow and deep crustal levels of Abu Dabbab Neoproterozoic basement succession, where the maximum principal stress axis ($\sigma 1$) rotates from a subhorizontal position at the uppermost crustal levels practicing transpressional deformation to a near vertical attitude in the deeper levels, where the transtensional deformation predominated.

13 Effect of Gravitational Tectonics

The structural architecture of the crystalline basement complex of the Eastern Desert is attributed to the Pan-African Orogeny that led to the formation of a wide variety of tectonic structures, such as thrusting and thrust-related structures, and shearing and shear-related structures. Nevertheless, effect of gravitational collapse in fracturing and deforming some domains is worth mentioning. Best example of this effect could be detected in Abu Fas area in Wadi Allaqi District in the extreme SED. Lithologic units outcropping in this area comprise metavolcanics, metagabbros, metaultramafics, and metasediments, intruded by tonalite, layered gabbro and muscovite-biotite granite. Striking features in Abu Fas gabbroic mass are margin-parallel arcuate faulting and inward symmetric dipping of layering and the remarkable decrease in the amount of dip from very steep layers in the outermost part of the intrusion to mildly dipping layers toward the center (Fig. 35). El-Kazzaz and Hamimi (2000) attributed the arcuate faulting to the gravitational forces, and believed that the inward dipping of foliation in the enveloping rocks close to the layered gabbro is related to a sagging of the preexisting structure post-dating the gabbro emplacement. Such observations may give a clue to the role of gravitational tectonics and crustal relaxation in the structural history of the Egyptian Eastern Desert.

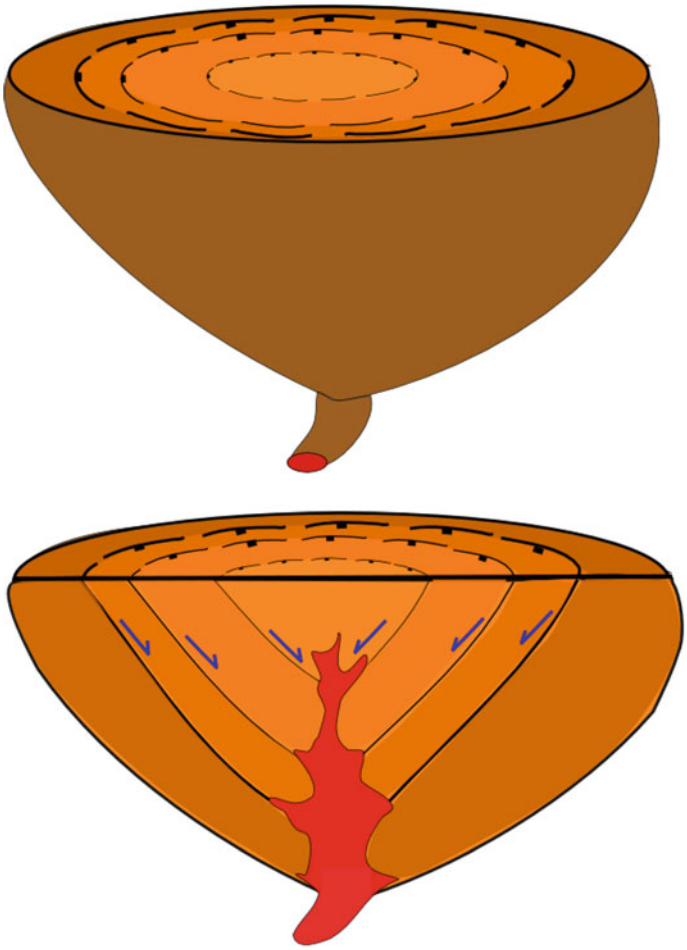

Fig. 35 Block diagrams showing arcuate faulting in Abu Fas layered gabbro, Gabal Muqsim area (after Hamimi et al. 2012c)

14 Discussion

In discussing the Neoproterozoic crustal evolution of the Pan-African belt and the tectonics of the Eastern Desert of Egypt the following enigmatic points are worthy to be addressed.

- Do we have pre-Pan-African infracrustal rocks?
- Thrusting, shearing, and folding relations.
- Gneiss domes vs. metamorphic core complexes.
- The conjugate pairs of Najd-related shears.
- Role of Najd Fault System in tectonic evolution of Gneiss domes.

- Rates and transport directions of metaultramafic nappes.
- The voluminous intrusives in NED.
- The post-amalgamation Hammamat sediments and their relation to Dokhan Volcanics.
- Northward decrease in intensity of deformation.

14.1 Do We Have Pre-pan-African Infracrustal Rocks?

The existence of the pre-Pan-African rocks in the Egyptian Eastern Desert is controversy and a matter of much debate. Also, the nature of the Pan-African orogeny and characteristics of the early crustal complex, are more controversial (Dixon 1981). Evaluating the extent of pre-ANS crustal input into the shield's core region carries important implications for the ongoing debate regarding its origin and evolution, because this affects critically models of crustal accretion rates and the interpretation of the Nd, Sr, Pb, and O isotope compositions of ANS rocks (Be'eri-Shlevin et al. 2009b). On scanning leading works done by influential scholars, once find that there are two principal schools of thoughts. The first school (e.g., Akaad and Noweir 1980; El-Gaby et al. 1988; Kroner et al. 1987a, b; Abdelkhalek et al. 1992; Khudeir et al. 1995) demonstrates that the exposed lithologic units are affiliated into two main rock groups; high-grade pre-Pan-African infrastructure (gneisses, migmatites, shear granites, and remobilized equivalents) and low-grade Pan-African suprastructure (ophiolites island arc volcanics and volcaniclastics). The contact (Pan-African thrusting) between the infrastructure and suprastructure is marked by a narrow zone of mylonite and intensive degree of shearing and cataclases, along with tightness of foliation. Affiliation of the gneisses, migmatites, and remobilized equivalents into the pre-Pan-African age is based mainly on the deformation and shearing, where these rocks are highly deformed and sheared compared to the ophiolites, island arc volcanics, and volcaniclastics. The Pan-African dating obtained for some gneisses and sheared granites elsewhere in the Eastern Desert are regarded to represent the age of metamorphism and not the protolith age. In this context, El-Gaby (1983), El-Gaby et al. (1988) and Hassan and Hashad (1990) believed that the mid-Proterozoic continental crust extends into the Eastern Desert and crops out in gneiss domes underneath overthrusted Pan-African island arc volcanics and volcaniclastics and associated ophiolites. Khudeir et al. (1995) contributed to the debate on the existence of pre-Pan-African continental crust in the Eastern Desert by presenting new data on the geology, petrography, and geochemistry of deformed granites exposed within the Sibai swell. The obtained results showed that the granite masses within the Sibai swell are intensely deformed and are older than the thrusting event which emplaces the overlying ophiolites and island arc volcanics and volcaniclastics of Pan-African age. The second school considered that (1) the rocks of the Eastern Desert have oceanic affinity characterized by mafic to intermediate volcanics and thick sequences of immature

sediments and volcaniclastic material (e.g., Engel et al. 1980), and (2) the gneisses are regarded to represent the highly deformed and metamorphosed equivalent of metavolcanics and metasedimentary rocks. Such opinion is in complete harmony with the arc assembly (arc accretion) model that shows, as mentioned before, that the EAO juvenile crust was generated around and within a Pacific-sized ocean (Mozambique Ocean) (Vail 1985; Stoeser and Camp 1985; Stern 1994).

14.2 Thrusting, Shearing, and Folding Relations

Structural styles and overprinting relations in the Egyptian Eastern Desert Shield rocks offer a good opportunity to decipher the relationship between folding, on the one hand, and thrusting and shearing on the other hand. Our investigations of key areas in the Eastern Desert indicate that these structures are geometrically and kinematically related. In many areas, a complete transition from slightly deformed to highly deformed rocks are potential in deducting such geometric and kinematic relations. Propagation of thrusting often took place according to "footwall-nucleating–footwall vergent rule". Accordingly, earlier hanging walls are carried forward in a piggyback manner, and newly formed thrusts grow in the footwalls of the older thrusts. Out-of-sequence thrusts are infrequently observed. The propagation of thrusting led to the formation of thrust-related folds which are best typified by Beitan major structure (Abdelkhalek et al. 1992; Abdeen et al. 2008). Other types of folds are shear zone-related. Overprinting relations between thrust-related folds and shear zone-related folds demonstrate that the former are in most case the older as documented in many deformed belts in the Eastern Desert, such as Mubarak–Baramiya belt, Um Nar-Gabal Elhadid Belt, and Wadi Khuda Belt.

14.3 Gneiss Domes Versus Metamorphic Core Complexes

The main structural feature of the Eastern Desert terrane comprises structural basement (lower and higher grade gneissic domes) overthrusted by structural cover nappes (lower grade volcaniclastic metasediments) (Sabet 1961; Akaad and El-Ramly 1960; El-Ramly 1972; El-Gaby 1983; El-Gaby et al. 1984, 1994; Kamal El Din et al. 1992; Khudeir et al. 1992, 1995; Kamal El Din 1993; Greiling et al. 1994; Akaad et al. 1996; El-Sayed et al. 1999, 2002; Ibrahim and Cosgrove 2001; Fritz et al. 1996, 2002, 2013; Fowler and Osman 2001; Bregar et al. 2002; Abdeen 2003; Abdeen and Greiling 2005; Fowler et al. 2007; Abd El-Wahed 2008; Youssef et al. 2009; Amer et al. 2010; Johnson et al. 2011; Abdeen et al. 2014; Abu Enen et al. 2016). The directions of nappe transport reported from the CED vary from top to the NE (e.g., El-Bayoumi and Greiling 1984), top to the NW (e.g., Ries et al. 1983; Greiling 1987), top to the SE (e.g., Kamal El Din et al. 1992), and top to the

SW (e.g., Abdeen et al. 2002; Abdelsalam et al. 2003). One remarkable feature of the Eastern Desert is the presence of a series of gneiss domes (e.g., Meatiq, Sibai, El-Shalul, Hafafit) surrounded by low-grade nappes (Fig. 34). Also, there are several gneissic windows in Sinai (e.g., Feiran–Solaf metamorphic complex: Abu Alam and Stuwe 2008; Kid area: Abu El-Enen et al. 2003; Blasband et al. 1997, 2000; Brooijmans et al. 2003; Eliwa et al. 2008; Taba area: Abu El-Enen et al. 2004; Eliwa et al. 2008). Abu Alam and Stuwe (2009) proposed that the fold-and-thrust deformation and exhumation of the Feiran–Solaf complex was a result of transpressional deformation and the NW-striking Najd Fault System exhuming the complex in an oblique transpressive regime.

The gneiss domes in the Eastern Desert terrane have been interpreted as metamorphic core complexes exhumed in extensional settings. The origin and mode of deformation and exhumation of these gneissic domes and their relation to the Najd Fault System are the subjects of many publications (e.g., Fritz et al. 1996, 2002, 2013; Loizenbauer et al. 2001; Bregar et al. 2002; Shalaby et al. 2005; Fowler et al. 2007; Abd El-Wahed 2008, 2014; Andresen et al. 2010; Fowler and Osman 2009; Abu Alam and Stüwe 2009; Abd El-Wahed and Kamh 2010; Shalaby 2010; Johnson et al. 2011; Abu Alam et al. 2014; Abd El-Wahed et al. 2016; Makroum 2017; Stern 2017; Hassan et al. 2016). Gneiss domes in Egypt are mostly bordered by NW-striking sinistral shear zones and low-angle normal faults (Fritz et al. 1996). Geochronology suggests that extension and exhumation of gneiss domes commenced around 620–606 Ma (Fritz et al. 2002; Andresen et al. 2009)

Within the Eastern Desert Terrane of Egypt, there is a general agreement on (i) significant NW–SE extension and crustal-scale thinning, (ii) NNW-thrust propagation and juxtaposition of low-grade volcano-sedimentary sequences against high-grade gneisses along extensional shears, and (iii) intense magmatic activity and emplacement of extension-related granitoids (Blasband et al. 2000; Fowler and El Kalioubi 2004; Fowler and Osman 2009; Andresen et al. 2010). But, the presence or absence of core complexes (e.g., Meatiq, Sibai, El-Shalul, and Hafafit) and the surrounding sinistral shear zones in the Eastern Desert is a matter of debate. Based on structural arguments and the succession of magmatic events, the gneiss domes were interpreted as a remobilized early Proterozoic older continental crust (Sturchio et al. 1983; El-Gaby et al. 1990, 1994; Hassan and Hashad 1990). Kinematically, four tectonic models were proposed to decipher origin, evolution, and exhumation of the gneiss-cored domes in the Eastern Desert: (1) development of fault-bend fold "antiformal stacks" (e.g., Hafafit domal structure; Greiling et al. 1988), (2) orogen-parallel crustal extension as a consequence of sinistral shearing along the NW-trending shear zones of the Najd Fault System (e.g., Hafafit, Sibai, El-Shalul and Meatiq domal structures; Wallbrecher et al. 1993; Fritz et al. 1996, 2002, 2013; Bregar et al. 2002; Loizenbauer et al. 2001; Abd El-Wahed 2008; Khudeir et al. 2008), (3) emplacement within regional domal structures (Ibrahim and Cosgrove 2001) followed by extension parallel to their fold axes (e.g., Sibai dome, Fowler et al. 2007), and (4) interference patterns of sheath folds (e.g., Hafafit domal structure, Fowler and El Kalioubi 2002). Shalaby (2010) assigned the development of the northern dome of Wadi Hafafit culmination to oblique

convergence in a scissor-like wrench corridor model not to regional-scale lithospheric extension associated with formation of core complexes.

14.4 The Conjugate Pairs of Najd-Related Shears

The structures in the Najd Fault zone were developed in response to a sinistral transpressional and transtensional tectonic regimes, with the axis of maximum compressional stress oriented at oblique angles to the NW-trending orogenic front (Fritz et al. 1996). Transpression resulted in formation of ESE- to ENE-shortening that produced NNW- to NW-trending folds throughout the Central Eastern Desert (Abd El-Wahed 2014). These are superimposed on early NNW-directed thrusts and related structures (Abdeen et al. 2014). The structures associated with the NW-sinistral shear zones are strongly superimposed by the NE-trending structures of the Mubarak–Barramiya shear belt that extends from Wadi Mubarak in the East to Wadi Barramiya in the west across the whole width of the CED forming a remarkable structural feature in the eastern desert of Egypt. This belt constitutes well-defined ophiolite-decorated linear belt where serpentinites represent the most characteristic lithological unit. It is oriented orthogonal to the major NW-trending fabric characterizing the CED. In the D_{2b}, D_{2b} is the NE-trending dextral transpression along Wadi Mubarak overprinted on D1 and D2a structures. D_{2b} structures include the NNE- to NE-trending WUSZ, NNE- and NE-trending (NNW-verging) folds, NNW-directed thrusts (Shalaby et al. 2005; Abd El-Wahed and Kamh 2010; Abd El-Wahed 2014). D_{2a} and D_{2b} represent a non-coaxial progressive event formed in a dextral NE- over NW-sinistral shear zone during a partitioned transpression in response to E–W-directed compression during oblique convergence between East and West Gondwana developed due to closure of the Mozambique Ocean and amalgamation of the Arabian–Nubian Shield in Cryogenian-early Ediacaran time (Abd El-Wahed and Kamh 2010; Abd El-Wahed 2014). Superimposition of the NW Najd-related shear zones by the NE-trending transpressional deformation (Fig. 30) demonstrates that both trends are not conjugate. In this framework, the entire Pan-African Belt of the Eastern Desert represents a megashear, called in the present study as the Eastern Desert Megashear (Fig. 36). This megashear exhibits sinistral sense of movement and the NE-trending shears were formed by the same way as the domino structure.

14.5 Role of Najd Shear System in Tectonic Evolution of Gneiss Domes

Another controversy in the Eastern Desert is about the role of sinistral shearing and transpression related to the Najd Fault System in the exhumation of these gneiss

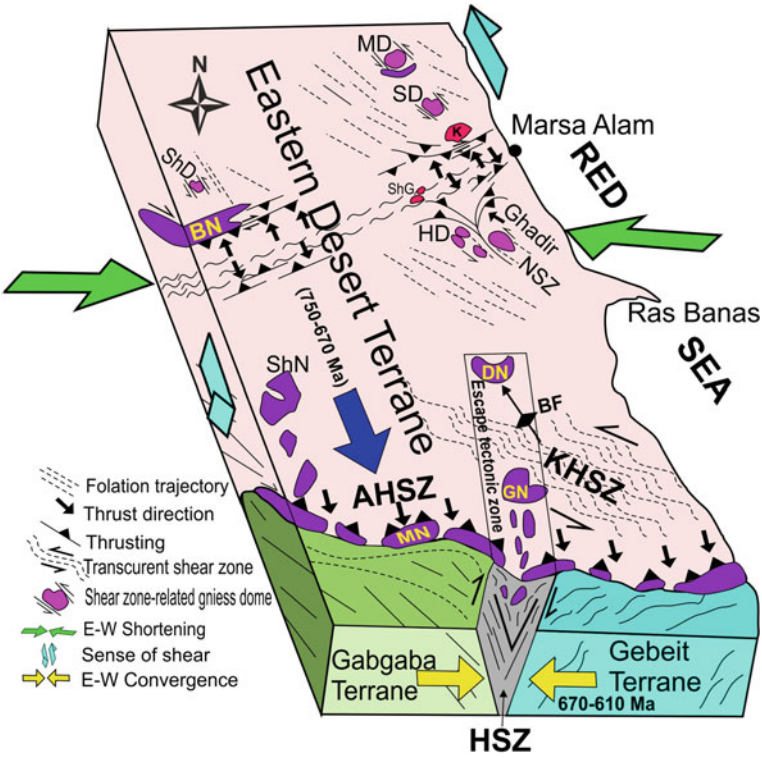

Fig. 36 Tectonic style sketch of the Southern and Central Eastern Desert. MD, Meatiq dome; SD, Sibai dome; HD, Hafafit dome, ShD, Shalul dome; K, Kadabbora granite; ShG, Sheikh Salem granite; BN, Barramiya nappe; NSZ, Nugrus shear zone; DN, Abu Dahr nappe; BF, Beitan fold; KHSZ, Kharit-Hodein shear zone; Gn, Gerf nappe; Mn, Moqsem nappe; ShN, Shilman nappe; AHSZ, Allaqi–Heiani shear zone; and HSZ, Hamisana shear zone

domes and in the crustal structure of the Central Eastern Desert. Northwest-striking shear zones and faults of the Najd Fault System are the dominant structural elements within the Afif–Hijaz and Midyan terranes of northwestern Saudi Arabia and the Eastern Desert terrane of Egypt. The Najd Fault System consists of brittle–ductile shears in a zone as much as 300 km wide and more than 1100 km long, extending across the northern part of the Arabian Shield and developed during the interval 540–620 Ma (Stern 1985). The Najd Fault System in Saudi Arabia extends northwest in the Central Eastern Desert of Egypt affecting the area between Duwi shear zone to the north and Kharit-Hodein shear zone to the south (Sultan et al. 1993; Abd El-Wahed 2014). The major shear zones bounding the gneiss domes have been interpreted as sinistral strike-slip shear zones combined with extensional shears that formed during exhumation of domes (e.g., Fritz et al. 1996, 2002) or as remnants of NW-directed thrusts (Andresen et al. 2010). Nowadays, sinistral shearing along the NW-trending shear zones of the Najd Fault System is genetically

linked with deposition of sediments, exhumation of gneiss domains, and emplacement of syn-tectonic granitoids (e.g., Fritz et al. 1996, 2002, 2013; Bregar et al. 2002; Shalaby et al. 2005; Abd El-Wahed 2008, 2010; Abd El-Wahed and Kamh 2010; Abdeen et al. 2014; Abd El-Wahed et al. 2016; Makroum 2017).

There are some points support the role of the Najd shear zones in the evolution and exhumation of core complexes in the Eastern Desert: (i) The large-scale, oblique transpressive shear zones of the Najd Fault System in the Eastern Desert and Sinai was developed during the second tectonometamorphic event (D2) occurred between 680 and 640 Ma (Johnson et al. 2011). During D_2 the Arabian–Nubian Shield collided with the Sahara Metacraton and moved toward the Paleo-Tethys ocean (Stern 1994), (ii) the gneiss domes is bounded by transtensional marginal shears linked by low-angle normal faults (Fritz et al. 1996, 2002, 2013), (iii) The oblique setting of the gneiss domes to the main NW-trending shear zones (Abu Alam et al. 2014), (iv) Exhumation history of the core complexes is accompanied by crustal thickening, development of molasse sedimentary basins (e.g., Kareim Basin to the north of Sibai core complex; Abd El-Wahed 2010), and (v) There is relationship between change of the Najd shear kinematics from transpressive to transtension through time and emplacement of transpressive- and transtension-related granitoids (655 and 645 Ma, respectively, Bregar et al. 2002; Abu Enen et al. 2016).

14.6 Rates and Transport Directions of Metaultramafic Nappes

Several metaultramafic nappes have been the subject matter of detailed field-structural studies in the Egyptian Eastern Desert. The largest nappe, not only in the Eastern Desert but also in the ANS as a whole, is the Gerf nappe which exists in a remarkable escape tectonic zone (Fig. 36) includes the southern tip of Hamisana Shear Zone and extends further north to Abu Dahr nappe that ranks the second after the Gerf nappe by volume. Other eye-catching nappes area is observed in Moqsem, Shilman, and Barramiya areas. Both Moqsem and Shiman nappes form part of an ophiolite-decorated belt defining the Allaqi–Heiani Suture which is itself regarded to represent the western extension of the greater Allaqi–Heiani–Onib–Sol Hamed–Yanbu (Abdelsalam and Stern 1996; Abdelsalam et al. 2003). However, the rates and directions of transport of these metaultramafic nappes are debatable, although there is a general agreement that these nappes follow two main directions in their transportation; W- (to WSW) and N- (to NNW-) direction. The first transport direction is mostly a consequence of the final assembly and accretion of the entire ANS to the Saharan Metacraton (SM) (Abdelsalam et al. 2011; Liégeois et al. 2013) which was concurrent with the assembly of eastern and western Gondwana during the late Cryogenian–Ediacaran (650–542 Ma). The second transport direction is linked to the N-directed tectonic escape of the ANS, and

proved by N- (to NNW-) trending stretched lineations. The rates of transportation of the metaultramafic nappes vary considerably from deformed belt to another in the Eastern Desert depending upon several factors, such as nappe size, shearing rate, and enveloping lithologies.

14.7 The Voluminous Intrusives in NED

Dissimilar to the Arabian Shield, the Nubian Shield had been invaded by anorogenic/within-plate magmatism (500–30 Ma) (El-Ramly and Hussein 1983; Abdel-Rahman and Martin 1987). The Pan-African basement of the NED of Egypt differs from the southern continuation by (1) voluminous calc-alkaline batholithic magmatism (635–590 Ma) and alkaline A-type magmatism (~600 Ma), (2) scarcity of older metasedimentary, metavolcanic, and ophiolitic rocks, (3) the absence of igneous activity younger than 475 Ma, and (4) the absence of megashear zone like the Najd-related shears (e.g., El-Ramly 1972; Engel et al. 1980; Ries et al. 1983; Bentor 1985; Stern and Hedge 1985; Abdel-Rahman and Martin 1987; Beyth et al. 1994; Cosca et al. 1999; Garfunkel 1999).

The voluminous magmatism of the NED includes: (1) batholithic post-collisional high-K calc-alkaline plutons (~635–590 Ma) of granodiorite and monzogranite, as well as some minor gabbros and quartz-diorites; and (2) within-plate alkaline to peralkaline high-level plutons and the associated bimodal (mafic–felsic) volcanic rocks and dyke swarms of similar age (~608–580 Ma) and geochemical affinity (e.g., Garfunkel 1999; Jarrar et al. 2003, 2004; Katzir et al. 2006, 2007a, b; Be'eri-Shlevin et al. 2009b). These magmas intruded the older deformed island arc complexes of c. 820–740 Ma (e.g., Be'eri-Shlevin 2009, and references therein). In the post-collisional calc-alkaline suite, the voluminous pulse of granodiorite to granite intrusions (610–600 Ma) characterized the change from mafic to felsic magmatism in most of the northeastern African region. Contemporaneously, the alkaline magmatism commenced at the peak of the latter calc-alkaline activity at ~608 Ma and had continued to ~580 Ma (Be'eri-Shlevin 2009).

The calc-alkaline magmatic suite of the NED is generally characterized by low initial $^{87}Sr/^{86}Sr$ ratios, low-Nb contents, and progression from intermediate to felsic calc-alkaline magmatism. Accordingly, the NED crustal segment can be compared to the modern continental arc magmatic suits, such as the Cordilleran magmatic suite (e.g., Abdel-Rahman and Martin 1987). The cease of subduction is characterized by alkaline/within-plate magmatism that emplaced into the orogenic calc-alkaline suite. Accordingly, a continental margin tectonomagmatic model (e.g., western North America) can be adopted for the NED crustal evolution.

The voluminous post-collisional magmatism in the NED/northernmost ANS is possibly the result of cratonization of the juvenile crust. According to Jackson (1986), the post-collisional magmatic activity in the ANS has generated large volumes of melt from crust and mantle. Černý (1991) proposed that peraluminous

A-type granitoids were generated by partial melting of undepleted (possible the ANS oceanic crust), previously unmelted, crustal sources. The first volumetrically important melting event of the ANS crust was most likely during the post-collisional magmatic activity (610–530 Ma) (e.g., Kuster 2009). The voluminous felsic magmatism took place during a period of ~40–45 Ma and was interpreted to represent the migration of melting zone from mantle to lower crustal levels (Be'eri-Shlevin et al. 2009). The latter felsic magmatism could lead to the internal differentiation of the ANS juvenile crust and cratonization of the nascent shield (e.g., Kuster 2009). The post-collisional setting of the NED voluminous magmatism can be supported by (1) the absence of arc formation in the northernmost ANS at ca 620–600 Ma, and (2) the absence of subduction-related features (e.g., accretionary prisms, paired metamorphic belts and linear alignment of calc-alkaline intrusions and volcanic rocks) (e.g., Be'eri-Shlevin et al. 2009).

14.8 The Post-amalgamation Hammamat Sediments and Their Relation to Dokhan Volcanics

Post-amalgamation depositional basins (each of which covers a surface area from 200 to 72,000 km^2) occur in some forty areas in the ANS (e.g., Abdeen et al. 1992; Johnson 2003; Matsah and Kusky 1999, 2001; Willis et al. 1988; Johnson and Woldehaimanot 2003; Abdeen and Greiling 2005; Eliwa et al. 2006, 2010; Hamimi et al. 2012b, 2013a, b, 2014; Hamimi and Kattu 2014). These basins encompass slightly to moderately metamorphosed, and at the same time variably deformed, volcano-sedimentary successions that were deposited after 650 Ma over newly amalgamated arc terranes (Johnson et al. 2011). They are commonly structurally controlled (fault-controlled down sags, pull aparts, rifts, half-grabens, thrusting, normal faulting, magmatic doming, etc.) (e.g., Abdeen and Greiling 2005; Shalaby et al. 2006; Hamimi et al. 2014), and autochthonous as attested by their unconformable basal contacts vs. older basement rocks. Depending on their carbonate succession, relative abundances of gray–green and red–purple rocks and other sedimentary structures, Johnson and Woldehaimanot (2003) subdivided these basins into marine, terrestrial and mixed terrestrial–marine basins. Marine post-amalgamation basins are prominent in the eastern part of the ANS, such as in Murdama, Bani Ghayy, Fatima, and Ablah areas.

In NED and CED, the post-amalgamation Hammamat basins (590–585 Ma depositional age, Rice et al. 1993) are epicontinental and showing mostly NW–SE and N–S directions (Rice et al. 1993; Abdeen and Greiling 2005). The sedimentary section of the Hammamat sediments in the type locality reaches up to 4000 m. It comprises polymictic conglomerates, gritstone, sandstone, siltstone, claystone, and rare limestone intercalated with volcaniclastic layers (Akaad and Now-eir 1969, 1980). The Hammamat sediments have been deposited in three main types of basins (Abd El-Wahed 2010) including foreland, intermontane (El-Gaby et al. 1990), and

strike-slip basins (Fritz and Messner 1999). They were deposited by alluvial fan and braided stream systems in intermontane (Grothaus et al. 1979) and foreland basins (El-Gaby et al. 1988) formed during the late stage of the Pan-African orogeny. The Hammamat sediments were deposited in late Precambrian after the eruption of subduction-related Dokhan Volcanics of andesitic to rhyolitic composition (Eliwa et al. 2006) and prior to the emplacement of the post-orogenic granitoids (Akaad and Noweir 1980). Hamimi et al. (2014) believed that the Hammamat basins are fault-bounded basins affected by a NW–SE- to NNW–SSE-oriented shortening phase just after the deposition of the molasse sediments, proved by NW- to NNW-verging folds and SE- to SSE-dipping thrusts that were refolded and thrusted in the same direction. The shortening phase in the Hammamat was followed by a transpressional wrenching phase related to the Najd Shear System, which resulted in the formation of NW–SE sinistral-slip faults associated with positive flower structures that comprise NE-verging folds and SW-dipping thrusts.

The Hammamat sediments show nearly the same deformation patterns and underwent the same deformation history of the post-amalgamation marine sediments in Western Arabia (Hamimi et al. 2014). The only exception is the absence of the earlier-formed structures (D_1) that predating the conspicuous transpressional phase (D_2) and formed due to the effect of an early E–W (to ENE–WSW) shortening phase accompanied with the convergence between East and West Gondwana. Such a conclusion is attested by MRL and CESS quantitative strain calculations. A general agreement is established that the deposition of the Hammamat was after the eruption of subduction-related Dokhan Volcanics (El-Gaby et al. 1988) and prior to the emplacement of the post-orogenic granitoids (Akaad and Noweir 1980).

14.9 Northward Decrease in Intensity of Deformation

One of the most amazing issues in dealing with the tectonics of the Pan-African Belt of the Egyptian Eastern Desert is the northward decrease in intensity of deformation. Although this point will be the subject matter of detailed investigation and will be addressed in the near future, the wealth of collected data from key areas in CED and SED attribute such variation in the intensity of deformation to several factors such as (1) presence of the Allaqi–Heiani suture zone at the southern end of the SED, (2) the NNE-SSW convergence of the Eastern Desert terrane (750–670 Ma) with the Gabgaba and Gebeit terranes, and (3) the effect of the N- to NNE-oriented Hamisana Shear Zone which in fact concomitant with the N-directed escape of the entire ANS.

References

Abd El-Naby H, Frisch W (2006) Geochemical constraints from the Hafafit Metamorphic Complex (HMC): evidence of Neoproterozoic back-arc basin development in the central Eastern Desert of Egypt. J Afr Earth Sci 45:173–186

Abd El-Rahman Y, Polat A, Dilek Y, Fryer BJ, El-Sharkawy M, Sakran S (2009a) Geochemistry and tectonic evolution of the Neoproterozoic Wadi Ghadir ophiolite, Eastern Desert, Egypt. Lithos 113:158–178

Abd El-Rahman Y, Polat A, Dilek Y, Fryer BJ, El-Sharkawy M, Sakran S (2009b) Geochemistry and tectonic evolution of the Neoproterozoic incipient arc–forearc crust in the Fawakhir area, Central Eastern Desert of Egypt. Precambr Res 175:116–134

Abd El-Wahed MA (2007) Pan-African strike-slip tectonics of Wadi El-Dabbah area, north Sibai core complex, Central Eastern Desert, Egypt. Ann Egypt Geol Surv 29:1–36

Abd El-Wahed MA (2008) Thrusting and transpressional shearing in the Pan-African nappe southwest El-Sibai core complex, Central Eastern Desert, Egypt. J Afr Earth Sci 50:16–36

Abd El-Wahed MA (2010) The role of the Najd fault system in the tectonic evolution of the Hammamat molasse sediments, Eastern Desert, Egypt. Arab J Geosci 3:1–26

Abd El-Wahed MA (2014) Oppositely dipping thrusts and transpressional imbricate zone in the Central Eastern Desert of Egypt. J Afr Earth Sci 100:42–59

Abd El-Wahed MA, Abu Anbar MM (2009) Syn-oblique convergent and extensional deformation and metamorphism in the Neoproterozoic rocks along Wadi Fatira shear zone, Northern Eastern Desert, Egypt. Arab J Geosci 2:29–52

Abd El-Wahed MA, Kamh SZ (2010) Pan-African dextral transpressive duplex and flower structure in the Central Eastern Desert of Egypt. Gondwana Res 18:315–336

Abd El-Wahed MA, Kamh SZ (2013) Evolution of conjugate strike-slip duplexes and wrench-related folding in the Central part of Al Jabal Al Ahkdar, NE Libya. J Geol 12 (2):173–195

Abd El-Wahed MA, Harraz HZ, El-Behairy MH (2016) Transpressional imbricate thrust zones controlling gold mineralization in the Central Eastern Desert of Egypt. Ore Geol Rev 78:424–446

Abdeen MM (2003) Tectonic history of the Pan-African orogeny in Um Gheig area, central Eastern Desert, Egypt. Egypt J Geol 47(1):239–254

Abdeen MM, Abdelghaffar AA (2011) Syn- and post-accretionary structures in the Neoproterozoic Central Allaqi-Heiani suture zone, Southeastern Egypt. Precambr Res 185:95–108

Abdeen MM, Greiling RO (2005) A quantitative structural study of late Pan-African compressional deformation in the Central Eastern Desert (Egypt) during Gondwana assembly. Gondwana Res 8(4):457–471

Abdeen MM, Dardir AA, Greiling RO (1992) Geological and structural evolution of the Wadi Queih Area (N Quseir), Pan-African basement of the Eastern Desert of Egypt. Zbl Geol Palfiontol Teil I:2653–2659

Abdeen MM, Allison TK, Abdelsalam MG, Stern RJ (2001) Application of ASTER band-ratio images for geological mapping in arid regions; the Neoproterozoic Allaqi Suture, Egypt. Abstr. Program Geol. Soc. Am. 3:289

Abdeen MM, Abdelsalam MG, Dowidar HM, Abdelghaffar AA (2002) Varying structural style along the Neo-Proterozoic Allaqi-Heiani suture, Southern Egypt. In: 19th Colloquium of African Geology. El Jadida, Morocco. (Abstract)

Abdeen MM, Sadek MF, Greiling RO (2008) Thrusting and multiple folding in the neoproterozoic pan-African basement of Wadi Hodein area, south Eastern Desert, Egypt. J Afr Earth Sci 52:21–29

Abdeen MM, Greiling RO, Sadek MF, Hamad SS (2014) Magnetic fabrics and Pan-African structural evolution in the Najd Fault corridor in the Eastern Desert of Egypt. J Afr Earth Sci 99:93–108

Abdel Khalek ML (1979) Tectonic evolution of the basement rocks in the Southern and Central Eastern Desert of Egypt. Bull Inst Appl Geol 3(1):53–62. (King Abdel Aziz University, Jeddah)

Abdel Khalek ML, Takla MA, Sehim A, Hamimi Z, El Manawi AW (1992) Geology and tectonic evolution of Wadi Beitan area, south Eastern Desert, Egypt. In: International Conference Geology. The Arab World, Cairo University, Egypt (GAW1), pp 369–393

Abdel Khalek ML, Takla MA, Sehim A, Abdel Wahed M, Hamimi Z, Sakran Sh (1999) Geology and tectonic evolution of the shield rocks, East Wadi Beitan area, south Eastern Desert, Egypt. Egypt J Geol 43(1):1–15

Abdel Rahman AM (1996) Pan-African volcanism: petrology and geochemistry of the Dokhan volcanic suite in the northern Nubian shield. Geol Mag 133:17–31

Abdel Rahman AM, El-Kibbi MM (2001) Anorogenic magmatism: chemical evolution of the Mount El-Sibai A-type complex (Egypt), and implications for the origin of within-plate felsic magmas. Geol Mag 138:67–85

Abdel Rahman AM, Martin RF (1987) Late Pan-African magmatism and crustal development in northeastern Egypt. Geol J 22:281–301

Abdel Wahed AA, Ali KG, Khalil MMA, Abdel Gawad A (2012) Dokhan volcanics of Gabal Monqul area, North Eastern Desert, Egypt: geochemistry and petrogenesis. Arab J Geosci 5:29–44

Abdelsalam MG (1994) The Oko shear zone: post-accretionary deformation in the Arabian-Nubian shield. J Geol Soc, London 151:767–776

Abdelsalam MG, Stern RJ (1996) Sutures and shear zones in the Arabian-nubian shield. J Afr Earth Sci 23:289–310

Abdelsalam MG, Abdeen MM, Dowaidar HM, Stern RJ, Abdelghaffar AA (2003) Structural evolution of the Neoproterozoic Western Allaqi-Heiani suture, southeastern Egypt. Precambr Res 124:87–104

Abdelsalam MG, Gao SS, Liégeois J-P (2011) Upper mantle structure of the Saharan metacraton. J Afr Earth Sci 60:328–336

Aboelkhair H, Yoshiki N, Yasushi W, Isao S (2010) Processing and interpretation of ASTER TIR data for mapping of rare-metal-enriched albite granitoids in the Central Eastern Desert of Egypt. J Afr Earth Sci 58(1):141–618

Abou El-Magd K, Emam A, Ali-Bik MW (2013) Chemostratigraphy, petrography and remote sensing characterization of the Middle Miocene-Holocene sediments of Ras Banas peninsula, Red Sea Coast, Egypt. Carpathian J Earth Environ Sci 8(3):27–42

Abou El-Magd I, Mohy H, Basta F (2015) Application of remote sensing for gold exploration in the Fawakhir area, Central Eastern Desert of Egypt. Arab J Geosci 8(6):3523–3536

Abu El-Ela FF (1997) Geochemistry of an island-arc volcanic suit: Wadi Dabr intrusive complex, Eastern Desert, Egypt. J Afr Earth Sci 24:473–496

Abu El-Enen MM, Okrusch M, Will TM (2003) Metapelitic assemblages in the Zariq schists, central western Kid Belt, Sinai Peninsula, Egypt. Neues Jahrbuch Mineralogie Abhandlungen 178:277–306

Abu El-Enen MM, Okrusch M, Will TM (2004) P-T evolution of the Taba metamorphic belt, Egypt: constraints from the metapelite assemblages. J Afr Earth Sci 38:59–78

Abu El-Enen MM, Abu-Alam TS, Whitehouse MJ, Ali K, Okrusch M (2016) P-T path and timing of crustal thickening during amalgamation of East and West Gondwana: a case study from the Hafafit Metamorphic Complex, Eastern Desert of Egypt. Lithos 263:213–238

Abu-Alam TS, Stüwe K (2008) Metamorphic evolution of the Wadi Feiran-Solaf core complex, Sinai, Egypt. J Alpine Geol 49:2. (PANGEO-Austria 2008)

Abu-Alam TS, Stüwe K (2009) Exhumation during oblique transpression: the Feiran-Solaf region, Egypt. J Metamorph Geol 27:439–459

Abu-Alam TS, Hassan M, Stüwe K, Meyer S, Passchier C (2014) Multistage tectonism during Gondwana collision: Baladiyah Complex, Saudi Arabia. J Petrol 55:1941–1964

Ahmed AH (2013) Highly depleted harzburgite–dunite–chromitite complexes from the Neoproterozoic ophiolite, south Eastern Desert, Egypt: a possible recycled upper mantle lithosphere. Precambr Res 233:173–192

Ahmed AH, Arai S, Attia AK (2001) Petrological characteristics of podiform chromitites and associated peridotites of the Pan African ophiolite complexes of Egypt. Miner Deposita 36:72–84

Akaad MK (1996) Rock succession of the basement: an autobiography and assessment. In: The Egyptian geological survey, centennial conference, paper no 71, p 87

Akaad MK (1997) On the behavior of serpentinites and its implications. Geol Surv Egypt, Paper, p 74

Akaad MK, Abu El Ela AM (2002) Geology of the basement rocks in the eastern half of the belt between latitudes 25 30′ and 26 30′ N Central Eastern Desert. Egypt, Geol Surv Egypt, p 78

Akaad MK, El Ramly MF (1960) Geological history and classification of the basement rocks of the central Eastern Desert of Egypt. Geol Surv Egypt 9:24

Akaad MK, Noweir AM (1969) Lithostratigraphy of the Hammamat-Umm Seleimat district, Eastern Desert of Egypt. Nature 223:284–285

Akaad MK, Noweir AM (1977) The post Hammamat felsites and their age relation with the younger granites of Egypt. Proc Acad Sci 30:163–168

Akaad MK, Noweir AM (1980) Geology and lithostratigraphy of the Arabian Desert orogenic belt of Egypt between latitudes 25 35′ S and 26°30′ N. Inst Appl Geol Jeddah Bull 3:127–135

Akaad MK, Noweir AM, Kotb H (1979) Geology and petrochemsitry of the granite association of the Arabian Desert Orogenic Belt of Egypt between 25 35′ and 26°30′. Delta J Sci 3:107–151

Akaad MK, Abu El Ela AM, El Kamshoshy HI (1993) Geology of the region West of Mersa Alam, Eastern Desert, Egypt. Ann Egypt Geol Surv 19:1–18

Akaad MK, Nowei AM, Abu El-Ela AM (1996) Geology of the Pan-African basement rocks of the Jabal al Hadid–Wadi Mubarak district, Eastern Desert, Egypt. Geol Surv Egypt 73:78

Akawy A (2003) Fault characterization and paleostress analysis in the Precambrian rocks west of the Meatiq Dome, Central Eastern Desert, Egypt. Neues Jahrbuch Mineralogie Abhandlungen 228:135

Akawy A (2007) Geometry and texture of quartz veins in Wadi Atalla area, Central Eastern Desert. J Afr Earth Sci 47:73–87

Al-Husseini M (2000) Origin of the Arabian plate structures: Amar collision and Najd rift. Geo Arabia 5:527–542

Ali KA, Stern RJ, Manton WI, Kimura J-I Khamees HA (2009) Geochemistry, Nd isotopes and U–Pb SHRIMP dating of Neoproterozoic volcanic rocks from the Central Eastern Desert of Egypt: new insights into the 750 Ma crust-forming event. Precambr Res 171:1–22

Ali KA, Azer MK, Gahlan HA, Wilde SA, Samuel MD, Stern RJ (2010) Age constraints on the formation and emplacement of Neoproterozoic ophiolites along the Allaqi-Heiani Suture, South Eastern Desert of Egypt. Gondwana Res 18:583–595

Ali KA, Andresen A, Stern RJ, Manton WI, Omar SA, Maurice AE (2012) U-Pb zircon and Sr–Nd–Hf isotopic evidence for a juvenile origin of the c 634 Ma El-Shalul Granite, Central Eastern Desert, Egypt. Geol Mag 149:783–797

Ali K, Wilde S, Stern RJ, Moghazi A, Mahbubul Ameen S (2013) Hf isotopic composition of single zircons from Neoproterozoic arc volcanics and post-collision granites, Eastern Desert of Egypt: implications for crustal growth and recycling in the Arabian-Nubian Shield. Precambr Res 239:42–55

Ali KA, Kröner A, Hegner E, Wong J, Li S, Gahlan HA, Abu El Ela F (2015) U-Pb zircon geochronology and Hf–Nd isotopic systematics of Wadi Beitan granitoid gneisses, South Eastern Desert, Egypt. Gondwana Res 27:811–824

Ali-Bik MW, Taman Z, El Kalioubi B, Abdel Wahab W (2012) Serpentinite-hosted talc–magnesite deposits of Wadi Barramiya area, Eastern Desert, Egypt: Characteristics, petrogenesis and evolution. J Afr Earth Sci 64:77–89

Ali-Bik MW, Sadek MF, Ghabrial DS (2014) Late Neoproterozoic metamorphic assemblages along the Pan-African Hamisana Shear Zone, southeastern Egypt: Metamorphism, geochemistry and petrogenesis. J Afr Earth Sci 99:24–38

Amer RM, Kusky TM, Ghulam A (2010) New methods of processing ASTER data for lithological mapping. Examples from Fawakhir, Central Eastern Desert of Egypt. J Afr Earth Sci 56:75–82

Andresen A, Abu El-Rus MA, Myhre PI, Boghdady GY, Corfu F (2009) U-Pb TIMS age constraints on the evolution of the Neoproterozoic Meatiq Gneiss Dome, Eastern Desert, Egypt. Int J Earth Sci (Geol Rundsch) 98:481–497

Andresen A, Augland LE, Boghdady GY, Elnady OM, Lundmark AM, Hassan MA, Abu El-Rus MA (2010) Structural constraints on the evolution of the Meatiq Gneiss Dome (Egypt), East African Orogen. J Afr Earth Sci 57:413–422

Anonymous (1972) Penrose field conference on ophiolites. Geotimes 17:24–25

Asran AM, Kabesh M (2003) Evolution and geochemical studies on a stromatic migmatite-amphibolite association in Hafafit area CED Egypt. Egypt J Geol 47:1–24

Asran AM, Rkh Bekir, Abdel Rahman E, Abdel El-Rashed A (2013) Petrology, geochemistry and remote sensing data of island arc assemblage along Wadi Abu Marawat, Central Eastern Desert, Egypt. Arab J Geosci 6:2285–2298

Augland LE, Andresen A, Boghdady GY (2012) U-Pb ID-TIMS dating of igneous and metaigneous rocks from the El-Sibai area: time constraints on the tectonic evolution of the Central Eastern Desert, Egypt. Int J Earth Sci 101:25–37

Azer MK, Stern RJ (2007) Neoproterozoic (835–720 Ma) serpentinites in the Eastern Desert, Egypt: fragments of fore-arc mantle. J Geol 115:457–472

Azer MK, Obeid M, Gahlan HA (2016) Late Neoproterozoic layered mafic intrusion of arc-affinity in the Arabian-Nubian Shield: a case study from the Shahira layered mafic intrusion, southern Sinai, Egypt. Geol Acta 14:237–259

Azza M, Hosny A, Gharib A (2012) Rupture process of Shallow Earthquakes of Abou-Dabbab Area, South East of Egypt. Egypt J Appl Geophys 11(1):85–100

Badawy A, El-Hady Sh, Abdel-Fattah AK (2008) Microearthquakes and neoteconics of Abu-Dabbab, Eastern Desert of Egypt. Seismol Res Lett 79(1):55–67

Basta EZ, Kotb H, Awadallah MF (1980) Petrochemical and geochemical characteristics of the Dokhan Formation at the type locality, Gabal Dokhan, Eastern Desert, Egypt. Bull Inst Appl Geol 4(3):121–140 King Abdel Aziz University, Jeddah

Be'eri-Shlevin Y, Katzir Y, Whitehouse MJ, Kleinhanns IC (2009a) Contribution of pre Pan-African crust to formation of the Arabian Nubian Shield: new secondary ionization mass spectrometry U-Pb and O studies of zircon. Geol Soc Am 37(10):899–902

Be'eri-Shlevin Y, Katzir Y, Whitehouse M (2009b) Postcollisional tectono-magmatic evolution in the northern Arabian-Nubian Shield (ANS): time constraints from ion probe U-Pb dating of zircon. J Geol Soc London 166(1):71–8

Be'eri-Shlevin Y, Samuel MD, Azer MK, Rämö OT, Whitehouse MJ, Moussa HE (2011) The Ediacaran Ferani and Rutig volcano-sedimentary successions of the northernmost Arabian–Nubian Shield (ANS): new insights from zircon U-Pb geochronology, geochemistry and O-Nd isotope ratios. Precambr Res 188:21–44

Bennett JD, Mosley PN (1987) Tiered-tectonics and evolution, Eastern Desert and Sinai. In: Matheis G, Schandelmeier H (eds) Current research in African earth sciences. Balkema, Rotterdam, pp 79–82

Bentor YK (1985) The crustal evolution of the Arabian-Nubian Massif with special reference to the Sinai Peninsula. Precambr Res 28:1–74

Berhe SM (1990) Ophiolites in northeast and east Africa: implications for Proterozoic crustal growth. J Geol Soc 147:41–57

Beyth M, Stern RJ, Altherr R, Kroner A (1994) The late Precambrian Timna igneous complex, Southern Israel: evidence for comagmatic-type sanukitoid monzodiorite and alkali granite magma. Lithos 31:103–124

Blasband B, Brooijmans P, Dirks P, Visser W, White S (1997) A pan-African core complex in the Sinai, Egypt. Geologie en Mijnbouw 76:247–266

Blasband B, White S, Brooijmans P, De Brooder H, Visser W (2000) Late Proterozoic extensional collapse in Arabian-Nubian Shield. J Geol Soc 157:615–628

Bregar M, Bauernhofer A, Pelz K, Kloetzli U, Fritz H, Neumayr P (2002) A late Neoproterozoic magmatic core complex in the Eastern Desert of Egypt; emplacement of granitoids in a wrench-tectonic setting. Precambr Res 118:59–82

Breitkreuz C, Eliwa H, Khalaf I, El Gameel K, Bühler B, Sergeev S, Larionov A (2010) Neoproterozoic SHRIMP U-Pb zircon ages of silica-rich Dokhan Volcanics in the northeastern Desert, Egypt. Precambr Res 182:163–174

Brooijmans P, Blasband B, White SH, Visser WJ, Dirks P (2003) Geothermobarometric evidence for a metamorphic core complex in Sinai, Egypt. Precambr Res 123:249–268

Brown GB (1972) Tectonic map of the Arabian Peninsula. Saudi Arabian Directorate General of Mineral Resources Map AP-2, Scale 1:4,000,000

Brown GF, Jackson RO (1960) The Arabian shield. In: XIX international geological congress, Pt. 9, pp 69–77

Bulter CA, Holdsworth RE, Strachan RA (1995) Evidence for Caledonian sinistral strike-slip motion and associated fault zone weakening, Outer Hebrides Fault Zone, NW Scotland. J Geol Soc 152:743–746

Černý P (1991) Fertile granites of Precambrian rare-element pegmatite fields: is geochemistry controlled by tectonic setting or source lithologies? Precambr Res 51:429–468

Chetty TRK, Bhaskar Rao YJ (2006) The Cauvery Shear Zone, Southern Granulite Terrain, India: a crustal-scale flower structure. Gondwana Res 10(1–2):77–85

Clark RN (1999) Spectroscopy of rocks, and minerals and principles of spectroscopy. In: Rencz AN, Ryerson RA (eds) Remote sensing for the earth sciences, manual of remote sensing, 3rd edn. Wiley, New York, NY, pp 3–58

Collins AS, Pisarevsky SA (2005) Amalgamating eastern Gondwana: the evolution of the Circum-Indian Orogens. Earth Sci Rev 71(3–4):229–270

Cosca MA, Shimron A, Caby R (1999) Late Precambrian metamorphism and cooling in the Arabian-Nubian Shield: petrology and 40Ar/39Ar geochronology of metamorphic rocks of the Elat area (Southern Israel). Precambr Res 98:107–127

Coward MP (1990) Shear Zones at the Laxford Front, NW Scotland and their significance in the interpretation of lower crust structure. J Geol Soc 147:279–286

Crane RB (1971) Preprocessing techniques to reduce atmospheric and sensor variability in multispectral scanner data. In: Proceedings of 7th International Symposium Remote Sensing Environment Ann Arbor Michigan 2, pp 1345–1355

Daggett PH, Morgan P, Boulos FK, Hennin SF, El-Sherif AA, El Sayed AA, Basta NZ, Melek YS (1986) Seismicity and active tectonics of the Egyptian Red Sea margin and the northern Red Sea. Tectonophysics 125:313–324

David WL, Wooil MM (2012) Landsat-TM-Based discrimination of lithological units associated with the Purtuniq Ophiolite, Quebec, Canada. Remote Sens 4:1208–1231

de Wall H, Greiling RO, Sadek MF (2001) Post-collisional shortening in the late Pan-African Hamisana high strain zone, SE Egypt: field and magnetic fabric evidence. Precambr Res 107:179–194

Dewey JF, Holdsworth RE, Strachan RA (1998) Transpression and transtension zones. In: Holdsworth RE, Strachan RA, Dewey JE (eds) Continental transpressional and transtensional tectonics. J Geol Soc 135:1–14

Di Tommaso I, Rubinstein N (2007) Hydrothermal alteration mapping using ASTER data in the Infiernillo porphyry deposit, Argentina. Ore Geol Rev 32:275–290

Dixon TH (1981) Age and chemical characteristics of some pre-Pan-African rocks in the Egyptian shield. Precambr Res 14:119–133

Dixon TH, Stern RJ, Hussein IM (1987) Control of red sea rift geometry by Precambrian Structures. Tectonics 6:551–571

Doblas M, Faulkner D, Mahecha V, Aparicio A, Lopez-Ruiz J, Hoyos M (1997) Morphologically ductile criteria for the sense of movement on slickensides from an extensional detachment fault in Southern Spain. J Struct Geol 19:1045–1054

Drury S (1987) Image interpretation in geology. Allen & Unwin, London, p 243
Drury S (1993) Image interpretation in geology, 2nd edn. Chapman and Hall, London
Drury S (2013) The East African orogen: neoproterozoic tectonics on display. Research news from the Earth Sciences, Earth-pages. https://earth-pages.co.uk/2013/09/19/the-east-african-orogen-neoproterozoic-tectonics-on-display/
Egyptian Geological Survey and Mining Authority (EGSMA) (1996) Geological map of Wadi Jabjahah Quadrangle, Egypt, Scale 1:250.000
El Khrepy S, Koulakov I, Al-Arifi N (2015) Crustal Structure in the area of the cannon earthquakes of Abu Dabbab (Northern Red Sea, Egypt), from seismic tomography inversion. Bull Seismo Soc Am 105(4): 13. http://dx.doi.org/10.1785/ 0120140333
El Mahallawi MM, Ahmed AF (2012) Late Proterozoic older granitoids from the North Eastern desert of Egypt: petrogenesis and geodynamic implications. Arab J Geosci 5:15–27
El-Bayoumi RM, Greiling R (1984) Tectonic evolution of a Pan-African plate margin in southeastern Egypt—a suture zone overprinted by low angle thrusting? In: Klerkx J, Michot J (eds), African geology. Tervuren, pp 47–56
El-Bialy MZ, Omar MM (2015) Spatial association of Neoproterozoic continental arc I-type and post-collision a-type granitoids in the Arabian-Nubian Shield: the Wadi Al-Baroud older and younger granites, North Eastern Desert, Egypt. J Afr Earth Sci 103:1–29
El-Gaby S (1975) Petrochemistry and geochemistry of some granites from Egypt. Neues Jahrbuch für Mineralogie Abhandlungen 124:147–189
El-Gaby S (1983) Architecture of the Egyptian basement complex. In: Riad lS, Baars DL (eds) Proceedings of 5th international conference on basement tectonics, Cairo University, Egypt, pp 1–8
El-Gaby S, El Nady O, Khudeir A (1984) Tectonic evolution of the basement complex in the central Eastern Desert of Egypt. Geol Rundsch 73:1019–1036
El-Gaby S, List FK, Tehrani R (1988) Geology, evolution and metallogenesis of the pan-African Belt in Egypt. In: El-Gaby S, Greiling RO (eds) The pan-African belt of Northeast Africa and adjacent areas. Vieweg & Sohn, Weisbaden, pp 17–68
El-Gaby S, Khudier AA, El Taky M (1989) The Dokhan volcanics of wadi Queh area, Central Eastern Desert, Egypt. In: 1st conference on geochemistry, Alexandria, Egypt, pp 42–62
El-Gaby S, List FK, Tehrani R (1990) The basement complex of the Eastern Desert and Sinai. In: Said R (ed) The geology of Egypt. Balkema, Rotterdam, pp 175–184
El-Gaby S, Khudeir AA, Abdel Tawab M, Atalla RF (1991) The metamorphosed volcanosedimentary succession of Wadi Kid, Southeastern Sinai, Egypt. Ann Geol Surv Egypt 17:19–35
El-Gaby S, El Aref M, Khudeir A, El Habbak G (1994) Geology and genesis of banded iron formation at Wadi Kareim, Eastern Desert, Egypt. 7th Ann Meeting, Min Soc, Egypt. Abstract
El-Hady ShM (1993) Geothermal Evolution of the red sea margin and its relation to Earthquake Activity. M.Sc. thesis, Cairo University, Cairo, Egypt
Eliwa HA, Kimura JI, Itaya T (2006) Late Neoproterozoic Dokhan Volcanics, N Eastern Desert, Egypt: geochemistry and petrogenesis. Precambr Res 151:31–52
Eliwa HA, Abu El-Enen MM, Khalaf IM, Itaya T, Murata M (2008) Metamorphic evolution of Neoproterozoic metapelites and gneisses in Sinai, Egypt: insights from petrology, mineral chemistry and K-Ar age dating. J Afr Earth Sci 51:107–122
Eliwa H, Breitkreuz C, Khalaf I, El Gameel K (2010) Depositional styles of early Ediacaran terrestrial volcanosedimentary succession in Gebel El Urf area, N Eastern Desert, Egypt. J Afr Earth Sci 57:328–344
El-Kalioubi BA, Osman AF (1996) Petrological and structural aspects of the mylonitized felsite at Wadi Atalla, Central Eastern Desert, Egypt. Proc Geol Surv Egypt 159–184
El-Kazzaz YA (1999) Active faulting along along Qena-Safaga road. In: The first international conference on the geology of Africa, p 2
El-Kazzaz YA, Hamimi Z (1999) Polyphase deformation of Wadi Murra, south Eastern Desert, Egypt. Int Conf Geol Afr 1(1):353–368 Assiut University

El-Kazzaz YA, Hamimi Z (2000) Temporal and spatial relationships of Abu Fas geologic structures, south Eastern Desert, Egypt. In: Fifth international conference of geology of Arab world, Cairo University, Egypt, (GAW5), pp 619–634

El-Kazzaz YA, Taylor WE (2000) Tectonic evolution of the Allaqi Shear Zone and implications for the pan-African terrain amalgamation in the South Eastern Desert of Egypt. J Afr Earth Sci 33(2):177–197

El-Rabaa SM, Al-Shumaimri MS, Al-Mishwat AT (2001) Fate of the Najd fault system in northwestern Saudi Arabia and southwestern Jordan. Gondwana Res 4:164–165

El-Ramly MF (1972) A new geological map for the basement rocks in the Eastern and Southwestern Deserts of Egypt. Ann Geol Surv Egypt 2:1–18

El-Ramly MF, Akaad MK (1960) The basement complex in the CED of Egypt between lat. 24°30′ and 25°40′. Geol Surv Egypt 8:33

El-Ramly MF, Hussein AAA (1983) The ring complexes of the Eastern Desert of Egypt. J Afr Earth Sci 3(1/2):77–82

El-Ramly MF, Greiling R, Kroner A, Rashwan AA (1984) On the tectonic evolution of the Wadi Hafafit area and environs, Eastern Desert of Egypt. Bull Fac Earth Sci 6:114–126 King Abdulaziz University, Jiddah

El-Ramly MF, Greiling RO, Rashwan AA, Ramsy AH (1993) Explanatory note to accompany the geological and structural maps of Wadi Hafafit area, Eastern Desert of Egypt. Ann Geol Surv Egypt 9:1–53

EL-Sayed MM, Furnes H, Mohamed FH (1999) Geochemical constraints on the tectonomagmatic evolution of the late Precambrian Fawakhir ophiolite, Central Eastern Desert, Egypt. J Afri Earth Sci 29:515–533

EL-Sayed MM, Mohamed FH, Furnes HS, Kanisawa S (2002) Geochemistry and petrogenesis of the Neoproterozoic granitoids in the Central Eastern Desert, Egypt. Chem Erde 62:317–346

El-Sharkawy MA, El-Bayoumi RM (1979) The ophiolites of Wadi Ghadir area Eastern Desert, Egypt. Ann Geol Surv Egypt 9:125–135

Engel AEJ, Dixon TH, Stern RJ (1980) Late Precambrian evolution of Afro-Arabian crust from ocean to craton. Geol Soc Am Bull 91:699–706

Essawy MA, Abu Zeid KM (1972) Atalla felsite intrusion and its neighbouring rhylitic flows and tuffs, Eastern Desert, Egypt. Ann Geol Surv Egypt 2:271–280

Fairhead JD, Girdler RW (1970) The seismicity of the Red Sea, Gulf of Aden and Afar triangle. Phil Trans R Soc A 267:49–74

Farahat ES, Abdel Ghani MS, Ahmed AF (2004a) Mineral chemistry as a guide to magmatic evolution of I- and A-type granitoids, Eastern Desert, Egypt. In: Proceedings of the 6th international conference on geochemistry, Alexandria University, Egypt, pp 1–23

Farahat ES, El Mahalawi MM, Hoinkes G, Abdel Aal AY (2004b) Continental back-arc basin origin of some ophiolites from the Eastern Desert of Egypt. Miner Petrol 82:81–104

Farahat ES, Mohamed HA, Ahmed AF, El Mahallawi MM (2007) Origin of I- and A-type granitoids from the Eastern Desert of Egypt: implications for crustal growth in the northern Arabian-Nubian shield. J Afr Earth Sci 49:43–58

Farahat ES, Zaki R, Hauzenberger C, Sami M (2011) Neoproterozoic calc-alkaline peraluminous granitoids of the Deleihimmi pluton, Central Eastern Desert, Egypt: implications for transition from late- to post-collisional tectonomagmatic evolution in the northern Arabian-Nubian Shield. Geol J 46:544–560

Finger F, Dorr W, Gerdes A, Gharib M, Dawoud M (2008) U-Pb zircon ages and geochemical data for the monumental granite and other granitoid rocks from Aswan, Egypt. Implications for geological evolution of the western margin of the Arabian-Nubian Shield. Miner Petrol 93:153–183

Fleck RJ, Greenwood WR, Hadley DG, Anderson RE, Schmidt DL (1979) Rubidium-Strontium geochronology and plate-tectonic evolution of the southern part of the Arabian Shield. US Geological Survey Saudi Arabian Mission Report 245, p 105

Fossen H (2010) Structural geology. Cambridge University Press, London, p 457

Fossen H, Tikoff B (1998) Extended models of transpression/transtension and application to tectonic settings. In: Holdsworth RE, Strachan RA, Dewey JF (eds) Continental transpressional and transtensional tectonics. J Geol Soc London, Special Pub 135, pp 15–33

Fossen H, Tikoff B, Teyssier C (1994) Strain modeling of transpressional and transtensional deformation. Norsk Geol Tidsskr 74:134–145

Fowler A, El Kalioubi B (2002) The Migif-Hafafit gneissic complex of the Egyptian Eastern Desert: fold interference patterns involving multiply deformed sheath folds. Tectonophysics 346:247–275

Fowler AR, El-Kalioubi B (2004) Gravitational collapse origin of shear zones, foliations and linear structures in the Neoproterozoic cover nappes, Eastern Desert, Egypt. J Afr Earth Sci 38:23–40

Fowler TJ, Osman AF (2001) Gneiss-cored interference dome associated with two phases of late Pan-African thrusting in the Central Eastern Desert, Egypt. Precambr Res 108:17–43

Fowler AR, Osman AF (2009) The Sha'it-Nugrus shear zone separating Central and South Eastern Deserts, Egypt: a post-arc collision low-angle normal ductile shear zone. J Afr Earth Sci 53:16–32

Fowler A, Khamees H, Dowidar H (2007) El Sibai gneissic complex, Central Eastern Desert, Egypt: folded nappes and syn-kinematic gneissic granitoid sheets-not a core complex. J Afr Earth Sci 49(4):119–135

Frei M, Jutz S (1990) Use of thematic mapper data for the detection of gold bearing formations in the Eastern Desert of Egypt. In: 7th thematic conference on remote sensing for exploration geology—methods, integration, solutions, Calgary, Canada, pp 1157–1172

Fritz H, Messner M (1999) Intramontane basin formation during oblique convergence in the Eastern Desert of Egypt: magmatically versus tectonically induced subsidence. Tectonophysics 315:145–162

Fritz H, Wallbrecher E, Khudier AA, Abu El Ela F, Dallmeyer RD (1996) Formation of Neoproterozoic metamorphic core complexes during oblique convergence, Eastern Desert, Egypt. J Afr Earth Sci 23:311–329

Fritz H, Dalmeyer DR, Wallbrecher E, Loizenbauer J, Hoinkes G, Neumayr P, Khudeir AA (2002) Neoproterozoic tectonothermal evolution of the Central Eastern Desert, Egypt: a slow velocity tectonic process of core complex exhumation. J Afr Earth Sci 34:543–576

Fritz H, Abdelsalam M, Ali KA, Bingen B, Collins AS, Fowler AR, Ghebreab W, Hauzenberger CA, Johnson PR, Kusky TM, Mace P, Muhongo S, Stern RG, Viola G (2013) Orogen styles in the East African Orogen: a review of the Neoproterozoic to Cambrian tectonic evolution. J Afr Earth Sci 86:65–106

Gabr S, Ghulam A, Kusky T (2010) Detecting areas of high-potential gold mineralization using ASTER data. Ore Geol Rev 38(1):59–69

Gabr SS, Hassan SM, Sadek MF (2015) Prospecting for new gold-bearing alteration zones at El-Hoteib area, South Eastern Desert, Egypt, using remote sensing data analysis. Ore Geol Rev 71:1–13

Gad S, Kusky TM (2006) Lithological mapping in the Eastern Desert of Egypt, the Barramiya area using Landsat thematic mapper (TM). J Afr Earth Sci 44:196–202

Gad S, Kusky TM (2007) ASTER spectral ratioing for lithological mapping in the Arabian-Nubian shield, the Neoproterozoic Wadi Kid area, Sinai, Egypt. Gondwana Res 11(3):326–335

Gagnon É, Schneider D, Kalbfleisch T, Habler G, Biczok J (2016) Characterization of transpressive deformation in shear zones of the Archean North Caribou greenstone belt (NW Superior Province) and the relationship with regional metamorphism. Tectonophysics 693 (B):261–276

Gahlan HA (2003) Geology of the area of Wadi Fiqo, South Eastern Desert, Egypt. M.Sc. thesis, Assiut University, Assiut, Egypt, p 141

Gahlan HA (2006) Petrological characteristics of the mantle section in the Proterozoic ophiolites from the Pan-African Belt. Ph.D. thesis, Kanazawa University, Kanazawa, Japan, p 227

Gahlan H, Arai S, Abu El-Ela F, Tamura A (2012) Origin of wehrlite cumulates in the Moho Transition zone of the Neoproterozoic Ras Salatit Ophiolite, Central Eastern Desert, Egypt. Contrib Mineral Petrol 163:225–241

Gahlan HA, Azer MK, Khalil AES (2015) The Neoproterozoic Abu Dahr ophiolite, South Eastern Desert, Egypt: petrological characteristics and tectonomagmatic evolution. Mineral Petrol 109:611–630

Gahlan HA, Azer MK, Asimow P, Al-Kahtany K (2016) Late Ediacaran post-collisional a-type syenites with shoshonitic affinities, northern Arabian-Nubian Shield: a possible mantle-derived a-type magma. Arab J Geosci 9:603. https://doi.org/10.1007/s12517-016-2629-x

Gapais D, Bale P, Choukroune P, Cobbold PR, Mahjoub Y, Marquer D (1987) Bulk kinematics from shear zone patterns: some field examples. J Struct Geol 9:635–646

Garfunkel Z (1999) History and paleogeography during the Pan-African orogen to stable platform transition: reappraisal of the evidence from Elat area and the northern Arabian-Nubian Shield. Israel J Earth Sci 48:135–157

Goscombe BD, Gray R (2008) Structure and strain variation at mid-crustal levels in a transpressional orogen: a review of Kaoko Belt structure and the character of West Gondwana amalgamation and dispersal. Gondwana Res 13(1):45–85

Greiling RO (1985) Thrust tectonics in Pan-African rocks of SE Egypt. Terra Cognita 5

Greiling RO (1997) Thrust tectonics in crystalline domains: the origin of a gneiss dome. Proc Ind Acad Sci (Earth Planet Sci) 106:209–220

Greiling RO, Kröner A, El-Ramley MF (1984) Structural interference patterns and their origin in the Pan-African basement of the Southeastern Desert of Egypt. In: Kröner A, Greiling RO (eds) Precambrian tectonics illustrated. Schweitzerbart'sche Verlagsbuchhandlung, Stuttgart, Germany, pp 401–412

Greiling RO, Kröner A, El-Ramly MF, Rashwan AA (1988) Structural relationship between the southern and central parts of the Eastern desert of Egypt: details of a fold and thrust belt. In: El-Gaby S, Greiling RO (eds) The Pan-African belt of Northeast Africa and adjacent areas. Vieweg & Sohn, Weisbaden, Germany, pp 121–146

Greiling RO, Abdeen MM, Dardir AA, El Akhal H, El Ramly MF, Kamal El Din GM, Osman AF, Rashwan AA, Rice AH, Sadek MF (1994) A structural synthesis of the Proteorozoic Arabian-Nubian Shield in Egypt. Geol Rundsch 83:484–501

Grothaus B, Eppler D, Ehrlish R (1979) Depositional environments and structural implications of the hammamat formation, Egypt. Ann Geol Surv Egypt 9:564–590

Gupta RP (1991) Remote sensing geology. Springer, Heidelberg, p 356

Hamimi Z (1996) Tectonic evolution of the shield rocks of Gabal El Sibai area, Central Eastern Desert, Egypt. Egypt J Geol 40:423–453

Hamimi Z (1999) Kinematics of some major shear zones in the Eastern Desert of Egypt. Egypt J Geol 43(10):53–71

Hamimi Z, El-Kazzaz YA (2000) Structure and metamorphism of Rawd El-Bil area, south Eastern Desert, Egypt. Egypt J Geol 43(1):297–310

Hamimi Z, Hagag W (2016) A new tectonic model for Abu-Dabbab seismogenic zone (Eastern Desert, Egypt): evidence from field-structural, EMR and seismic data. Arab J Geosci (2017) 10:11. https://doi.org/10.1007/s12517-016-2786-y

Hamimi Z, Hagag W (2017) A new tectonic model for Abu-Dabbab seismogenic zone (Eastern Desert, Egypt): evidence from field-structural, EMR and seismic data. Arab J Geosci 10:11. https://doi.org/10.1007/s12517-016-2786-y

Hamimi Z, Kattu G (2014) Post-Accretionary structures in the Ediacaran Ablah Group volcanosedimentary sequence, Asir Terrane, Saudi Arabia. Gondwana 15, Madrid, Spain, 14–18 July 2014

Hamimi Z, El Amawy MA, Wetait M (1994) Geology and structural evolution of El Shalul Dome and environs, central Eastern Desert, Egypt. Egypt J Geol 38(2):575–595

Hamimi Z, El-Shafei M, Kattu G, Matsah M (2012a) Transpressional regime in southern Arabian Shield: insights from Wadi Yiba Area, Saudi Arabia. Mineral Petrol 107(5):849–860. http://dx.doi.org/10.1007/s00710-012-0198-6

Hamimi Z, Matsah MI, El-Shafei M, El-Fakharani A, Shujoon A, Al-Gabali M (2012b) Wadi Fatima thinskinned foreland FAT belt: a post amalgamation marine basin in the Arabian Shield. Open J Geol 2:271–293. http://dx.doi.org/10.4236/ojg.2012.24027

Hamimi Z, El-Kazzaz Y, El-Fakharani A (2012c) Deformation history of Jabal Muqsim Ophiolitic Nappe and Environs, Allaqi District: implications for the tectonic evolution of the South Eastern Desert Tectonic Terrane In NE Nubian Shield. American Geophysical Union, Fall Meeting 2012, abstract id. V33B-2863

Hamimi Z, Matsah M, Shujoon A, Al-Jabali M (2013b) The NE-Oriented Wadi Fatima Fault Zone, Near Jeddah, Saudi Arabia: a possible arc-arc suture in western Arabian shield. The abstract submitted to the CAG24, Addis Ababa, January 8–14

Hamimi Z, El-Fakharani A, Abdeen M (2014) Polyphase deformation history and strain analysis of the post-amalgamation depositional basins in the Arabian-Nubian Shield: Evidence from Fatima, Ablah and Hammamat basins. In: Fowler AR, Greiling RO and Abdeen MM (eds) Special issue: Arabian-Nubian Precambrian basement geology—progress and developments, J Afr Earth Sci 99(1):64–92

Hamimi Z, Kassem OMK, El-Sabrouty MN (2015a) Application of kinematic vorticity techniques for mylonitized rocks in Al Amar Suture, Eastern Arabian Shield, Saudi Arabia. Geotectonics 49(5):439–450

Hamimi Z, Zoheir BA, Younis MH (2015b) Polyphase deformation history of the Eastern Desert tectonic terrane in northeastern Africa. In: XII international conference "new ideas in earth sciences", Muscow, April 2015 (Abstract)

Hamimi Z, Ghazaly MK, Mohamed EA, Younis AM (2016) Structural history of Wadi Kharit transpressional Shear Zone, Eastern Desert tectonic terrane, Northern Nubian Shield. Ann Meet Egypt Geol Soc (Abstract)

Hanmer S, Passchier C (1991) Shear sense indicators: a review. Geology Survey, Canada, paper no 90, p 71

Harland WB (1971) Tectonic transpression in Caledonian Spitsbergen. Geol Mag 108:27–42

Hashad AH (1980) Present status of geochronological data on the Egyptian basement complex. In: Al-Shanti AMS (eds) Evolution and mineralization of the Nubian-Arabian Shield vol 3, pp 31–46. King Abdulaziz University, Jeddah, Saudi Arabia

Hassaan MM, El-Sawy E (2009) Tectonic environments and distribution of gold deposits in the Pan African Nubian Shield, Egypt. Aust J Basic Appl Sci 3(2):797–809

Hassaan MM, Ramadan TM, Abu El Leil I, Sakr SM (2009) Lithochemical surveys for ore metals in arid region, Central Eastern Desert, Egypt: using Landsat ETM + imagery. Aust J Basic Appl Sci 3:512–528

Hassan MA, Hashad AH (1990) Precambrian of Egypt. In: Said R (ed) The geology of Egypt. Balkema, Rotterdam, pp 201–245

Hassan SM, Ramadan TM (2014) Mapping of the late Neoproterozoic Basement rocks and detection of the gold-bearing alteration zones at Abu Marawat-Semna area, Eastern Desert, Egypt using remote sensing data. Arab J Geosci 8(7):4641–4656

Hassan SM, Sadek MF, Greiling RO (2015) Spectral analyses of basement rocks in El-Sibai-Umm Shaddad area, Central Eastern Desert, Egypt using ASTER thermal infrared data. Arab J Geosci 8(9):6853–6865

Hassan M, Stüwe K, Abu-Alam TS, Klötzli U, Tiepolo M (2016) Time constraints on deformation of the Ajjaj branch of one of the largest Proterozoic shear zones on Earth: the Najd Fault System. Gondwana Res 34:346–362

Hassoup A (1987) Microearthquakes and magnitude studies on Earthquake activity at Abu Dabbab region, Eastern Desert Egypt. M.Sc. thesis. Faculty of science, Cairo University, pp 1–169

Helmy H, Kaindl R, Fritz H, Loizenbauer J (2004) The Sukari gold mine, Eastern Desert, Egypt: structural setting, mineralogy and fluid inclusion study. Miner Deposita 39:495–511

Hermina M, Klitzsch E, List FK (1989) Stratigraphic lexicon and explanatory notes to the geological map of Egypt 1:500,000. Conoco Inc, Cairo, Egypt

Hippertt J (1993) "V"-pull-apart microstructures: a new shear sense indicator. J Struct Geol 15 (12):1393–1403

Hoffman PF (1999) The break-up of Rodinia, birth of Gondwana, true polar wander and the snowball earth. J Afr Earth Sc 17:17–33

Hosny A, El Hady SM, Mohamed AA, Panza GF, Tealeb A, El Rahman MA (2009) Magma intrusion in the upper crust of Abu Dabbab area, south east of Egypt, from Vp and Vp/Vs tomography. Rend Fis Acc Lincei 20:1–19. http://dx.doi.org/; https://doi.org/10.1007/s12210-009-0001-8

Hosny A, El-Hady SM, Guidarelli M, Panza GF (2012) Source moment tensors of the earthquake Swarm in Abu-Dabbab area, South-East Egypt. Rend Fis Acc Lincei 23:149–163

Hudleston PJ (1983) Strain patterns in an ice cap and implications for strain variations in shear zones. J Struct Geol 5:455–463

Hudleston PJ, Schultz-Ela DD, Southwick DL (1988) Transpression in an Archean greenstone belt, northern Minnesota. Can J Earth Sci 25:1060–1068

Hussein AA, Aly MM, El Ramly MF (1982) A proposed new classification of the granites of Egypt. J Volcanol Geoth Res 14:187–198

Ibrahim S, Cosgrove J (2001) Structural and tectonic evolution of the Umm Gheig/El-Shush region, central Eastern Desert of Egypt. J Afr Earth Sci 33:199–209

Ibrahim ME, Yokoyama I (1998) Probable origin of the Abu Dabbab earthquakes swarms in the Eastern Desert of Egypt. In: Bull IISEE 32

Ishii K (1992) Partitioning of non-coaxiality in deforming layered rock masses. Tectonophysics 210:33–43

Jackson NJ (1986) Petrogenesis and evolution of Arabian felsic plutonic rocks. J Afr Earth Sci 4:47–59

Jakob S, Bühler B, Gloaguen R, Breitkreuz C, Eliwa HA, El Gameel K (2015) Remote sensing based improvement of the geological map of the Neoproterozoic Ras Gharib segment in the Eastern Desert (NE-Egypt) using texture features. J Afr Earth Sci 111:138–147

Jarrar G, Stern RJ, Saffarini G, Al-Zubi H (2003) Late- and postorogenic Neoproterozoic intrusions of Jordan: implications for crustal growth in the northernmost segment of the East African Orogen. Precambr Res 123:295–319

Jarrar G, Saffarini G, Wachendorf H, Baumann A (2004) Origin, age and petrogenesis of neoproterozoic composite dykes from the Arabian-Nubian Shield, SW Jordan. Geol J 39:157–178

Jiang D, Williams PF (1998) High-strain zones: a unified model. J Str Geology 20:1105–1120

Johnson PR (1998) Tectonic map of Saudi Arabia and adjacents areas (scale 1–4,000,000). Technical report USGSOF-98-3.Saudi Arabian Deputy Ministry for Mineral Resources, Saudi Arabia, Jeddah, p 2

Johnson PR (2003) Post-amalgamation basins of the NE Arabian shield and implications for Neoproterozoic tectonism in the northern East African Orogen. Precambr Res 123:321–337

Johnson PR, Woldehaimanot B (2003) Development of the Arabian–Nubian shield: perspectives on accretion and deformation in the northern East African Orogen and the assembly of Gondwana. In: Yoshida M, Windley BF, Dasgupta S (eds), Proterozoic East Gondwana: supercontinent assembly and breakup. Geol Soc London, Special Publ 206, pp 290–325

Johnson PR, Andresen A, Collins AS, Fowler AR, Fritz H, Ghebreab W, Kusky T, Stern RJ (2011) Late Cryogenian-Ediacaran history of the Arabian-Nubian Shield: a review of depositional, plutonic, structural, and tectonic events in the closing stages of the northern East African Orogen. J Afr Earth Sci 61:167–232

Jones RR, Holdsworth RE, Clegg P, McCaffrey K, Travarnelli E (2004) Inclined transpression. J Struct Geol 30:1531–1548

Kalelioglu O, Zorlu K, Kurt MA, Gul M, Guler C (2009) Delineating compositionally different dykes in the Ulukıs¸la basin (Central Anatolia, Turkey) using computer-enhanced multi-spectral remote sensing data. Int J Remote Sens 30(11):2997–3011

Kamal El, Din GM (1993) Geochemistry and tectonic significance of the pan-African El Sibai Window, Central Eastern Desert, Egypt. Unpubl. Ph.D. thesis. Forschungzentrum Julich GmbH, 19, p 154

Kamal El Din GM, Khudeir AA, Greiling RO (1992) Tectonic evolution of a pan-African gneiss culmination, Gabal El Sibai area, Central Eastern Desert, Egypt. Zbl Geol Palaont Teil I 11:2637–2640

Kamel M, Youssef M, Hassan M, Bagash F (2016) Utilization of ETM + Landsat data in geologic mapping of wadi Ghadir-Gabal Zabara area, Central Eastern Desert, Egypt. J Remote Sens Space Sci 19:343–360

Katzir Y, Litvinovsky BA, Jahn BM, Eyal M, Zanvilevich AN, Vapnik Y (2006) Four successive episodes of Late Pan-African dykes in the central Elat area, southern Israel. Israel J Earth Sci 55:69–93

Katzir Y, Eyal M, Litvinovsky BA, Jahn BM, Zanvilevich AN, Valley JW, Beeri Y, Pelly I, Shimshilashvili E (2007a) Petrogenesis of A-type granites and origin of vertical zoning in the Katharina pluton, area of Gebel Mussa (Mt. Moses), Sinai, Egypt. Lithos 95(3–4):208–228

Katzir Y, Litvinovsky BA, Jahn BM, Eyal M, Zanvilevich AN, Valley JW, Ye Vapnik, Beeri Y, Spicuzza MJ (2007b) Interrelations between coeval mafic and A-type silicic magmas from composite dykes in a bimodal suite of southern Israel, northernmost Arabian-Nubian Shield: geochemical and isotope constraints. Lithos 97(3–4):336–364

Kebeasy RM (1990) Seismicity. In: Said R (ed) Geology of Egypt. Balkema, Rotterdam, pp 51–59

Khalil KI (2007) Chromite mineralization in ultramafic rocks of the Wadi Ghadir area, Eastern Desert, Egypt: mineralogical, microchemical and genetic study. Neues Jahrbuch für Mineralogie Abhandlungen 183:283–296

Khan T, Murata M, Karim T, Zafar M, Ozawa H, Rehman H (2007) Cretaceous dike swarm provides evidence of a spreading axis in the back-arc basin of the Kohistan paleo-island arc, northwestern Himalaya, Pakistan. J Asian Earth Sci 29:350–360

Kharbish S (2010) Geochemistry and magmatic setting of Wadi El-Markh island-arc gabbro–diorite suite, central Eastern Desert, Egypt. Chemie der Erde 70:257–266

Khudeir AA, Asran AH (1992) Back-arc Wizr Ophiolites at Wadi Um Gheig district, Eastern Desert, Egypt. Bull Fac Sci 21:1–22 Assiut University

Khudeir AA, El-Gaby S, Greiling RO, Kamal El Din GW (1992) Geochemistry and tectonic significance of polymetamorphosed amphibolites in the Gebel Sibai window, Central Eastern Desert, Egypt. Geology of the Arab world conference. Cairo University, Egypt, pp 461–476

Khudeir AA, Kamal El-Gaby S, El Din GM, Asran AMH, Greiling RO (1995) The pre-Pan-African deformed granite cycle of the Gabal El-Sibai swell, Eastern Desert, Egypt. J Afr Earth Sci 21:395–406

Khudeir AA, Abu El-Rus MA, El-Gaby S, El-Nady O, Bishara WW (2008) Sr–Nd isotopes and geochemistry of the infrastructural rocks in the Meatiq and Hafafit core complexes, Eastern Desert, Egypt: evidence for involvement of Pre-Neoproterozoic crust in the growth of Arabian-Nubian shield. Island Arc 17:90–108

Klitzch C, List F, Pöhlmann A (1987) Geological Map of Egypt (CONOCO), NG 36NE. Qusier, scale 1:500000

Knopásek J, Kröner S, Kitt S, Passchier CW, Kröner A (2005) Oblique collision and evolution of large-scale transcurrent shear zones in the kaoko belt, NW Namibia. Precambr Res 136:139–157

Kröner A, Greiling RO, Reischmann T, Hussein IM, Stern RJ, Durr St, Kruger J, Zimmer M (1987a) Pan-African crustal evolution in northeast Africa. In: Kröner A (ed) Proterozoic lithospheric evolution. American geophysical union, geodynamic series 17, pp 235–257

Kröner A, Stern RJ, Dawoud AS, Compston W, Reischmann T (1987b) The Pan-African continental margin in northeast Africa: evidence from a geochronological study of granulites at Sabaloka, Sudan. Earth Planet Sci Lett 85:91–104

Kröner A, Todt W, Hussein IM, Mansour M, Rashwan AA (1992) Dating of late Proterozoic ophiolites in Egypt and the Sudan using the single grain zircon evaporation technique. Precambr Res 59:15–32

Kröner A, Krüger J, Rashwan AA (1994) Age and tectonic setting of granitoid gneisses in the Eastern Desert of Egypt and south-west Sinai. Geol Rundsch 83:502–513

Kumar RS, Prasannakumar V (2009) Fabric evolution in Salem-Attur Shear Zone, South India, and its implications on the kinematics. Gondwana Res 16:37–44

Kumar C, Shetty A, Raval S, Sharma R, Ray C (2015) Lithological discrimination and mapping using ASTER SWIR data in the Udaipur area of Rajasthan, India. Proc Earth Planet Sci 11:180–188

Kusky TM (2004) Precambrian ophiolites and related rocks. Elsevier, Amsterdam, p 748

Kusky TM, Ramadan TM (2002) Structural controls on Neoproterozoic mineralization in the South Eastern Desert, Egypt: an integrated field, Landsat TM, and SIR C/X SAR approach. J Afr Earth Sci 35(1):107–121

Kusky TM, Abdelsalam M, Tucker R, Stern RJ (2003) Evolution of the East African and related Orogens, and the assembly of Gondwana. Spec Iss Precambr Res 123:81–344

Kuster D (2009) Granitoid-hosted Ta mineralization in the Arabian-Nubian Shield: ore deposit types, tectono-metallogenetic setting and petrogenetic framework. Ore Geol Rev 35:68–86

Lacassin R, Van Den Driessche J (1983) Finite strain determination of gneiss: application of Fry's to porphyroid in Southern Massif Central (France). J Struct Geol 5:245–253

Li ZX, Evans DAD, Zhang S (2004) A 90○ Spin on Rodinia: possible causal links between the Neoproterozoic supercontinent, superplume, true polar wander and low-latitude glaciation. Earth Planet Sci Lett 220:409–421

Li S, Wilde SA, Wang T, Xiao WJ, Guo QQ (2016) Latest Early Permian granitic magmatism in southern inner Mongolia, China: implications for the tectonic evolution of the southeastern Central Asian orogenic belt. Gondwana Res 29:168–180

Liégeois JP, Stern RJ (2010) Sr–Nd isotopes and geochemistry of granite–gneiss complexes from the Meatiq and Hafafit domes, Eastern Desert, Egypt: no evidence for pre-Neoproterozoic crust. Int J Earth Sci 57:31–40

Liégeois J-P, Abdelsalam MG, Ennih N, Ouabadi A (2013) Metacraton: nature, genesis and behavior. Gondwana Res 23:220–237

Loizenbauer J, Wallbrecher E, Fntz H, Neumayr P, Khudeir AA, Kloetzil U (2001) Structural geology, single zircon ages and fluid inclusion studies of the Meatiq metamorphic core complex. Implications for Neoproterozoic tectonics in the Eastern Desert of Egypt. Precambr Res 110:357–383

Lundmark AM, Andresen A, Hassan MA, Augland LE, Abu El-Ru MA, Boghdady GY (2012) Repeated magmatic pulses in the East African Orogen of Central Eastern Desert, Egypt: an old idea supported by new evidence. Gondwana Res 22:227–237

Madani AA, Emam AA (2011) SWIR ASTER band ratios for lithological mapping and mineral exploration: a case study from El Hudi area, southeastern desert, Egypt. Arab J Geosci 4(1–2):45–52

Makroum FM (2001) Pan-African tectonic evolution of the Wadi El Mayit Area and its environs, Central Eastern Desert, Egypt. Second Int Conf Geol Afr 2:219–233 Assiut University, Egypt

Makroum FM (2003) Lattice preferred orientation (LPO) study of the orogen-parallel Wadi Nugrus and Wadi Um Nar shears, Eastern Desert-Egypt, using EBSD-technique. Third Int Conf Geol Afr 1:213–232

Makroum F (2017) Structural Interpretation of the Wadi Hafafit Culmination: a pan African gneissic dome in the central Eastern Desert. Lithosphere (in press), Egypt

Matin A (2006) Structural anatomy of the Kushtagi schist belt, Dharwar craton, south India-an example of archaean transpression. Precambr Res 147:28–40

Matsah MI, Kusky TM (1999) Sedimentary facies of the Neoproterozoic Al-Jifn basin, NE Arabian shield: relationships to the Halaban-Zarghat (Najd) faults system and the closure of the Mozambique Ocean. In: Greiling R (ed) Pan-African of northern Africa–Arabia. Forschungszentrum Jülich. Geologisch Palaeontoloigsches Institut, Ruprecht-Karls-Universitaet, Heidelberg, proceedings of a workshop, Oct 22–23, 1998

Matsah MI, Kusky TM (2001) Analysis of Landsat ratio imagery of the Halaban Zarghat fault and related Jifn basin, NE Arabian shield: implications for the kinematic history of the Najd fault. Gondwana Res 4(2):182

Miller MM, Dixon TH (1992) Late Proterozoic evolution of the north part of the Hamisana zone, northeast Sudan: constraints on Pan-African accretionary tectonics. J Geol Soc London 149:743–750

Moghazi AM (2002) Petrology and geochemistry of Pan-African granitoids, Kab Amiri area, Egypt-implications for tectonomagmatic stages of the Nubian Shield evolution. Miner Petrol 75:41–67

Moghazi AM, Andersen T, Oweiss GA, El Bouseily AM (1998) Geochemical and Sr–Nd–Pb isotopic data bearing on the origin of Pan-African granitoids in the Kid area, southeast Sinai, Egypt. J Geol Soc London 155:697–710

Moghazi AM, Hassanen MA, Hashad MH, Mohamed FH (2001) Garnet-bearing leucogranite in the El-Hudi area, southern Egypt: evidence of crustal anatexis during Pan-African low pressure regional metamorphism. J Afr Earth Sci 33:245–259

Moghazi AM, Hassanen MA, Mohammed FH, Ali S (2004) Late Neoproterozoic strongly peraluminous leucogranites, South Eastern Desert, Egypt—petrogenesis and geodynamic significance. Miner Petrol 81:19–41

Mohamed FH (1993) Rare metal-bearing and barren granites, Eastern Desert of Egypt: geochemical characterization and metallogenetic aspects. J Afr Earth Sci 17:525–539

Mohamed FH, Hassanen MA (1996) Geochemical evolution of arc-related mafic plutonism district, Eastern Desert of Egypt. J Afr Earth Sc 22:269–283

Mohamed FH, Moghazi AM, Hassanen MA (2000) Geochemistry, petrogenesis and tectonic setting of late Neoproterozoic Dokhan type volcanic rocks in the Fatira area, eastern Egypt. Int J Earth Sci 88:764–777

Mohamed AS, Hosny A, Abou-Aly N, Saleh M, Rayan A (2013) Preliminary crustal deformation model deduced from GPS and earthquakes' data at Abu-Dabbab area, Eastern Desert, Egypt. NRIAG J Astron Geophys 2(1):67–76

Moore JM (1979) Tectonics of the Najd transcurrent fault system, Saudi Arabia. J Geol Soc London 136:441–454

Moussa EMM, Stern RJ, Manton WI, Ali KA (2008) SHRIMP zircon dating and Sm/Nd isotopic investigations of Neoproterozoic granitoids, Eastern Desert, Egypt. Precambr Res 160:341–356

Nano L, Kontny A, Sadek MF, Greiling RO (2002) Structural evolution of metavolcanics in the surrounding of the gold mineralization at El Beida, South Eastern Desert, Egypt. Ann Geol Surv Egypt 25:11–22

Neumayr P, Hoinkes G, Puhl J, Mogessie A, Khudeir AA (1998) The Meatiq Dome, (Eastern Desert, Egypt) a precambrian metamorphic core complex: petrological and geological evidences. J Metamorph Geol 16:259–279

Noweir AM (1968) Geology of the Hammamat-Um Seleimat District, Eastern Desert, Egypt. Ph. D. thesis, Assiut University, Egypt

Oriolo S, Oyhantçabal P, Wemmer K, Basei MAS, Benowitz J, Pfänder J, Hannich F, Siegesmund S (2016) Timing of deformation in the Sarandí del Yí Shear Zone, Uruguay: implications for the amalgamation of the Western Gondwana during the Neoproterozoic Brasiliano–Pan-African Orogeny. Tectonics 35(3):754–771

Patchett PJ, Chase CG (2002) Role of transform continental margins in major crustal growth episodes. Geology 30:39–42

Phillips WJ (1972) Hydraulic fracturing and mineralization: geological society of London 128:337–361

Pisarevsky SA, Wingate MTD, Powell CM, Johnson S, Evans DAD (2003) Models of Rodinia assembly and fragmentation. In: Yoshida M, Windley Dasgupta BFS (eds) Proterozoic East Gondwana: supercontinent assembly and breakup. J Geol Soc London Special Publ 206:35–55

Pohl W (1979) Metallogenic/minerogenic analysis—contribution to the differentiation between Mozambiquian basement and Pan-African superstructure in the Red Sea region. Ann Geol Surv Egypt 9:32–44

Qaoud N (2014) Utilization of spaceborne imagery for lithologic mapping: a case study from Um Had area, Central Eastern Desert, Egypt. J Geogra Geol 6(2):113–123

Qiu F, Abdelsalam M, Thakkar P (2006) Spectral analysis of ASTER data covering part of the Neoproterozoic Allaqi-Heiani suture, southern Egypt. J Afr Earth Sci 44:169–180

Raharimahefa T, Kusky TM (2010) Structural and remote sending analysis of the Betsimisaraka Suture in northeastern Madagascar. Gondwana Res 15:14–27

Ramadan TM, Kontny A (2004) Mineralogical and structural characterization of alteration zones detected by orbital remote sensing at Shalatin District area, SE Desert, Egypt. J Afr Earth Sci 40:89–99

Ramsay JG, Huber MI (1987) The techniques of modern structural geology. Academic Press, New York, I & II, p 700

Ratschbacher L, Wenk HR, Sintubin M (1991) Calcite textures: an example from nappes with strain-path partitioning. J Struct Geol 13:369–384

Rice AHN, Greiling RO, Dardir AA, Rashwan AA, Sadek MF (1993) Pan-African extensional structures in the area S of the Hafafit Antiform, Eastern Desert of Egypt. Zentralblatt fur Geologie und Palaeontolgie Teil I 11:2641–2651

Ries AC, Shackelton RM, Graham RH, Fitches WR (1983) Pan-African structures, ophiolites and melange in the Eastern Desert of Egypt: a traverse at 26° N. J Geol Soc London 140:75–95

Rothery DA (1987) Improved discrimination of rock units using landsat thematic mapper imagery of the Oman ophiolite. J Geol Soc London 144:587–597

Rowan LC, Mars JC (2003) Lithologic mapping in the mountain pass, California, area using advanced spaceborne emission and reflection radiometer (ASTER) data. Remote Sens Environ 82:350–366

Rowan LC, Mars JC, Simpson CJ (2005) Lithologic mapping of the Mordor, NT, Australia ultramafic complex by using the advanced spaceborne thermal emission and reflection radiometer (ASTER). Remote Sens Environ 99:105–126

Sabet AH (1961) Geology and mineral deposits of Gebel El Sibai area, Red Sea hills, Egypt. Ph.D. thesis, Leiden State University, Netherlands, p 188

Sabet AH, Tsogoev V, Sarin LP, Azazi SA, Bedewi MA, Ghobrial GA (1976) Tin tantalum deposits of Abu Dabbab. Ann Geol Surv Egypt 6:93–117

Sabins F (1997) Remote Sensing: principles and interpretation, 3rd edn. Wiley Inc, New York, p 494

Sadek MF (2004) Discrimination of basement rocks and alteration zones in Shalatein area, Southeastern Egypt using Landsat Imagery data, Egypt. J Remote Sens Space Sci 7:89–98

Sadek MF (2005) Geology and spectral characterization of the basement rocks at Gabal Gerf area Southeastern Egypt. J Remote Sens Space Sci 8:109–128

Sadek MF, Hassan SM (2012) Application of remote sensing in lithological discrimination and geological mapping of Precambrian basement rocks in the Eastern Desert of Egypt. In: Proceedings of 33rd Asian conference remote sensing, Pattaya, Thailand, 26–30 Nov 2012

Sadek MF, Ali-Bik MW, Hassan SM (2015) Late Neoproterozoic basement rocks of Kadabora-Suwayqat area, Central Eastern Desert, Egypt: geochemical and remote sensing characterization. Arab J Geosci 8(12):10459–10479

Sakakibara N (1995) Structural evolution of multiple ductile shear zone system in the Ryoke Belt, Kinki Province. J Sci Hiroshima Univ Ser C 10(2):267–332

Sakran ShM, Hussein AA, Takla MA, Makhlouf AA (2001) Structural evolution of Um Radam area, south Eastern desert, Egypt. Ann Geol Surv Egypt XXII I(2):1–14

Salem SM, Soliman NM (2015) Exploration of gold at the east end of Wadi Allaqi, South Eastern Desert, Egypt, using remote sensing techniques. Arab J Geosci 8(11):9271–9282

Salem SM, Soliman NM, Ramadan TM, Greilling RO (2014) Exploration of new gold occurrences in the alteration zones at the Barramiya District, central Eastern Desert of Egypt using ASTER data and geological studies. Arab J Geosci 7:1717–1731

Salloum GM, Yehia MA, Tolba ME (1989) Tectonics of the Idfu-Marsa Alam area, central Eastern Desert, Egypt. In: The first conference on geochemistry, Alexandria University, pp 225–237

Sanderson DJ, Marchini WRD (1984) Transpression. J Struct Geol 6:449–458

Sarkarinejad K, Azizi A (2008) Slip partitioning and inclined dextral transpression along the Zagros thrust system, Iran. J Struct Geol 30:116–136

Seleim AM, Hammed MS (2016) Applications of remote sensing in lithological mapping of east Esh El Malaha area, southwest Gulf of Suez, Egypt. Int J Sci Eng Res 7(12):691–701

Sengör AMC, Natal'in BA (1996) Turkic-type orogeny and its role in the making of the continental crust. Ann Rev Earth Planet Sci 24:263–337

Shafiei Bafti S, Mohajjel M (2015) Structural evidence for slip partitioning and inclined dextral transpression along the SE San-andaj–Sirjan zone, Iran. Int J Earth Sci 104:587–601

Shalaby A (2010) The northern dome of Wadi Hafafit culmination, Eastern Desert, Egypt: structural setting in tectonic framework of a scissor-like wrench corridor. J Afr Earth Sci 57:227–241

Shalaby A, Stüwe K, Makroum F, Fritz H, Kebede T, Klotzli U (2005) The Wadi Mubarak belt, Eastern Desert of Egypt: a neoproterozoic conjugate shear system in the Arabian-Nubian Shield. Precambr Res 136:27–50

Shalaby A, Stüwe K, Fritz H, Makroum F (2006) The El Mayah molasse basin in the Eastern Desert of Egypt. J Afr Earth Sci 45:1–15

Shebl A (2018) Contribution of remote sensing and GIS in deciphering the structural and geomorphological attributes of Wadi Ghadir environs, Eastern Desert, Egypt. Unpublished M. Sc thesis, Geology Department, Faculty of Science, Tanta University, Egypt, 402 pp

Smith M, O'Connor E, Nasr BB (1999) Transpressional flower structures and escape tectonics: a new look at the pan-African collision in the Eastern desert, Egypt. In: de Wall H, Greiling RO (eds) Aspects of pan-African tectonics. International Cooperation, Bilateral Seminars Int Bureau, Forschungszentrum Jülich, Germany, pp 81–82

Souza Filho CR, Drury SA (1997) Remote sensing strategies for lithological mapping of Pan African assemblages in arid environments—a case study in Eritrea, NE Africa. Bol./G-USP. Ser Gent 28:1–22

Stein M, Goldstein SL (1996) From plume head to continental lithosphere in the Arabian Nubian shield. Nature 382:773–778

Stern RJ (1979) Late precambrian ensimatic volcanism in the Central Eastern Desert of Egypt. Ph. D. thesis, University of California, USA

Stern RJ (1985) The Najd fault system, Saudi Arabia and Egypt: a late precambrian rift-related transform system. Tectonics 4:497–511

Stern RJ (1994) Arc assembly and continental collision in the neoproterozoic East African orogen: implications for the consolidation of Gondwanaland. Ann Rev Earth Planet Sci 22:319–351

Stern RJ (2017) Neoproterozoic formation and evolution of Eastern Desert continental crust—the importance of the infrastructure-superstructure transition. J Afr Earth Sci (in press). http://dx.doi.org/10.1016/j.jafrearsci.2017.01.001

Stern RJ, Hedge CE (1985) Geochronologic and isotopic constraints on late precambrian crustal evolution in the Eastern Desert of Egypt. Am J Sci 258:97–127

Stern RJ, Gottfried D, Hedge CE (1984) Late Precambrian rifting and crustal evolution in the North Eastern Desert of Egypt. Geology 12:168–172

Stern RJ, Kroner A, Manton WI, Reischmann T, Mansour M, Hussein IM (1989) Geochronology of the late Precambrian Hamisana shear zone, Red Sea Hills, Sudan and Egypt. J Geol Soc London 146:1017–1030

Stern RJ, Nielsen KC, Best E, Sultan M, Arvidson RE, Kroner A (1990) Orientation of late precambrian sutures in the Arabian-Nubian shield. Geology 18:1103–1106

Stern RJ, Johanson PR, Kroner A, Yibas B (2004) Neoproterozoic ophiolites of the Arabian-Nubian shield. In: Kusky TM (ed) Precambrian Ophiolites and Related Rocks. Elsevier, Amsterdam, pp 95–128

Stoeser DB, Camp VE (1985) Pan-African microplate accretion of the Arabian shield. Geol Soc Am Bull 96:817–826

Sturchio NC, Sultan M, Batiza R (1983) Geology and origin of Meatiq Dome, Egypt: a precambrian metamorphic core complex? Geology 11:72–76

Sultan M, Arvidson RE, Sturchio NC (1986) Mapping of serpentinites in the Eastern Desert of Egypt by using Landsat thematic mapper data. Geology 14(12):995–999

Sultan M, Arvidson RE, Duncan IJ, Stern RJ, El Kalioubi B (1988) Extension of the Najd shear system from Saudi Arabia to the central Eastern Desert of Egypt based on integrated field and Landsat observations. Tectonics 7:1291–1306

Sultan M, Becker R, Arvidson RE, Shore P, Stern RJ, El Alfy Z, Attia RI (1993) New constraints on red-sea rifting from correlations of Arabian and Nubian neoproteozoic Outcrops. Tectonics 12:1303–1319

Takla MA, Hussein AA, Sakran ShM, Makhlouf AA (2002) Tectonometamorphic history of Um Radam area, south Eastern Desert, Egypt. Egypt. Ann Geol Surv Egypt XXIV:41–61

Tangestani MH, Jaffari L, Vincent RK, Sridhar BM (2011) Spectral characterization and ASTER-based lithological mapping of an ophiolite complex: a case study from Neyriz ophiolite. SW Iran Remote Sens Environ 115(9):2243–2254

Tavarnelli E, Holdsworth RE, Clegg P, Jones RR, McCaffrey KJW (2004) The anatomy and evolution of a transpressional imbricate zone, Southern Uplands, Scotland. J Struct Geol 26:1341–1360

Taylor WEG, El Hamad YA, El-Kazzaz YA, Rashwan AA (1993) An outline of the tectonic framework for the Pan-African orogeny in the vicinity of Wadi Um Relan, SE Desert, Egypt. In: Thorweihe U, Shandelmeier H (eds) Geoscientific research in NE Africa. Balkema, Rotterdam, pp 31–34

Tikoff B, Greene D (1997) Stretching lineations in transpressional shear zones: an example from the Sierra Nevada Batholith, California. J Struct Geol 19:29–39

Torres-Vera MA, Prol-Ledesma RM (2003) Spectral enhancement of selected pixels in thematic mapper images of the Guanajuato district (Mexico) to identify hydrothermally altered rocks. Int J Remote Sens 24:4357–4373

Treagus S (1983) A theory of finite strain variation through contrasting layers and its bearing on cleavage refraction. J Struct Geol 5:351–368

Vail JR (1985) Pan-African (late Precambrian) tectonic terrains and the reconstruction of the Arabian-Nubian shield. Geology 13:839–842

Wallbrecher E, Fritz H, Khudeir AA, Farahat F (1993) Kinematics of pan-African thrusting and extension in Egypt. Geosci Res Northeast Afr 27–30

Wallbrecher E, Loizenbauer J, Fritz H, Bauernhofer A, Hauzenherger C (1999) Convergence of East and West Gondwana-constraints from Egypt and East Africa. In: The first international conference on the geology of Africa (Abstract)

Willis KM, Stern RJ, Clauer N (1988) Age and geochemistry of Late Precambrian sediments of the Hammamat series from the Northeastern Desert of Egypt. Precambr Res 42:173–187

Yenne EY, Bala DA, Abalaka IE, Ozoji TM, Nimze LW (2015) Utilization of Landsat and field data in geological mapping of Vom-Kuru Area, North-central Nigeria. J Environ Earth Sci 5 (16):95–114

Youssef AM, Hassan AM, Mohamed MA (2009) Integration of remote sensing data with the field and laboratory investigation for lithological mapping of granitic phases: Kadabora pluton, Eastern Desert, Egypt. Arab J Geosci 2(1):69–82

Zimmer M, Kröner A, Jochum KP, Reischmann T, Todt W (1995) The Gabal Gerf complex: a Precambrian N-MORB ophiolite in the Nubian Shield, NE Africa. Chem Geol 123:29–51

Zoheir BA (2008) Characteristics and genesis of shear zone-related gold mineralization in Egypt: a case study from the Um El Tuyor mine, south Eastern Desert. Ore Geol Rev 34:445–470

Zoheir BA (2011) Transpressional zones in ophiolitic mélange terranes: potential exploration targets for gold in the SouthEastern Desert, Egypt. J Geochem Explor 111:23–38

Zoheir BA, Emam A (2012) Integrating geologic and satellite imagery data for high-resolution mapping and gold exploration targets in the South Eastern Desert, Egypt. J Afr Earth Sci 66:22–34

Zoheir BA, Emam A (2014) Field and ASTER imagery data for the setting of gold mineralization in Western Allaqi-Heiani belt, Egypt: a case study from the Haimur deposit. J Afr Earth Sci 99 (1):150–164

Zoheir BA, Lehmann B (2011) Listvenite-lode association at the Barramiya gold mine, Eastern Desert, Egypt. Ore Geol Rev 39:101–115